THE INITIAL MASS FUNCTION FOR MASSIVE STARS IN THE MAGELLANIC CLOUDS. 1. UBV PHOTOMETRY AND CM DIAGRAMS FOR 14 OB ASSOCIATIONS

Robert J. Hill[1,2]
Department of Astronomy
University of Toronto
60 St. George St.
Toronto, Ontario, Canada M5S 1 Al

Barry F. Madore[2]
NASA/IPAC Extragalactic Database
Infrared Processing and Analysis Center
California Institute of Technology
Jet Prepulsion laboratory, MS 100-22
Pasadena, CA 91125

Wendy L. Freedman
The Observatories
Carnegie institution of Washington
813 Santa Barbara St.
Pasadena, CA 91101

[1] Current address: The Observatories, Carnegie Institute of Washington, 813 Santa Barbara St., Pasadena, CA 91101
2 Visiting Astronomer, Las Campanas Observatory, Carnegie institution of Washington

Abstract

UBV CCD photometry has been obtained for 14 OB associations in the Magellanic Clouds using the University of Toronto's 0.6m telescope and the Carnegie Institution of Washington's 1.Om reflector, both on Las Campanas, Chile. 'l'he data arc presented and used to construct colour-magnitude diagrams for the purposes of investigating the massive-st.ar content of the associations.

Keywords: stars: OB associations - stars: photometry — galaxies: LMC and SMC

I. INTRODUCTION

Onc of the primary results of stellar evolution theory is that, to first order, the initial mass of a star determines its structure and subsequent evolution. The initial mass of a star also determines the chemical composition and amount of material returned to the interstellar medium during its lifetime. Therefore the distribution of stellar masses will control the evolution of populations of stars and hence also the chemical evolution of galaxies through quiescent and catastrophic mass loss from massive stars. Accordingly, the frequency distribution of stellar masses as they arrive on the main sequence (known as the initial mass function or IMF) along with the star formation rate arc required for any study of galaxy evolution and chemical enrichment.

Observational attempts to determine the shape of the massive star IMF from samples of stars in the Galaxy have been plagued by problems of small number statistics, a wide range in distance among the sample stars, and both large and uncertain amounts of reddening toward these stars. The resulting uncertainties in the derived mass function can be lessened by choosing samples of stars from nearby galaxies. Large numbers of massive stars in the LMC and SMC can be easily observed with the availability of modern CC]) technology. The interstellar reddening along the line-of-sight to the Magel-

lanic Clouds is much lower than towards massive stars in the Galaxy, which allows much more accurate absolute magnitudes to be obtained for the Magellanic Cloud stars. Also, since all the stars in the Magellanic Clouds can be considered to be at the same distance, any error in the assumed distance will result only in a scale error in the derived IMF, leaving the shape of the IMF unchanged. A serious drawback to this approach is that such studies will always be affected by crowding and confusion at absolute magnitude limits much brighter than are attainable in the Galaxy. in this study, wc restrict our investigation to those stars bright enough to be relatively unaffected by crowding problems.

This is the first in a series of papers aimed at observationally determining the shape of the upper initial mass function using samples of stars in the Magellanic Clouds. We present and discuss here the observational data. Subsequent papers will deal with the reddening and extinction toward these stars, and the construction of the luminosity and mass functions (Hill *et al.* 1992a, b).

II. THE SAMPLE OF ASSOCIATIONS

'l'he large number of OB associations and young clusters in the Magellanic Clouds combined with the small size of CCD chips currently available prohibits the observation of a complete sample of the massive stars in either

galaxy. We present here observations of a subsample of the associations in each galaxy, which we hope are representative.

The sample of associations observed in the LMC was chosen from the catalogue of associations compiled by Lucke and Hodge (1970). At the time this project was undertaken, no similar catalog existed for the SMC, and hence the associations selected were objects which had previously been observed to contain a young stellar component. A list of the associations included in this study is found in Table 1. The LH designations refer to the Lucke and Hodge (1970) catalog of LMC associations, while the N designations refer to the Henize (1956) catalog of emission nebulae in both Magellanic Clouds.

The associations cataloged by Lucke and Hodge (1970) in the LMC range in size from cluster-sized objects to the giant H 11 region 30 Doradus. All of the associations observed for this project were small objects, typically ≤ 10 arcmin in the longest dimension, corresponding to a physical size of ≤ 150 pc at the distance of the Magellanic Clouds. The reason for selecting only the smaller objects is that the interpretation of the mass function is much more straightforward if the stars which make up the mass function are close to coeval. In fact, in most studies, it is assumed that the stars are coeval simply because there is usually no means of determining the duration of the star formation event and the rate at which stars formed during the event.

Working within a spatially restricted area strengthens this assumption but by no means validates it. It is still possible that star formation has occurred over a significant fraction of the lifetimes of the associations containing the youngest, most massive stars.

Most of the associations which were observed were also loose, non-compact objects. The crowding of the more dense objects results in larger photometric errors due to the difficulty of determining the magnitudes of overlapping stellar images. Also, the severe crowding at the center of such objects sets a brighter limit on the completeness of the photometry. Therefore, low density systems were selected in order to minimize the contribution of the photometric errors to the uncertainties in the mass functions and to extend the observations to fainter magnitudes (or equivalently, to lower masses). Nevertheless, a fcw associations with dense clusters at their cores were observed (e.g., 1,11 111 = Lucke-Hodge association #1 11, and NGC 376) in order to investigate any potential differences between the more compact and less compact associations.

III. OBSERVATIONS

The observations were made during two observing runs at Las Campanas, Chile. The first set of observations were made between December 19, 1985 and January 5, 1986 using the 1.Om Swope Telescope, operated by the

Observatories of the Carnegie Institution of Washington. The detector was a Texas Instruments (T1) 500x500 pixel charge-coupled device (CCD), with a scale of 0.68 arcsec per pixel. The second set of observations were made during October 18-27, 1987, with a Thompson 384x576 CCD mounted on the University of Toronto Southern Observatory (UTSO) 0.61 m telescope, also at Las Campanas. This chip has a scale of 0.52 arcsec pcr pixel. The useful size of this chip was only 384x480 duc to a large number of charge traps near one edge. The properties of this chip arc completely described in McCall *et al.* (1989).

Finder charts for the LMC associations were taken from Lucke (1972) and from Hedge and Wright (1 977) for the SMC associations. A log of the observations is given in Table 2. Figures 1a-p are reproductions of the V images obtained for each of the associations. In the cases of NGC 460 and NGC 465, two frames were required in order to obtain complet e coverage of the associations.

IV. DATA REDUCTIONS

a) Preliminary Reductions

The first step in the reduction of CCD data is the removal of the background charge which is present because of the voltage bias on the chip. in the case of the TI chip, this bias subtraction was done by subtracting the

overscan column which is read out along with each image. Bias subtraction of the UTSO data was achieved by subtracting an average of 30 bias frames which were acquired along with each night's data. Following the bias subtraction, the data frames were fiat-fielded in the standard fashion.

b) DAOPHOT Reductions

The individual stellar magnitudes were determined using the computer program DAOPHOT and the companion program ALLSTAR. The procedures followed here in applying DAOPHOT arc essentially those recommended by Stetson (1987a) and the DAOPHOT user's manual (Stetson 1987 b).

The final step in obtaining instrumental magnitudes is to apply an aperture correction to the DAOPHOT magnitudes. The size of the aperture correction was determined by subtracting all but the brightest, least-crowded stars from the frame. Aperture photometry (using the DAOPHOT subroutine PHOT) was then performed on these stars using an aperture large enough to include all of the stellar image (typically 8–10 arcsec radius). The average of the differences between the magnitudes obtained from the aperture photometry and those obtained from the PSF fitting is the aperture correction for the frame. 'J'his zero-point aperture correction was then applied to the magnitudes of all the stars on the frame, before the next step

of transforming to the standard system was taken.

V. PHOTOMETRIC CALIBRATION

The instrumental magnitudes were transformed to standard UBV magnitudes and colors by using observations of standard stars from the lists of Landolt (1973,1983), Menzies *et al.* (1980), and Graham (1981) were also observed. Typically, between 15 and 20 standard stars spanning a large range in color were observed over a large range in air mass on each photometric night. in addition, a series of short exposure observations of several fields were obtained on the night of Nov. 15, 1988, by Patricio Ortiz, using the University of Toronto 0.61 m telescope, with the same instrumentation as described above. These fields had previously been observed on non-photometric nights, and the new observations were used to calibrate the earlier data.

The standard star instrumental (IIAOI'I1OT) magnitudes and colors were obtained from large aperture photometry using the PHOT subroutine, and normalized to a 1 sec exposure time. These instrumental magnitudes were transformed to the standard system using the equations

$$V = v + \epsilon(B - V) - k'_v X + \zeta_v \quad (1)$$

$$(B - V) = \mu J_x(b - v) - \mu k'_{bv} X + \zeta_{bv} \quad (2)$$

$$(U - B) \quad = \quad \psi G_x(u - b) - \psi k'_{ub} X + \zeta_{ub} \tag{3}$$

where v, (6– v), and $(u - b)$ arc the instrumental magnitudes and colors, c, μ and ψ arc the transformation coefficients, k'_v, k'_{bv}, and k'_{ub} arc the first-order extinction coefficients, $\zeta_v, \zeta_b v$, and $\zeta_u b$ are the zero-point constants, and X is the air mass. Also J_x = 1 – $k''_{bv} X$ and G_x = 1 – $k''_{ub} X$, where k''_{bv}, and k''_{ub} arc the second-order extinction coefficients.

In practice, the second-order coefficients arc usually found to be both small and stable from night to night (Hardie 1962). This has been verified for the Las Campanas sight by Hill (1986). 'J'bus, the second-order coefficients from that study (k''_{bv} = –0.023, k''_{ub} = –0.015) were adopted here and J_x and G_x arc simple constants.

The extinction coefficients, transformation coefficients and zero-point constants were found by least squares analysis. The transformation coefficients and zero-point constants for a given telescope, filter and detector system are usually stable over the course of an observing run and hence average values for each run are appropriate and have been adopted here. These values are given in Table 3.

On the other hand, the extinction coefficients can vary from night to night, and hence ndividual coefficients for each photometric night were used

to reduce that night's data. Average extinction values for each observing run arc given in Table 4. (Note: The extinction coefficient for V for the night of Nov. 15, 1988 is smaller than typically found, while the coefficient for (II-V) is large. However, when these coefficients arc used to reduce the standard star observations for that night, the rms residuals for the standards are no larger than those found for ot hcr nights. Hence, these values were accepted and the night judged to be photometric.)

Several of the objects in this study were observed on nights which were not photometric. However, short exposure observations of these fields obtained on a subsequent photometric night yields magnitudes and colors for the brightest stars in the frame. These stars can then be used as a set of '(standard" stars with which the observations from the non-photometric night can be calibrated. The transformation equations in this case are

$$\mathrm{v} = v + \epsilon(B - V) + \zeta_v \tag{4}$$

$$(B - V) = \mu(b - v) + \& \tag{5}$$

$$(U - B) = \psi(u - \mathrm{b}) + \zeta_{ub} \tag{6}$$

These equations differ from equations 1–3 in that the extinction terms arc irrelevant when comparing two frames and hence have been absorbed into

the other constants.

In Tables 5-18, wc present the UBV magnitudes and colors for the 14 associations included in this study. Also included in these tables are the DAOPI1OT estimates of the errors in the magnitudes and colors. Finally, columns 2 and 3 in each of the tables, give the xy coordinates of each star on the V images of the associations (Figures la–p). In the case of NGC 460, the stars numbered 1 through 500 can be found in Figure 1 m, while stars 507 through 1015 can be found in Figure In. For NGC 465, stars 11 through 589 arc located in Figure 10, while stars 590 through 1058 arc found in Figure 1p.

VI. PHOTOMETRIC ACCURACY

a) Internal Errors

The sources of error in the final magnitudes and colors considered here arc: a) photon statistics, b) sky determinations, c) crowding, d) aperture corrections, c) extinction corrections, and f) transformation errors.

The DAOPHOT errors include only an estimate of the first three sources of error and can be considered to be a reasonably accurate estimate of their combined effects. Examples of the typical DAOPHOT errors in V, B and U as a function of magnitude (for the association LH 4) arc displayed in Figures 2–4. Most of the errors follow the expected pattern in that they increase with magnitude, however, there arc some comparatively bright stars with large errors. Upon closer inspection, these stars were found to lie in crowded regions or in the wings of other stars.

The accuracy of the aperture corrections is not as easy to evaluate. In most cases, the aperture corrections are determined from only 3–5 bright uncrowded stars in the frame, so a standard deviation is not particularly meaningful. However, in the vast majority of cases, the aperture corrections for stars in any onc frame arc consistent to within 0.02-0.03 msg. In the worst cases, the error may be as large as 0.05 msg.

The errors introduced by the uncertainties in determining the extinction and transformation coefficients can be estimated by considering how accurately the magnitudes of the standard stars are reproduced when these coefficients are applied to the standard star observations. These observations do not suffer from an aperture correction (assuming that the aperture is large enough) and the first three sources of error should be minimal, since the standard stars are bright and in uncrowded regions. Typical rms errors arc ±0.02 mag in V and (11-V) and ±0.03 mag in (U-B).

The net effect is that the magnitudes and colors for even the brightest, most isolated program stars are probably accurate to no better than ±0.03 m ag.

c) ***External Accuracy***

A test of the external accuracy of the photometry may be made by comparing the magnitudes and colors obtained in this study with those from other work. Unfortunately, most previous observations of the objects included here used photographic plates as the detector, and hence the internal accuracy of such work is expected to be lower.

The comprehensive study by Lucke (1972) includes BV photographic photometry of all the LMC associations observed in this study. An example of the comparison between Lucke's photographic photometry of LH 111 and

the CC]) photometry present.cd here is found in Figures 5 and 6.

'I'here is a systematic difference between the two, in the sense that the photographic magnitudes arc brighter by 0.10 mag in V and 0.16 mag in B. This points out a serious problem that arises in attempting to determine photographic or photoelectric magnitudes in crowded fields with strong and variable unresolved backgrounds. Many of the stars identified as single by Lucke were found by DAOPHOT to be double and sometimes even triple, The differences in magnitude for the single stars are close to zero in most cases, while the points which have large positive differences in magnitude in the plots are, for the most part, the multiple objects.

In order to make a better comparison between the two measurements, the stars which were found to be multiple by DAOPHOT can be treated as single objects. Recalculating their magnitudes then gives a measurement of approximately the same flux as in the photographic case. Figures 7 and 8 show the results of this new comparison. The systematic differences between the two sets of measurements are much smaller, as is the scatter in both cases. While there is no systematic difference in the V magnitudes (AV = 0.01 mag), Lucke's B magnitudes arc still brighter by 0.08 mag, for this field. No further comparisons were attempted.

Lee (1990) has also made CCD observations of 1,11111. A comparison of

his data with that present.cd here is made in Figures 9-11. The systematic differences in the observations through each filter arc small (AV = –0.032 mag, ΔB = –0.002 mag, and AU = +0.034 mag, in the sense present study minus Lee), and fully consistent with the estimated total error suggested in the last section. The difference in the V magnitudes may be significant, but there is no simple method of determining which set of data is more accurate.

VII. COLOR-MAGNITUDE DIAGRAMS

The magnitudes and colors obtained from the observations can be used to construct color-magnitude (CM) diagrams for each of the associations. These CM diagrams are presented in Figures 12-25. The different symbols represent the photometric accuracy of the plotted data. Filled circles are used for stars with the most accurate photometry ($\sqrt{\sigma_V^2 + \sigma_{BV}^2} \leq 0.05$ mag), according to DAOPHOT. Open circles represent stars with photometry of intermediate accuracy ($0.05 < \sqrt{\sigma_V^2 + \sigma_{BV}^2} \leq 0.10$ mag), while plus signs are used for stars with the larges photometric errors ($\sqrt{\sigma_V^2 + \sigma_{BV}^2} > 0.10$ mag). The dashed line near the bottom of each plot is drawn parallel to the completeness limits of the photometry for illustrative purposes; it does not represent the actual photometric limits.

All of the associations show a very strong blue main sequence, which broadens at fainter magnitudes due to increasing photometric errors. The

bright, limit of the main sequence varies from association to association which indicates a range in their ages. Red supergiants are present in some, but not all, associations. Also, a background population of Magellanic Cloud giant stars is apparent in the red part of the CM diagrams below $V \simeq 16$ msg.

The CM diagrams can be used to study many of the properties, both global and individual, of the associations. in companion papers, wc will investigate the amounts and characteristics of the interstellar reddening towards these associations (Hill *et al.* 1992a) and determine the luminosity and mass functions of the brightest member stars (Hill *et al.* 1992b).

BFM was supported in part by the Jet Propulsion Laboratory, California Institute of Technology, under the sponsorship of the Astrophysics Division of *NASA's* Office of Space Science and Applications. WLF's research is supported in part by NSF Grant AST 87-13889.

Table 1: The Sample of Associations

Object		Other Designations	α (1950.0)	δ (1950.0)
LMC	1,114	NGC 1731, N4	045323	-670024
	1,1154	NGC 1955, N51	052615	-673214
	1,1158	NGC 1962, NGC 1965 N135, N144	052657	-6851 12
	1,1183	NGC 2030, N61, N63	053540	-660353
	1.1187	NGC 2048, N154	053619	-694052
	1,1193	NGC 2050, N135	053706	-692450
	1,11111	NGC 2100, N135	054223	-691339
SMC	N 24	...	004623	-733609
	NGC 249	N12	004334	-732112
	NGC 261	N12	004441	-732311
	NGC 376	...	010213	-730502
	NGC 456	N83	01 1236	-733156
	NGC 460	N84	011323	-723355
	NGC 465	N85	01 1425	-733455

Table 2: Log of Observations

Object	Date	Filter	Exposure Times (See)
LMC LH 4	29/30 Dec. 1985	v	20, 300
		B	10, 60, 400
		u	120,800
LMC 1,1154	22/23 Dec. 1985	v	90
		B	120
		u	300
	29/30 Dec. 1985	v	20, 300
		B	20, 400
		u	60, 800
LMC LH 58	29/30 Dec. 1985	v	10, 300
		B	10, 40,400
		u	80, 800
LMC 1,1183	30/31 Dec. 1985	v	30, 300
		B	60, 360
		u	800
	18/19 Oct. 1987	v	90, 90
		B	180, 180

Object	Date	Filter	Exposure Times (sCc)
		u	600
LMC 1,1187	22/23 *ŋ cc.* 1985	v	15, 60
		B	30, 90
		u	240
	15/16 Nov. 1988	v	180
		B	240
		u	600
LMC 1,1193	22/23 Dec. 1985	v	30,90
		B	120
		u	300
	28/29 Dec. 1985	v	30,240
		B	60,300
		u	600
	15/16 Nov. 1988	v	180
		B	240
		u	600

Object	Date	Filter	Exposure Times (See)
LMC 1,11 1 11	18/19 Oct. 1987	v	Go, 120
		B	90,240
		u	180,600
SMC N 24	18/19 Oct. 1987	v	180
		B	300
		u	900,900
SMC NGC 249	19/20 Oct. 1987	v	240,300
		B	300,300
		u	300, 900
SMC NGC 261	19/20 Oct. 1987	v	240,300
		B	360,360
		u	300,900
SMC NGC 376	19/20 Oct. 1987	v	30,90, 300
		B	60,360,360
		u	300,900

Object	Date	Filter	Exposure'1'imes (sCc)
SMC NGC 456	27/280 ct. 1987	v	90,300
		B	180, 360
		u	300, 900
SMC NGC 460(N)	27/28 Oct. 1987	v	90, 300
		B	180, 360
		u	300,900
SMC NGC 460(S)	28/29 Oct. 1987	v	90,300
		B	180, 360
		u	300, 900
SMC NGC 465(N)	28/29 Oct. 1987	v	90, 300
		B	180, 360
		u	300,900
SMC NGC 465(S)	29/30 Oct. 1987	V	30, 90,300
		B	180, 360
		u	90, 300, 900

Table 3: Transformation Coefficients

Dates	c	μ	ψ	ζ_V	ζ_B	ζ_U
Dec. 1985	-0.1516	1.3103	0.8497	-3.007	0.213	-2.229
Oct. 1987	0.0995	1.0048	0.9045	-5.852	-0.878	-0.906
Nov. 1988	0.1339	1.0176	0.9978	-5.980	-0.705	-1.138

Table 4: Transformation Coefficients

Dates	k'_v	k'_{bv}	k'_{ub}
Dec. 1985	0.150	0.030	0.255
Oct. 1987	0.168	0.073	0.341
Nov. 1988	0.102	0.209	0.244

REFERENCES

Graham, J. A. 1981, Pub. A. S. 1'., 93,29.

Hardie, R. 11.1962, in Astronomical Techniques, cd. W. A. Hiltner (Chicago: University of Chicago Press), p. 178.

Henize, K. 1956, Ap. J. Supp., 2, 315.

Hill, R., 1986, M. Sc. Thesis, University of Western Ontario.

Hill, R., Madore, B. F., & Freedman, W. L. 1992a, in preparation.

Hill, R., Madore, B. F., & Freedman, W. L. 1992b, in preparation.

Hodge, P. W., & Wright, F., W. 1977, The Small Magellanic Cloud (Seattle: University of Washington Press).

Landolt, A. U. 1973, A. J., 78, 959.

Landolt, A. U. 1983, A. J., 88,439.

Lee, M. G. 1990, Ph. D. Thesis, University of Washington.

Lucke, 1'.11. 1972, Ph. D. Thesis, University of Washington.

Lucke, P. B., & Hodge, 1'. W. 1970, A. J., 75, 171.

McCall, M. I,., English, J., & Shelton, I. 1989, A. J., 83, 179.

Menzies, J. W., Banfield, R. M., & Laing, J. D. 1980, SAAO Circ., Vol. 1, No. 5, p 149.

Stetson, P. B. 1987a, Pub. A. S. P., 99, 101.

Stetson, 1'.11. 1987b, DAOPHOT User's Manual,

FIGURE CAPTIONS

Figure la. V gray scale image of 1,114. North is at the bottom and east is at the right.

Figure lb. V gray scale image of 1,1154. North is at the bottom and cast is at t he right.

Figure 1c. V gray scale image of 1,1158. North is at the bottom and east is at the right,.

Figure 1 d. V gray scale image of 1,1183. North is at the bottom and east is at the right.

Figure le. V gray scale image of LH 87, North is at the left and east is at the bottom.

Figure 1f. V gray scale image of 1,1193. North is at the left and east is at the bottom,

Figure lg. V gray scale image of 1,11111. North is at the left and east is at the bottom.

Figure 1h. V gray scale image of N 24. North is at the left and east is at the bottom.

Figure Ii. V gray scale image of NGC 249. North is at the left and east is at the bottom.

Figure 1j. V gray scale image of NGC 261. North is at the left and east is at the bottom.

Figure lk. V gray scale image of NGC 376. North is at the left and east is at the bottom.

Figure 11. V gray scale image of NGC 456. North is at the left and cast is at the bottom.

Figure 1 m. V gray scale image of NGC 460(N). North is at the left and cast is at the bottom.

Figure 1n. V gray scale image of NGC 460(S). North is at the left and cast is at the bottom.

Figure 1o. V gray scale image of NGC 465(N). North is at the left and east is at the bottom.

Figure 1p. V gray scale image of NGC 465(S). North is at the left and east is at the bottom.

Figure 2. V error distribution for 1,114.

Figure 3. B error distribution for 1,114.

Figure 4. U error distribution for 1,114.

Figure 5. Comparison of the V photometry for 1,11111 with Lucke (1972).

Figure 6. Comparison of the B photometry for LH111 with Lucke (1972).

Figure 7. Comparison of the V photometry for 1,11111 with Lucke (1972).

Objects found to be multiple by DAOI'11OT have been treated as single stars in this comparison.

Figure 8. Comparison of the B photometry for 1,11111 with Lucke (1972). objects found to be multiple by I) AOI'I1OT have been treated as single stars in this comparison.

Figure 9. Comparison of the V photometry for 1,11111 with Lee (1990).

Figure 10. Comparison of the B photometry for 1,11111 with Lee (1 990).

Figure 11. Comparison of the U photometry for 1,11111 with Lee (1990).

Figure 12. CM diagram for LH 4. The filled circles represent stars with the most. accurate photometry, the open circles denote stars with intermediate accuracy, and the plus signs represent stars with the largest photometric errors. See the text for details. 'l'he dashed line is drawn parallel to the completeness limits of the data.

Figure 13. CM diagram for 1,1154. Symbols arc as in Figure 14.

Figure 14. CM diagram for LH 58. Symbols arc as in Figure 14.

Figure 15. CM diagram for 1,1183. Symbols are as in Figure 14.

Figure 16. CM diagram for LH 87. Symbols arc as in Figure 14.

Figure 17. CM diagram for 1,1193. Symbols are as in Figure 14.

Figure 18. CM diagram for 1,11111. Symbols are as in Figure 14.

Figure 19. CM diagram for N 24. Symbols are as in Figure 14.

Figure 20. CM diagram for NGC 249. Symbols are as in Figure 14.

Figure 21. CM diagram for NGC 261. Symbols arc as in Figure 14.

Figure 22. CM diagram for NGC 376. Symbols arc as in Figure 14.

Figure 23. CM diagram for NGC 456. Symbols arc as in Figure 14.

Figure 24. CM diagram for NGC 460. Symbols are as in Figure 14.

Figure 25. CM diagram for NGC 465. Symbols are as in Figure 14.

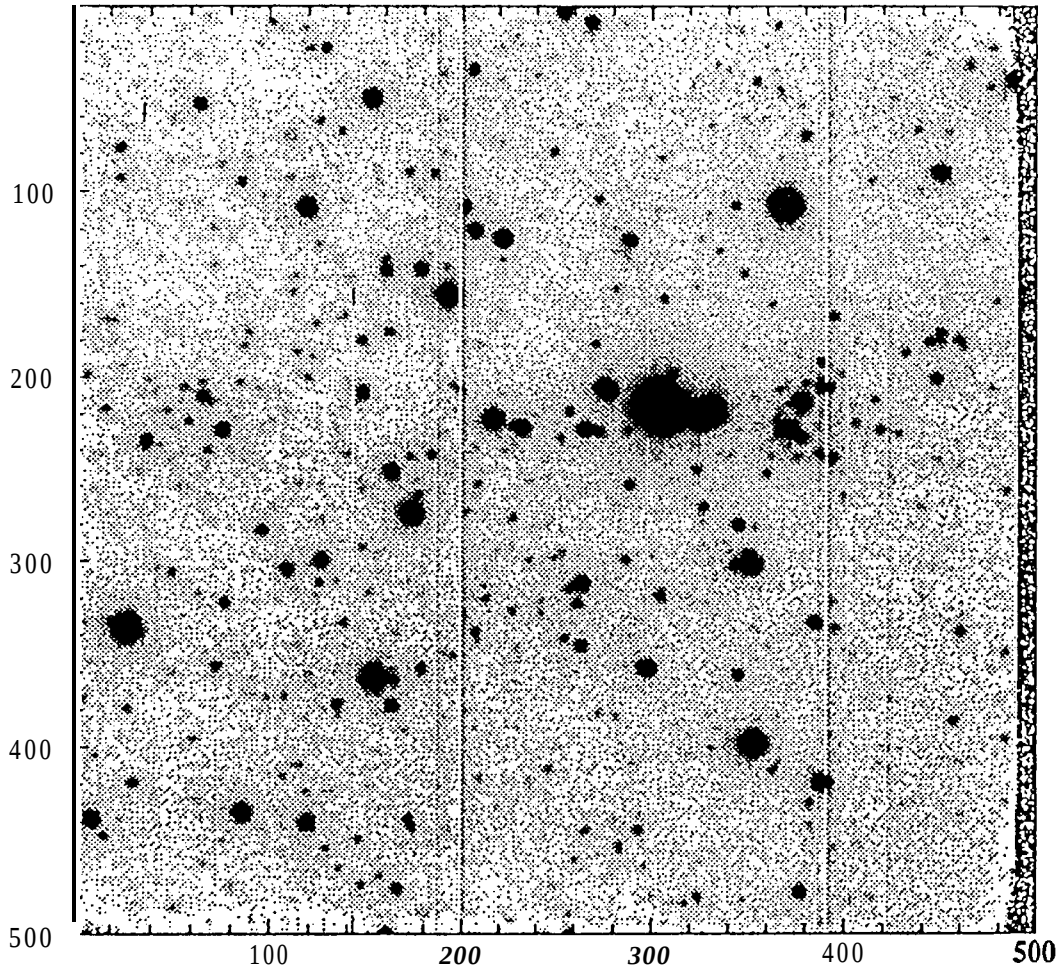

Figure ~~A.1~~ 1a: V gray scale image of LH 4. North is at the bottom and east is at the right.

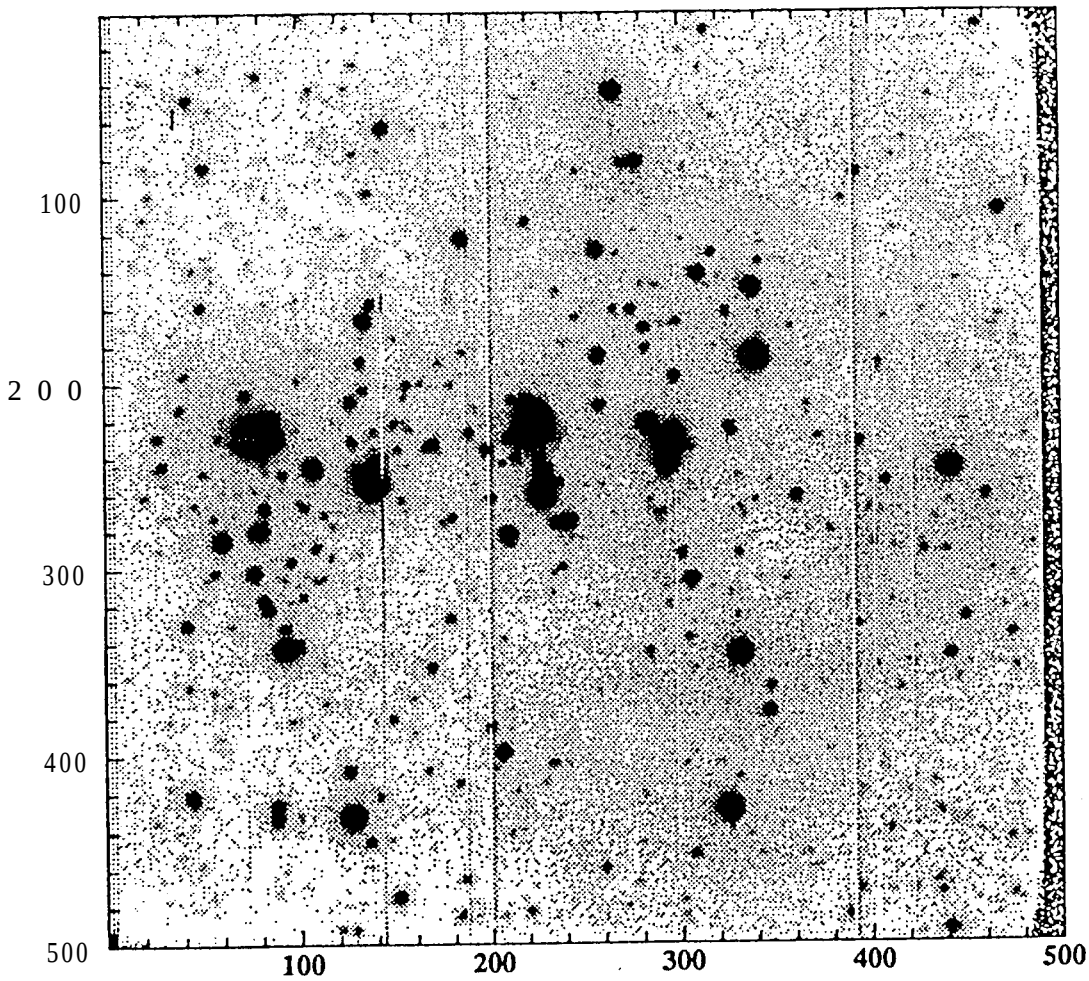

Figure ~~A.3~~ 1b: V gray scale image of LH 54. North is at the bottom and east is at the right.

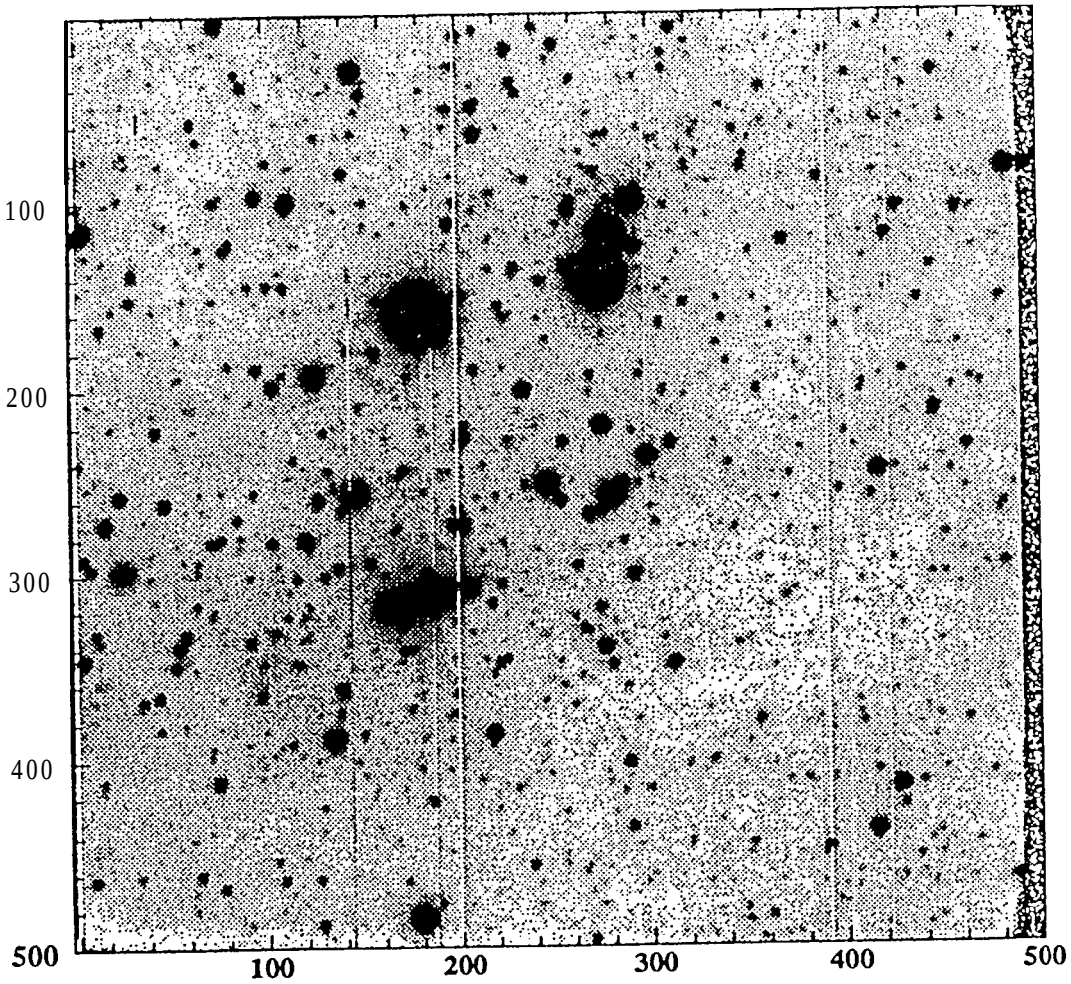

Figure ~~A.5~~ 1c: V gray scale image of LH *58.* North is at the bottom and east is at the right.

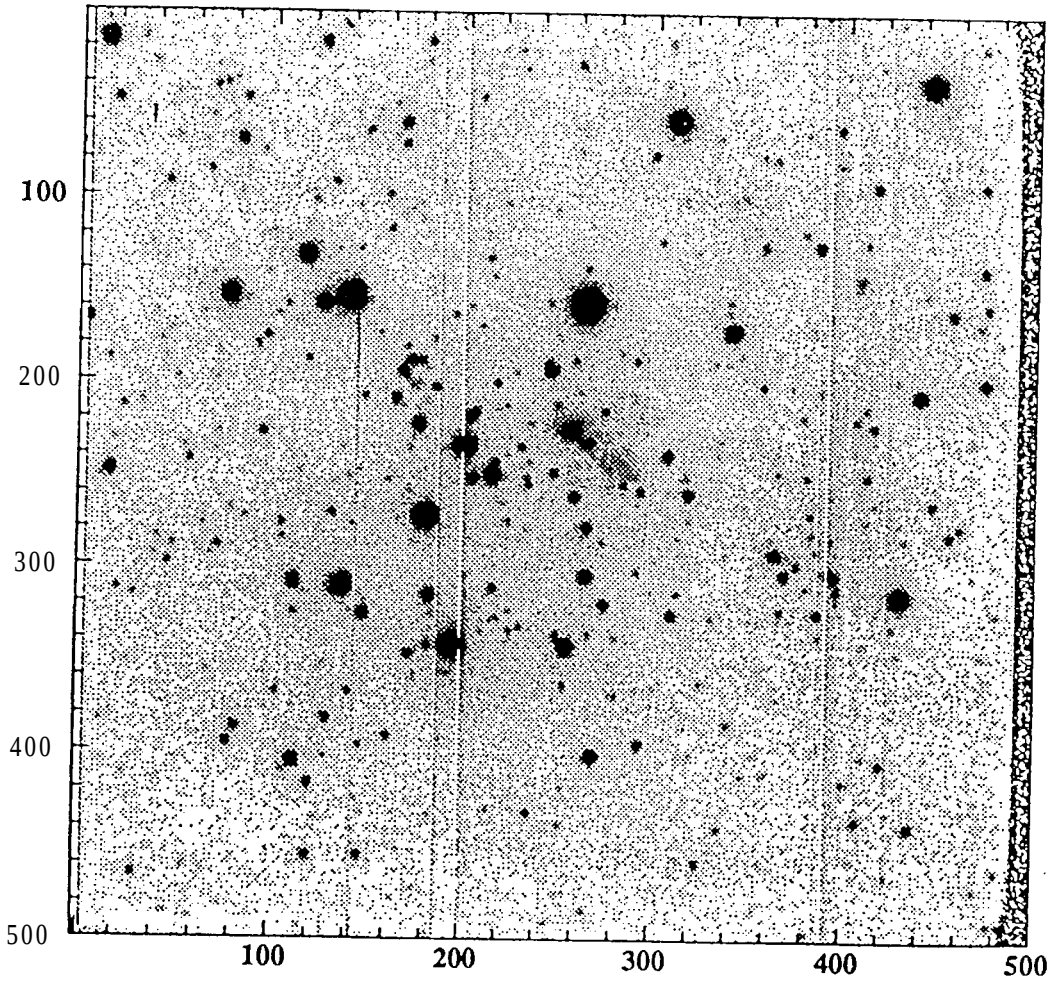

Figure ~~A.7~~ 1d: V gray scale image of LH *83.* North is at the bottom and east is at the right.

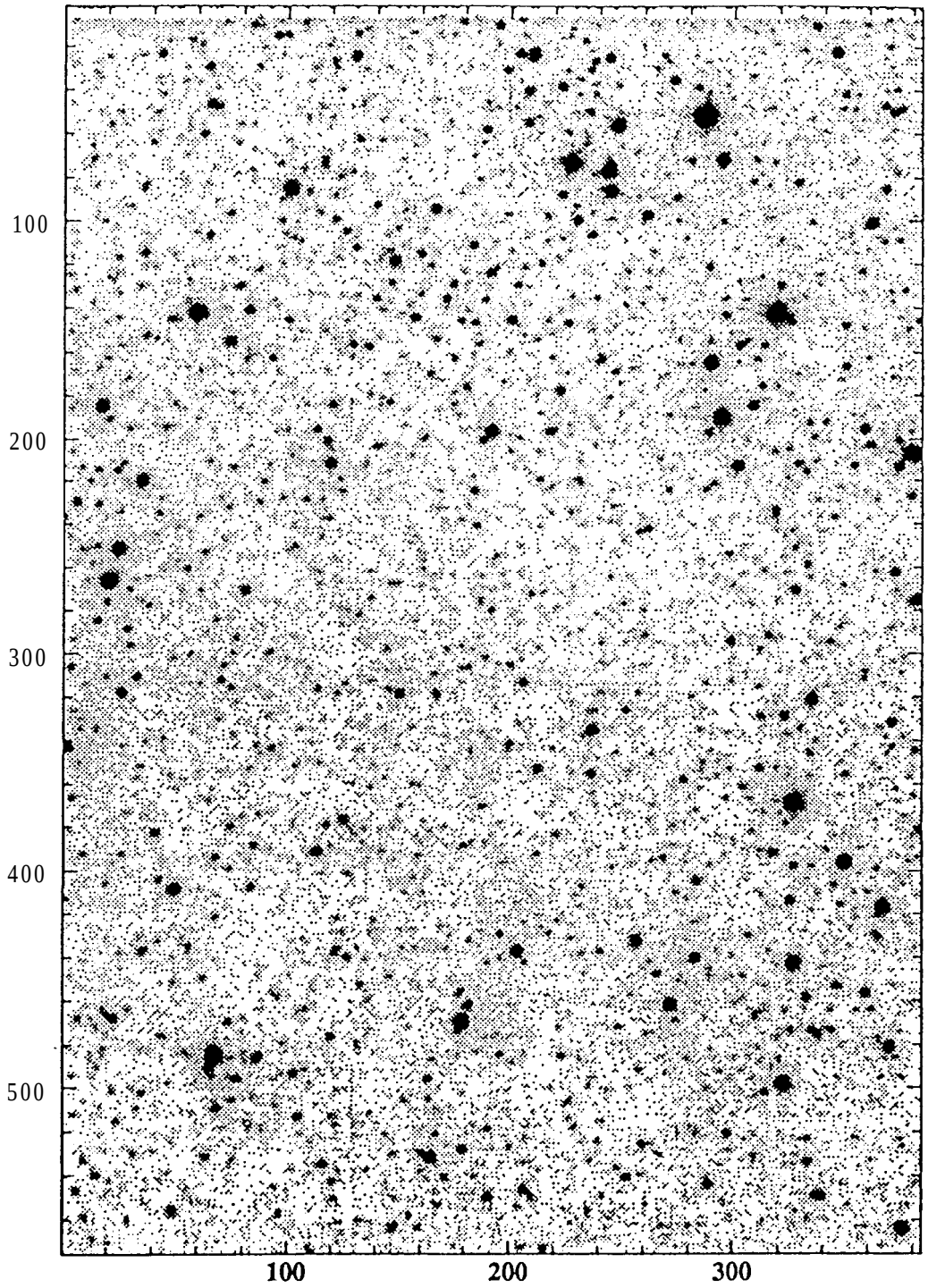

Figure ~~A.9~~ 1e: V gray scale image of LH 87. North is at the left and east is at the bottom.

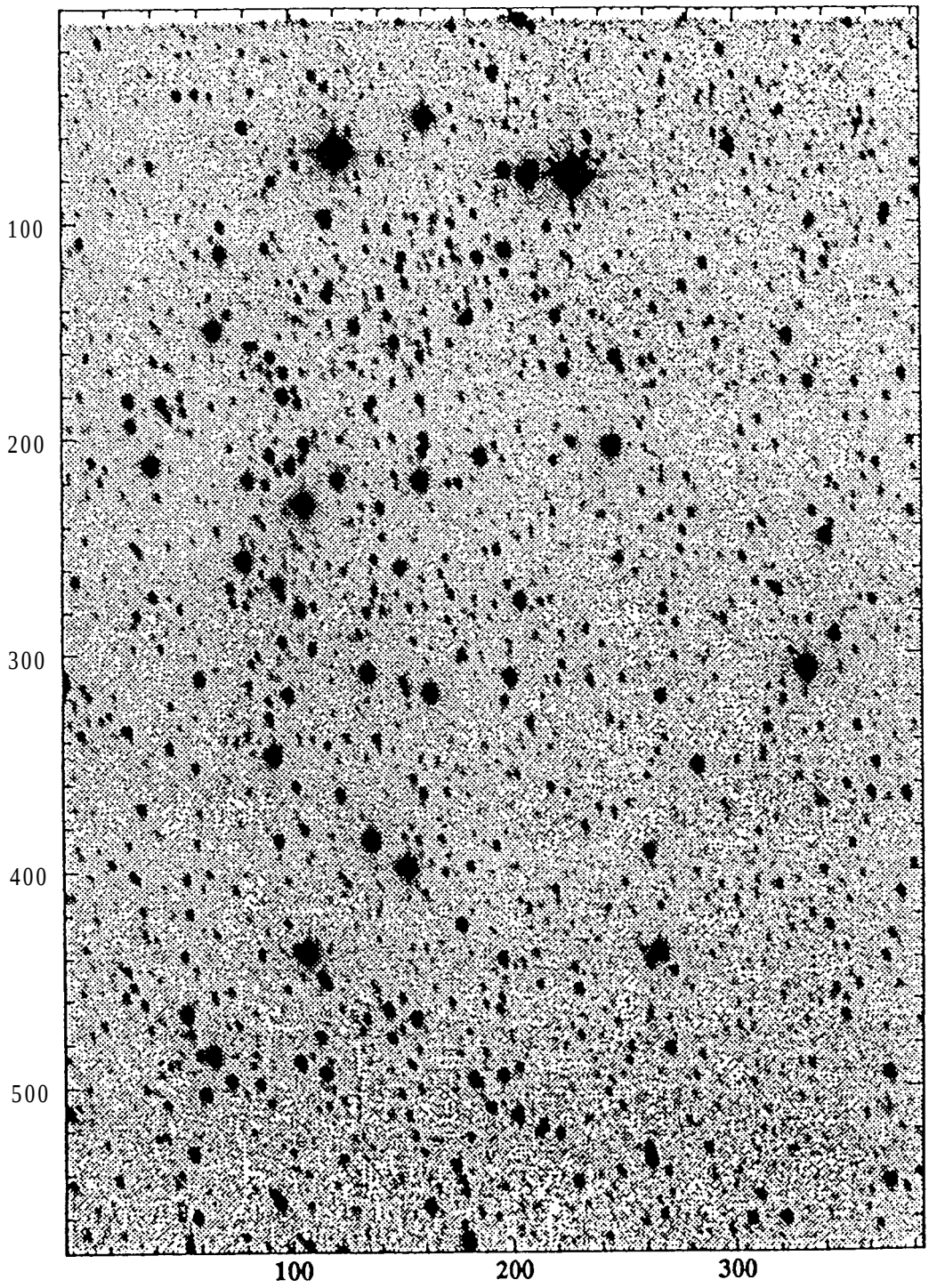

Figure ~~A.11~~ 1f: V gray scale image of LH 93. North is at the left and east is at the bottom.

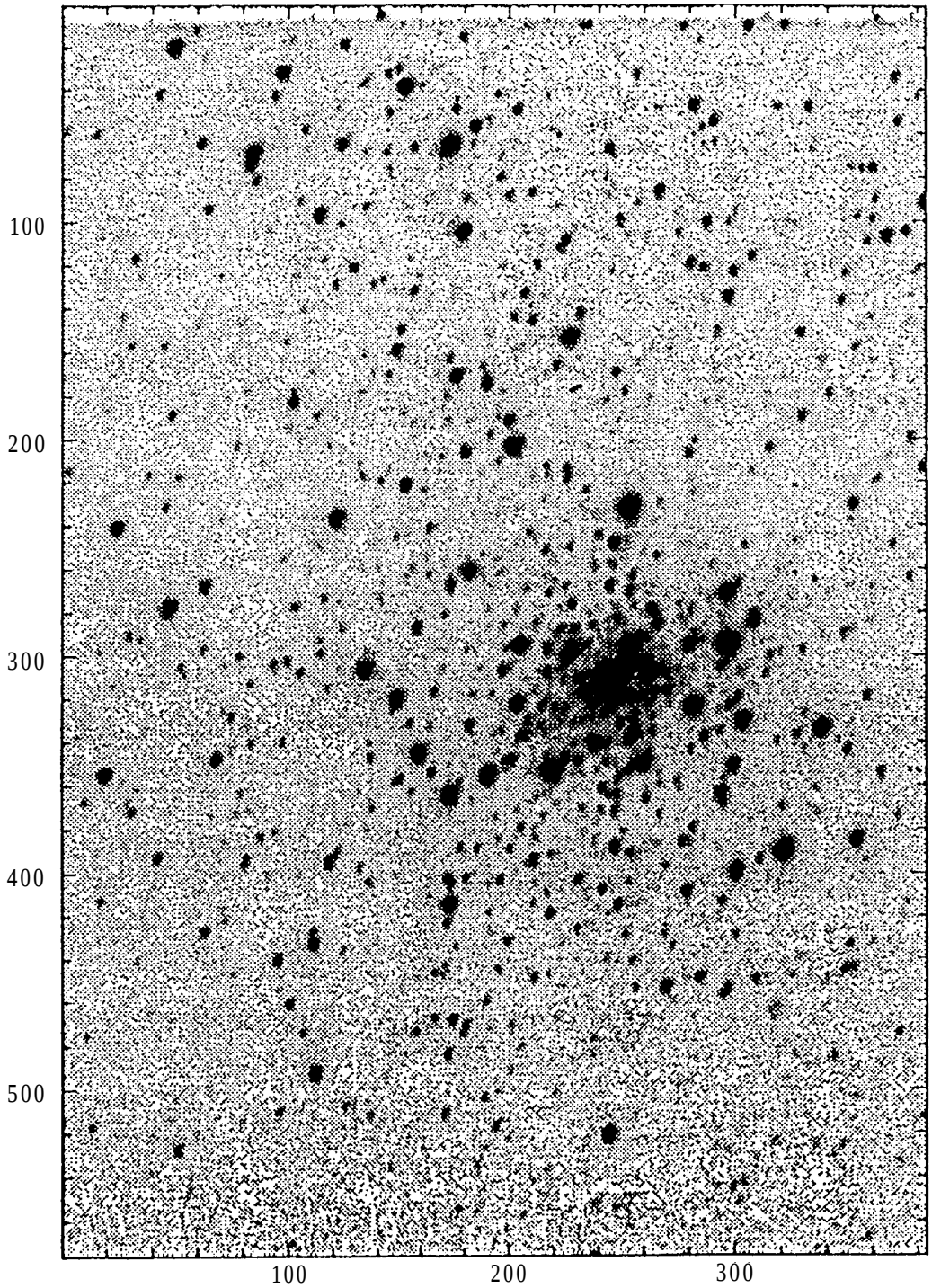

Figure ~~A.13~~ 1g: V gray scale image of LH 111. North is at the left and east is at the bottom.

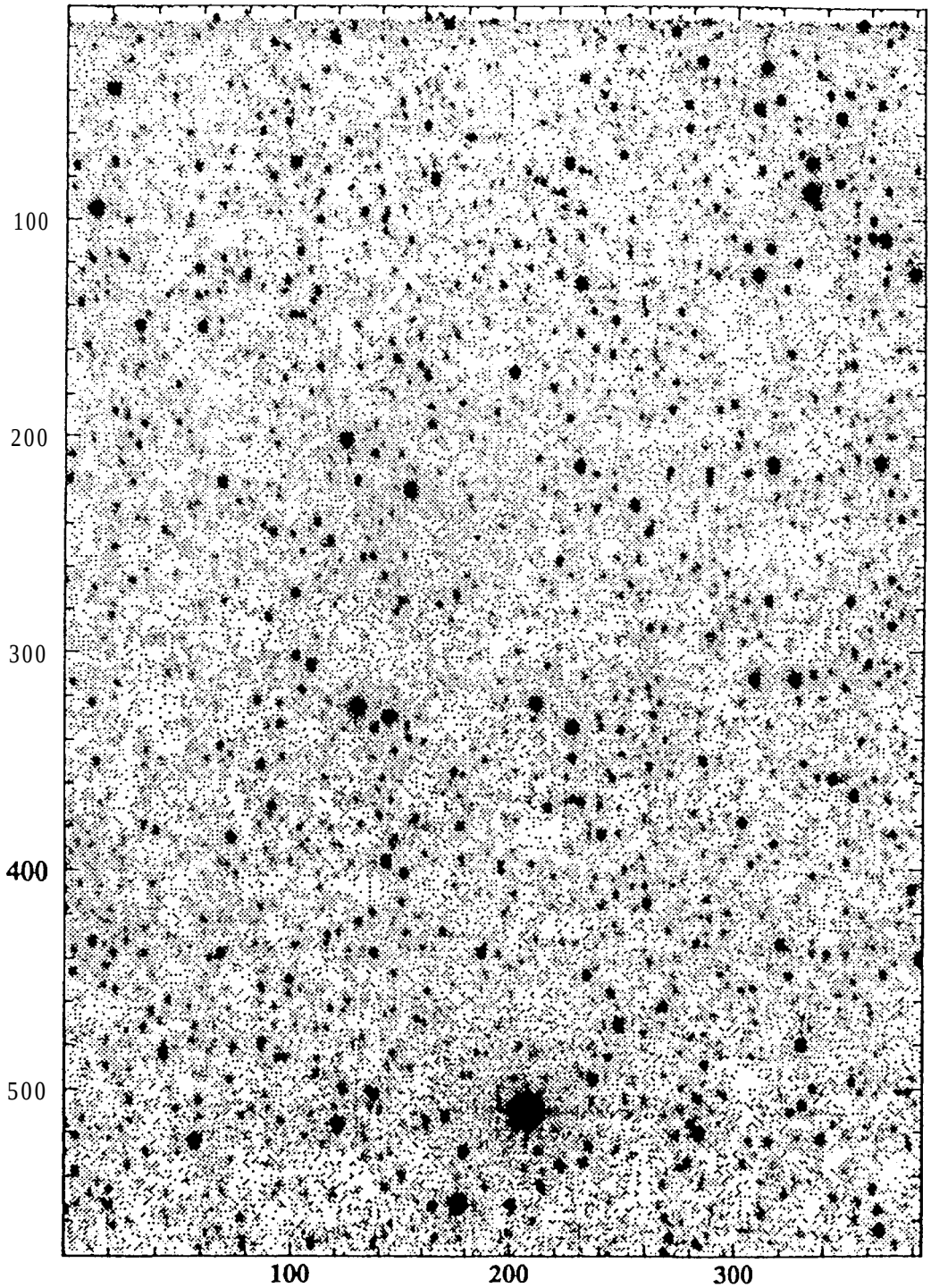

Figure ~~A.15~~ 1h: V gray scale image of N 24. North is at the left and east is at the bottom.

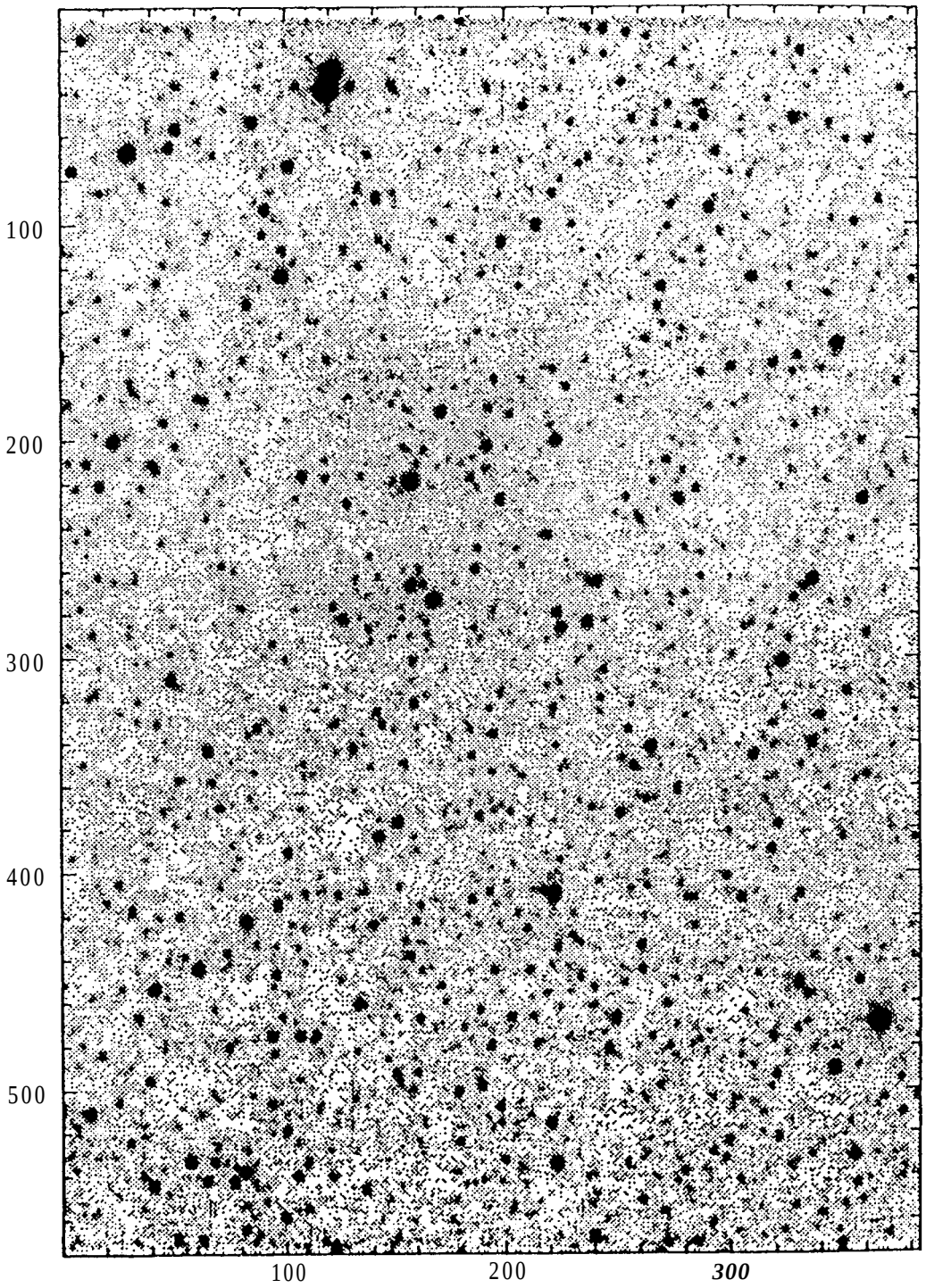

Figure ~~A.17~~ 1i: V gray scale image of NGC 249. North is at the left and east is at the bottom.

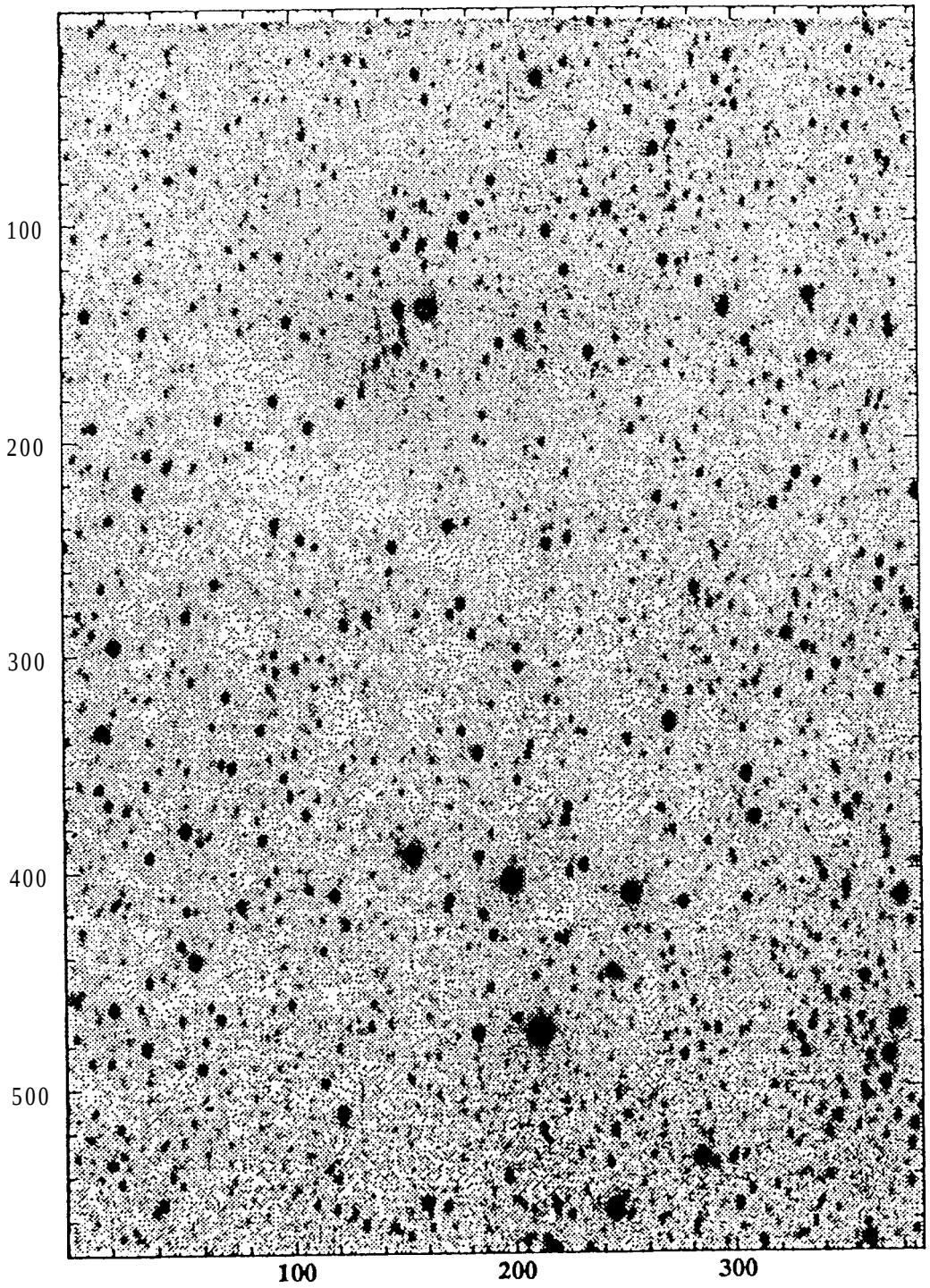

Figure ~~A.19~~ 1j: V gray scale image of NGC 261. North is at the left and east is at the bottom.

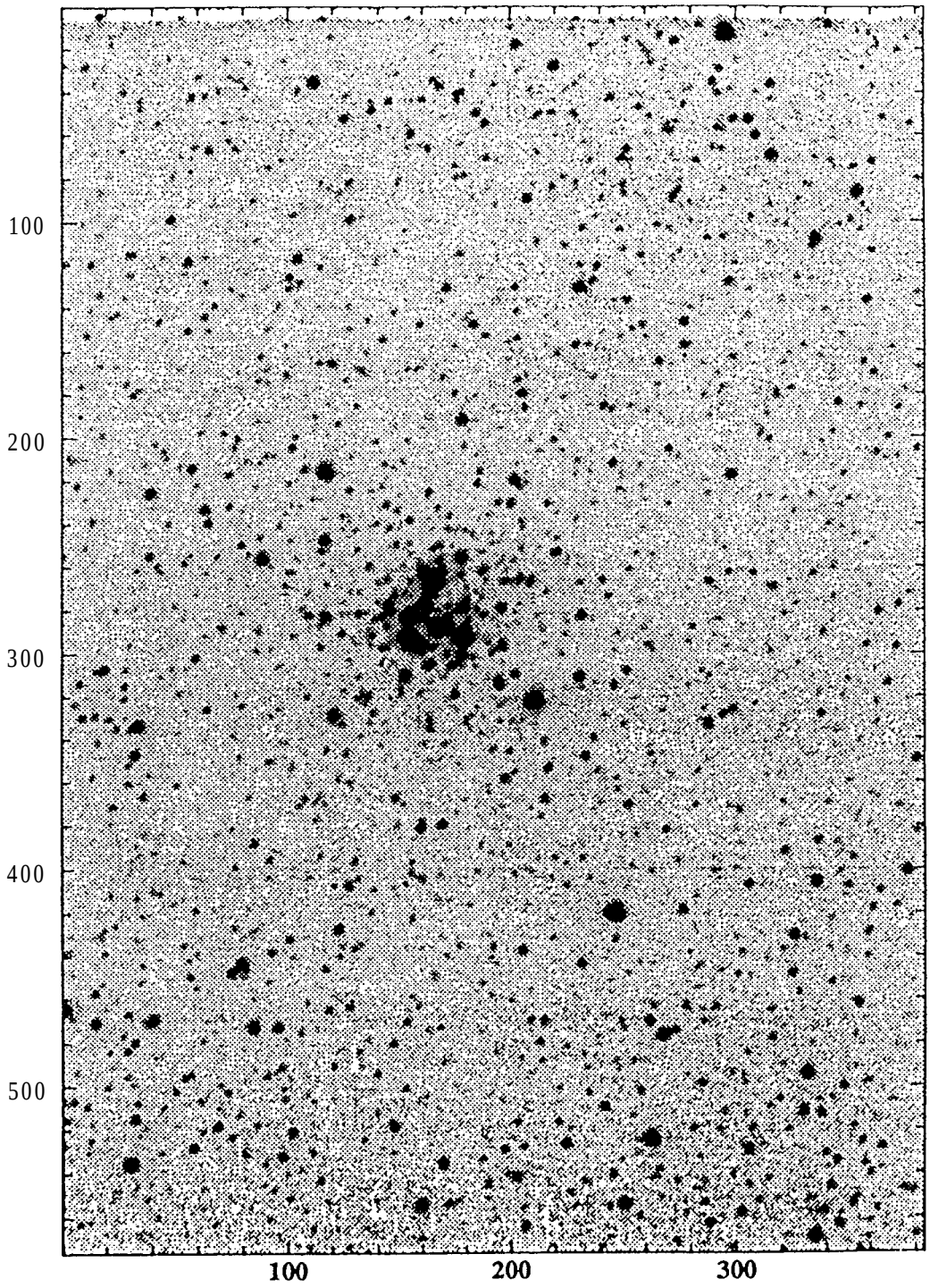

1k

Figure ~~A.21~~: V gray scale image of NGC 376. North is at the left and east is at the bottom.

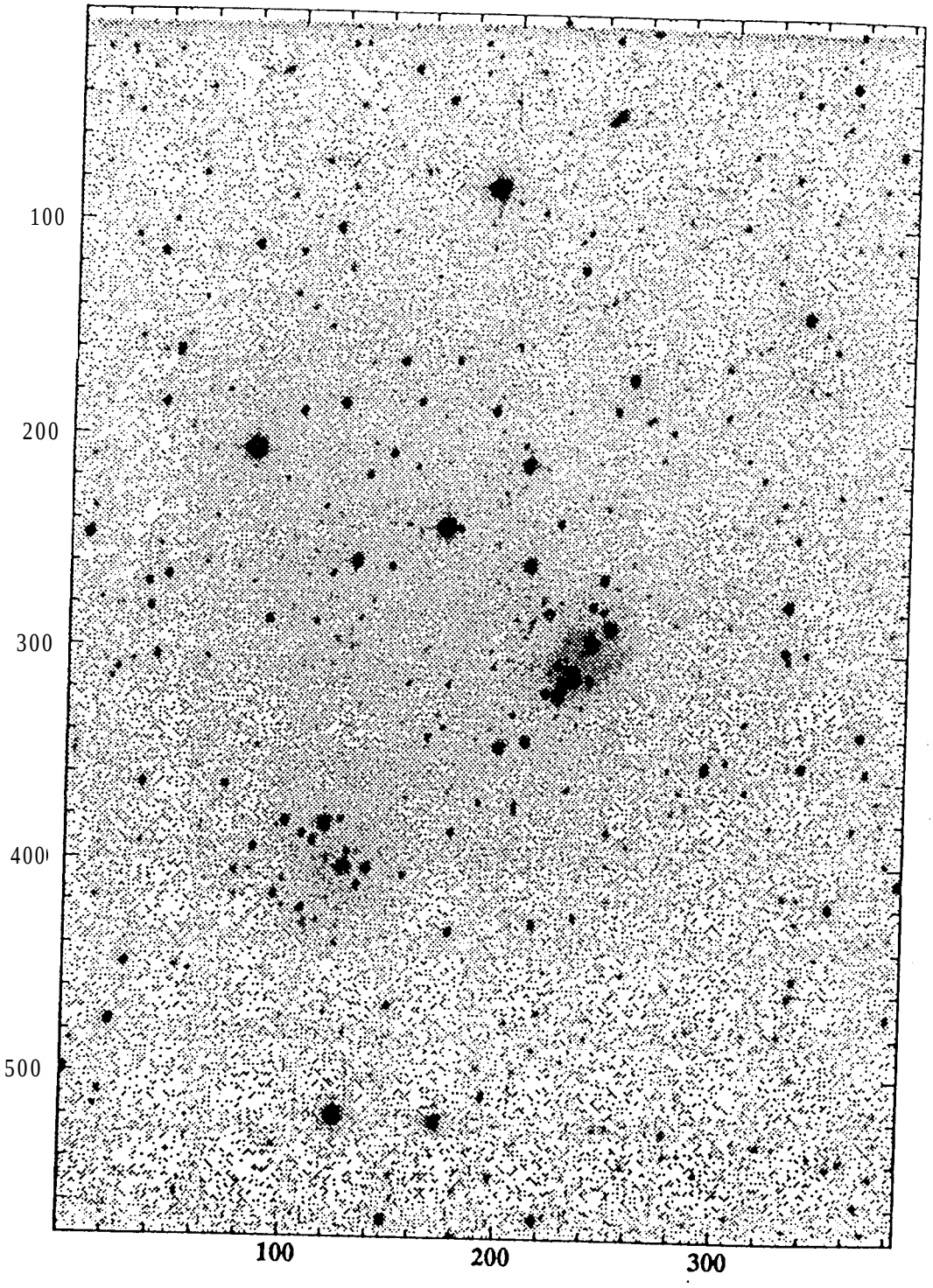

Figure ~~A.23~~ 1l: V gray scale image of NGC 456. North is at the left and east is at the bottom.

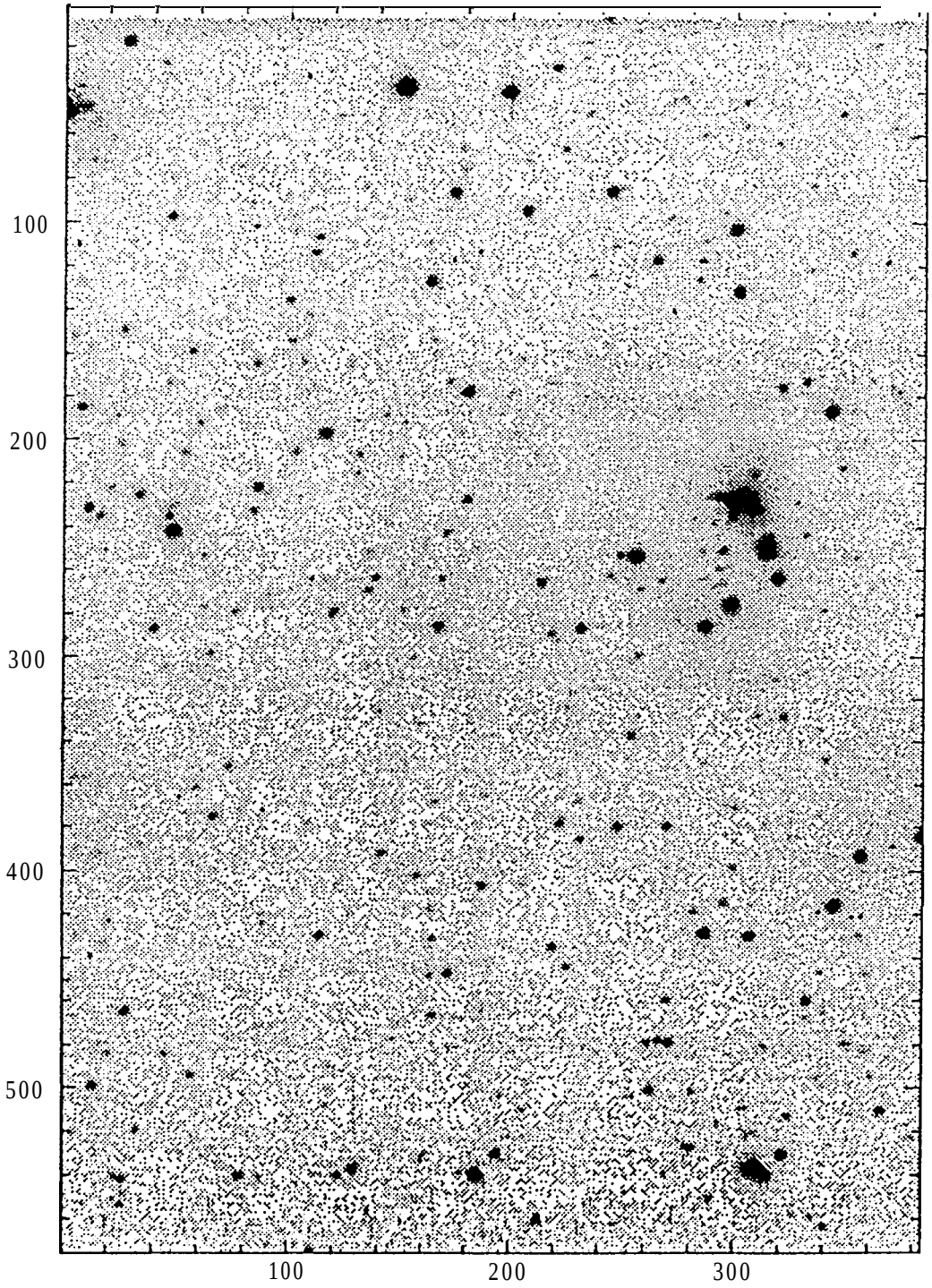

1m

Figure ~~A.25~~: V gray scale image of NGC 460(N). North is at the left and east is at the bottom.

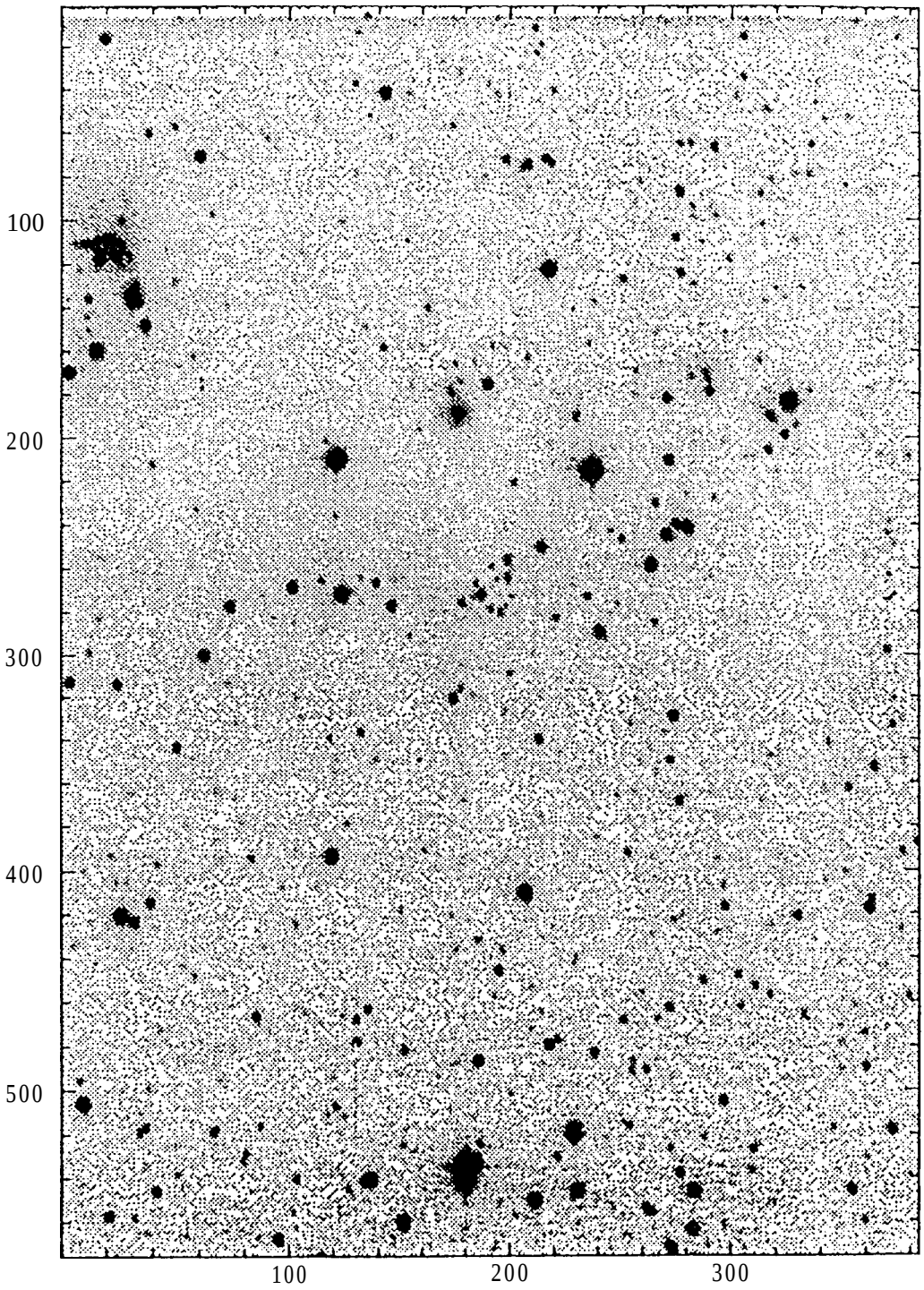

Figure ~~A.~~26: V gray scale image of NGC *460(S).* North is at the left and east is at the bottom.

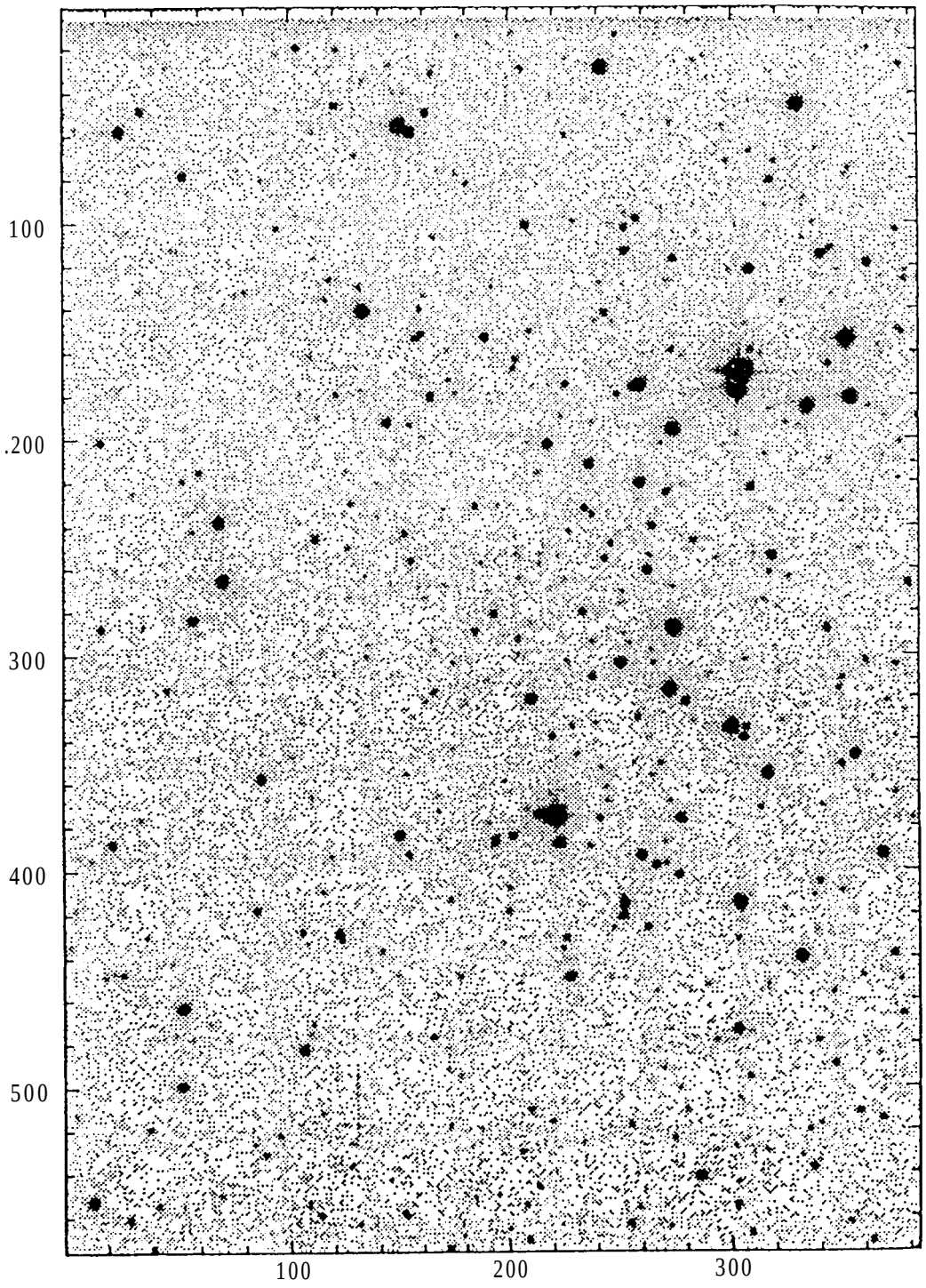

Figure ~~A.28~~ 10: V gray scale image of NGC 465(N). North is at the left and east is at the bottom.

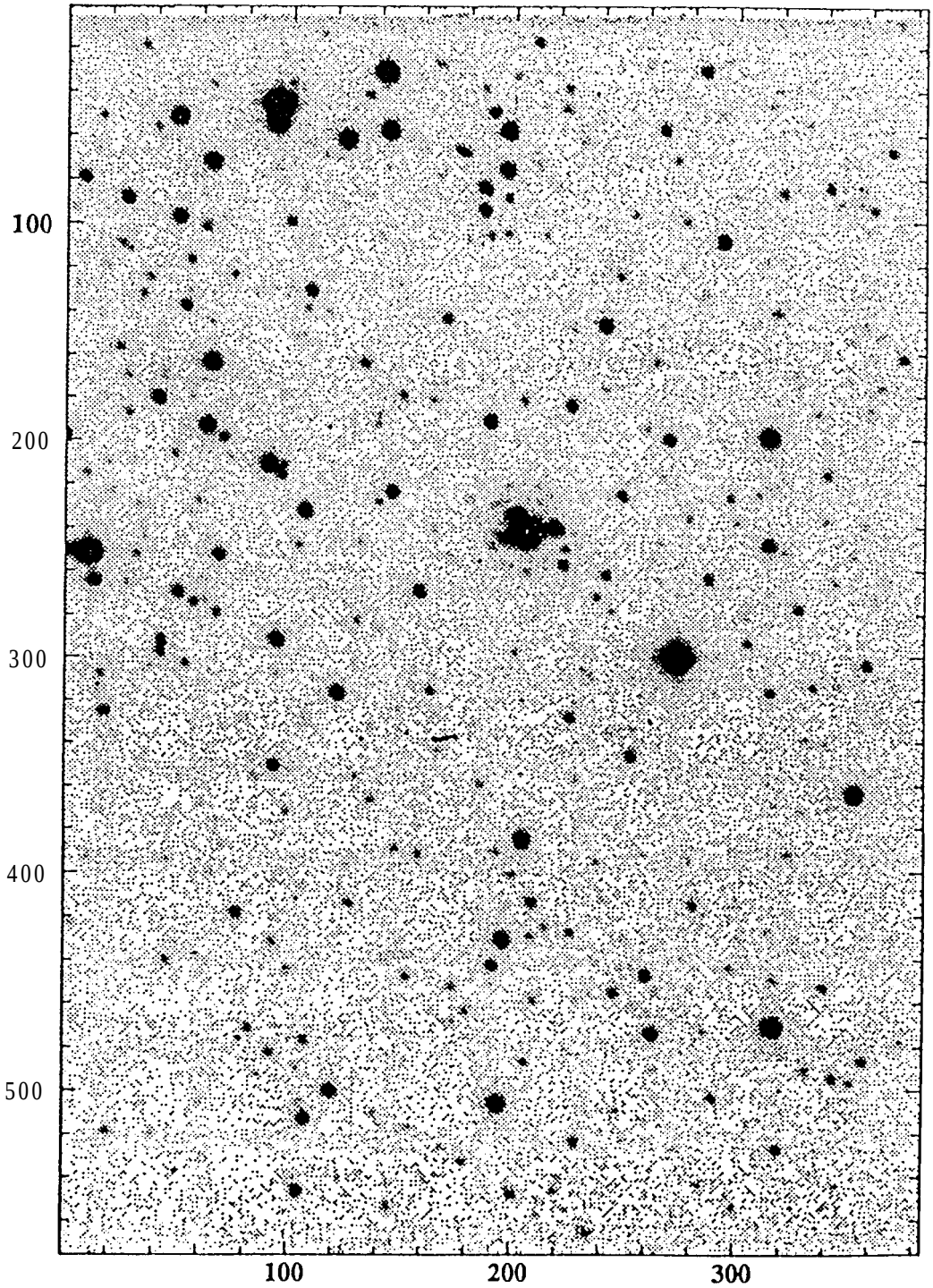

Figure ~~A.29~~ 1p: V gray scale image of NGC 465(S). North is at the left and east is at the bottom.

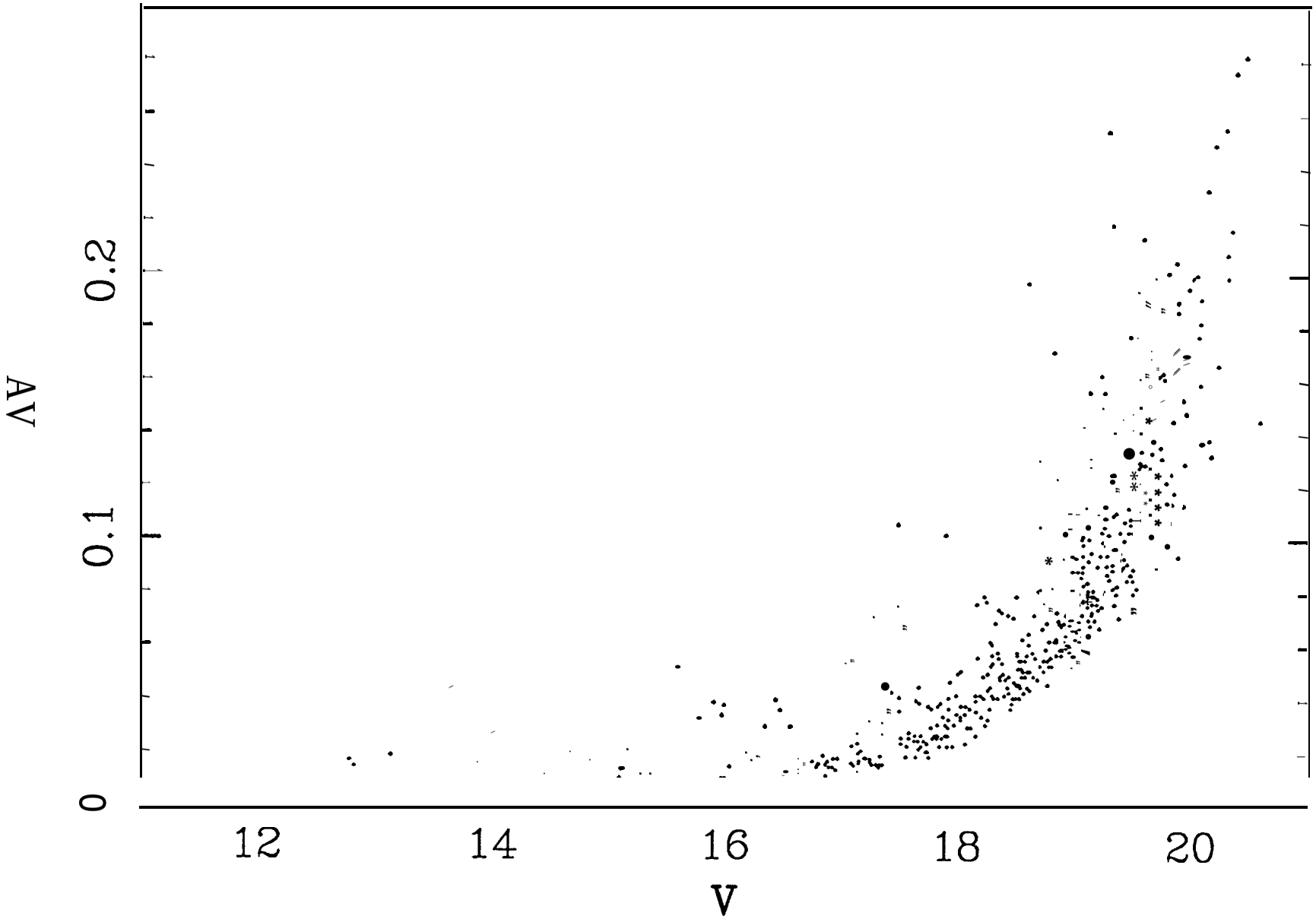
AV
0.2
0.1
0
12
14
16
18
20
V

Figure 3

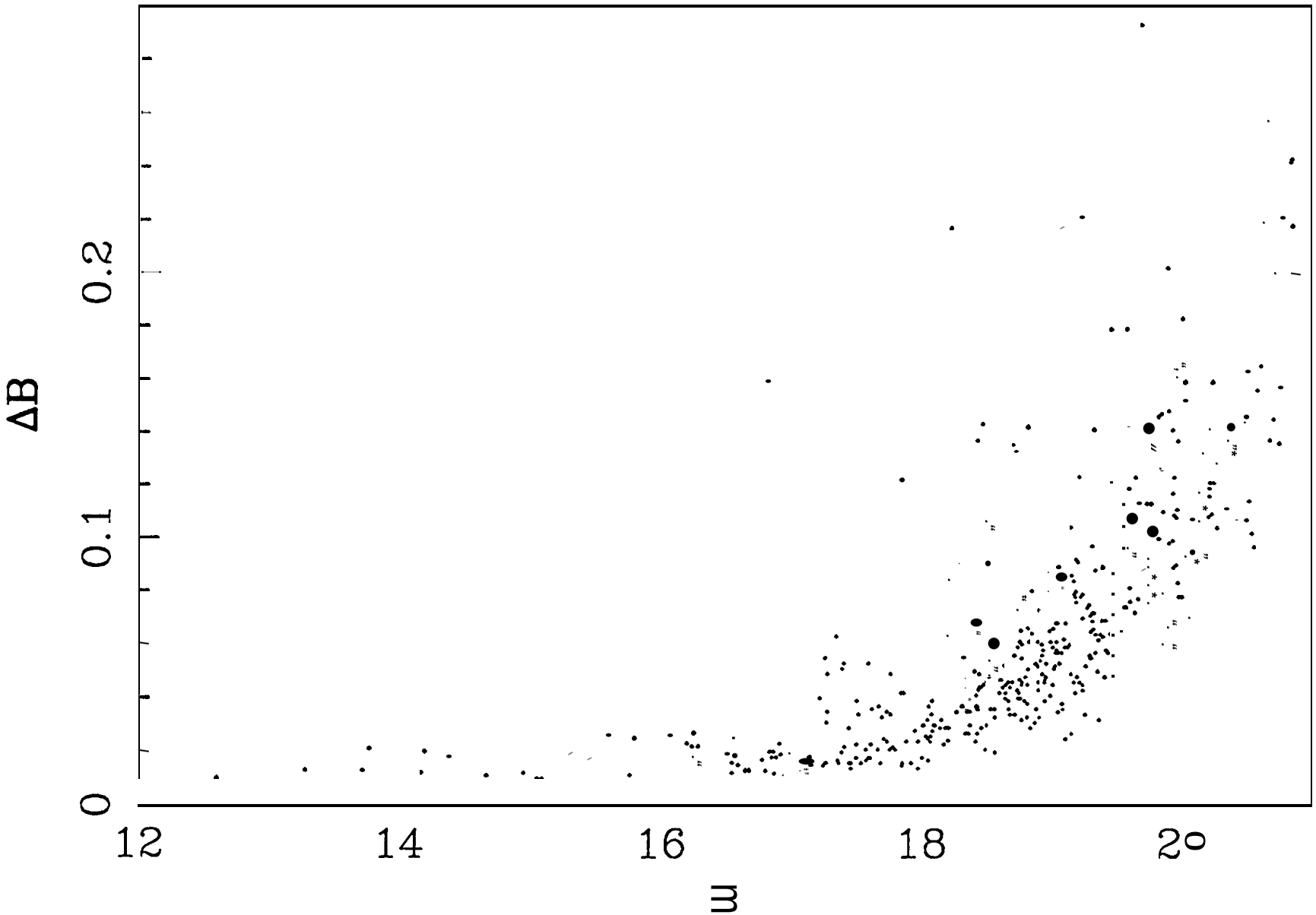

Figure 4

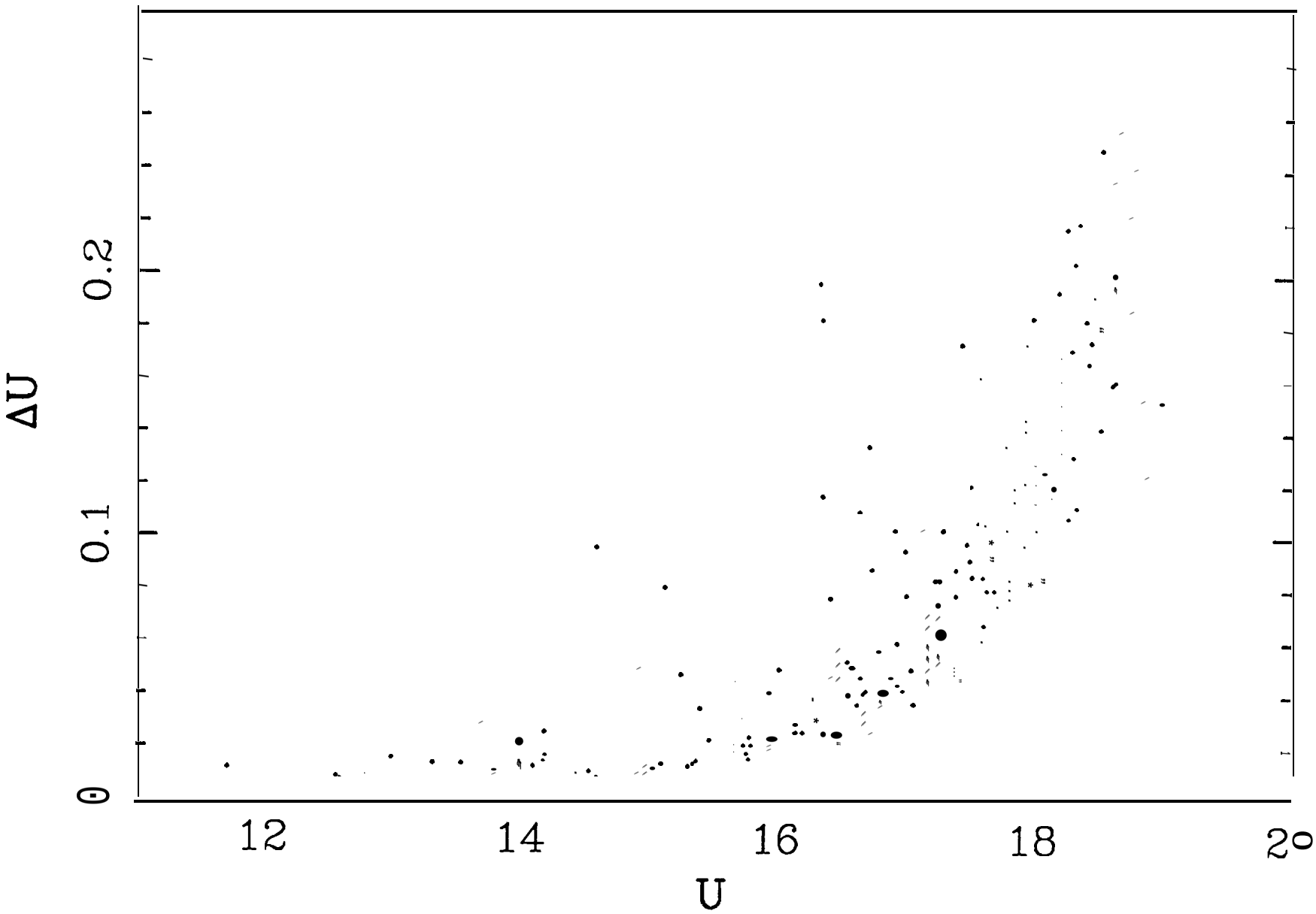

Figure 5

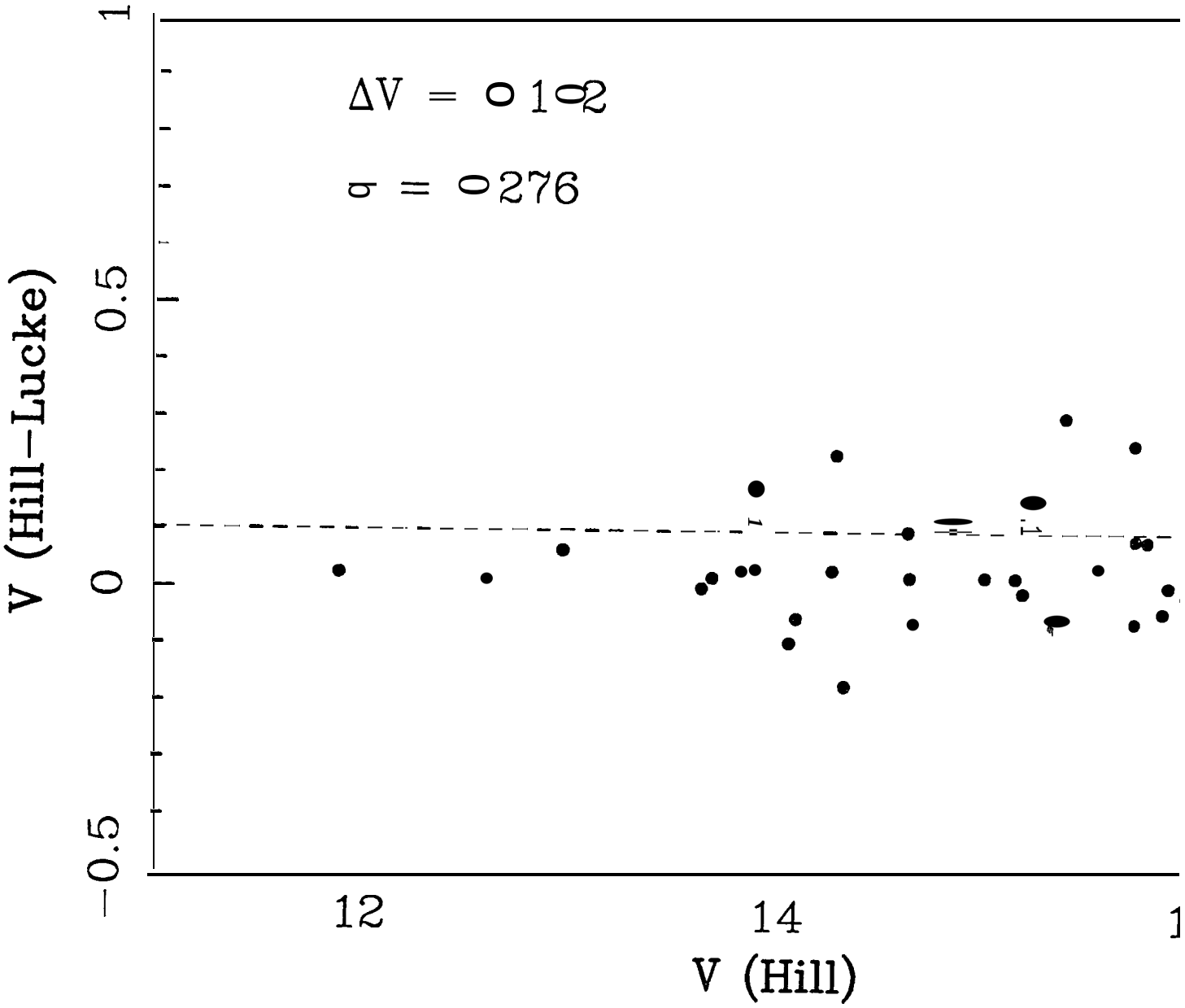

Figure 6

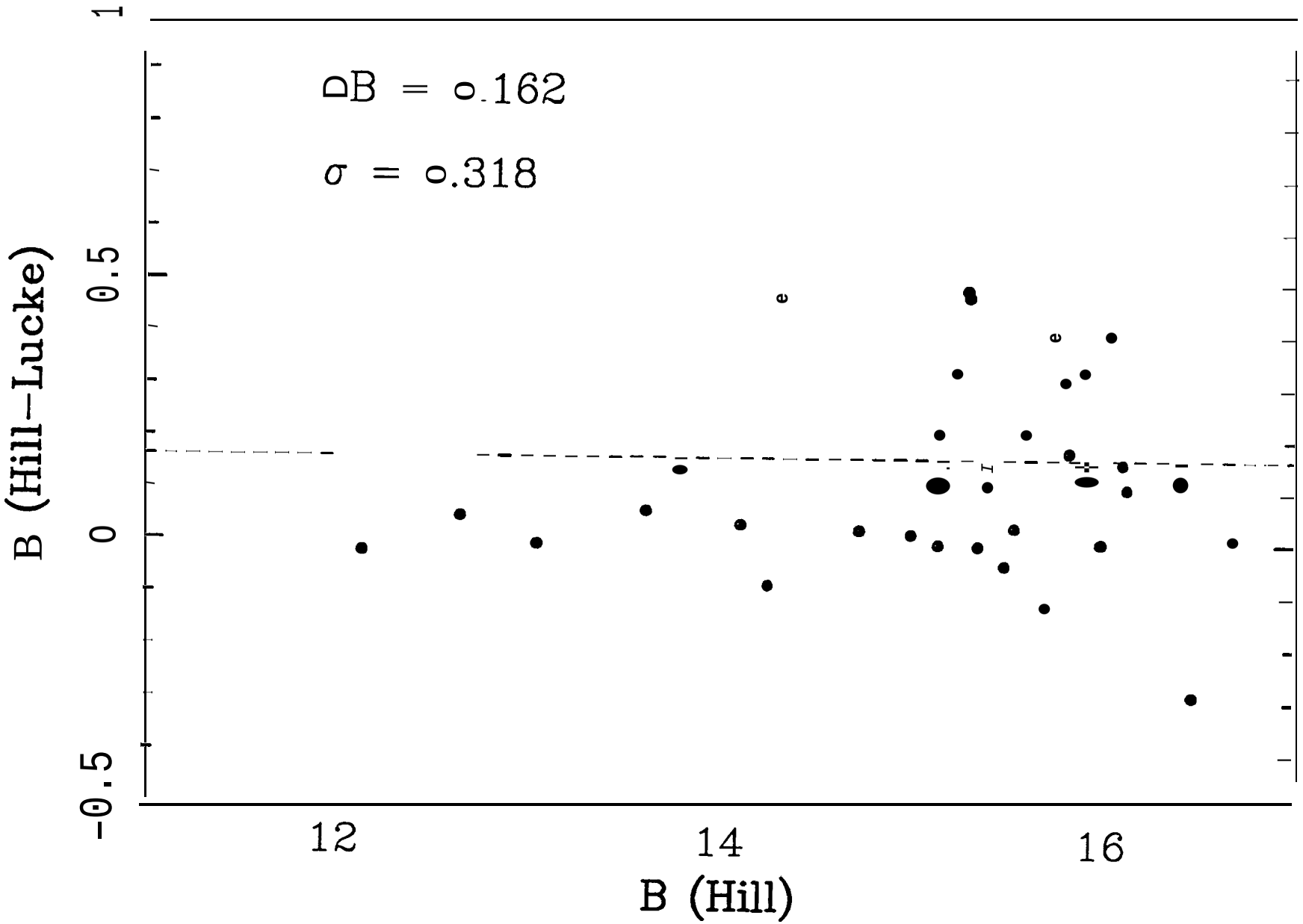

Figure 1

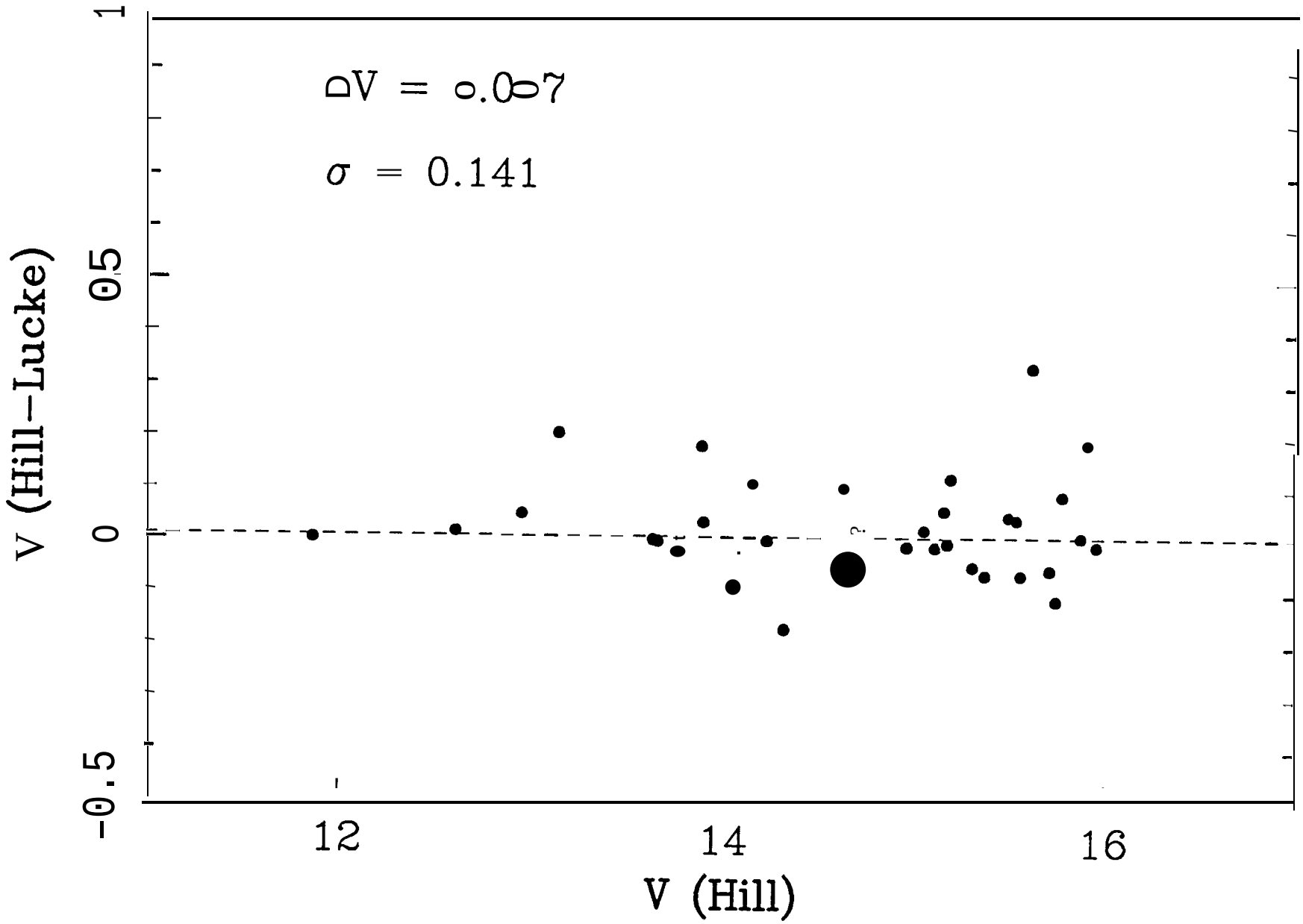

Figure 8

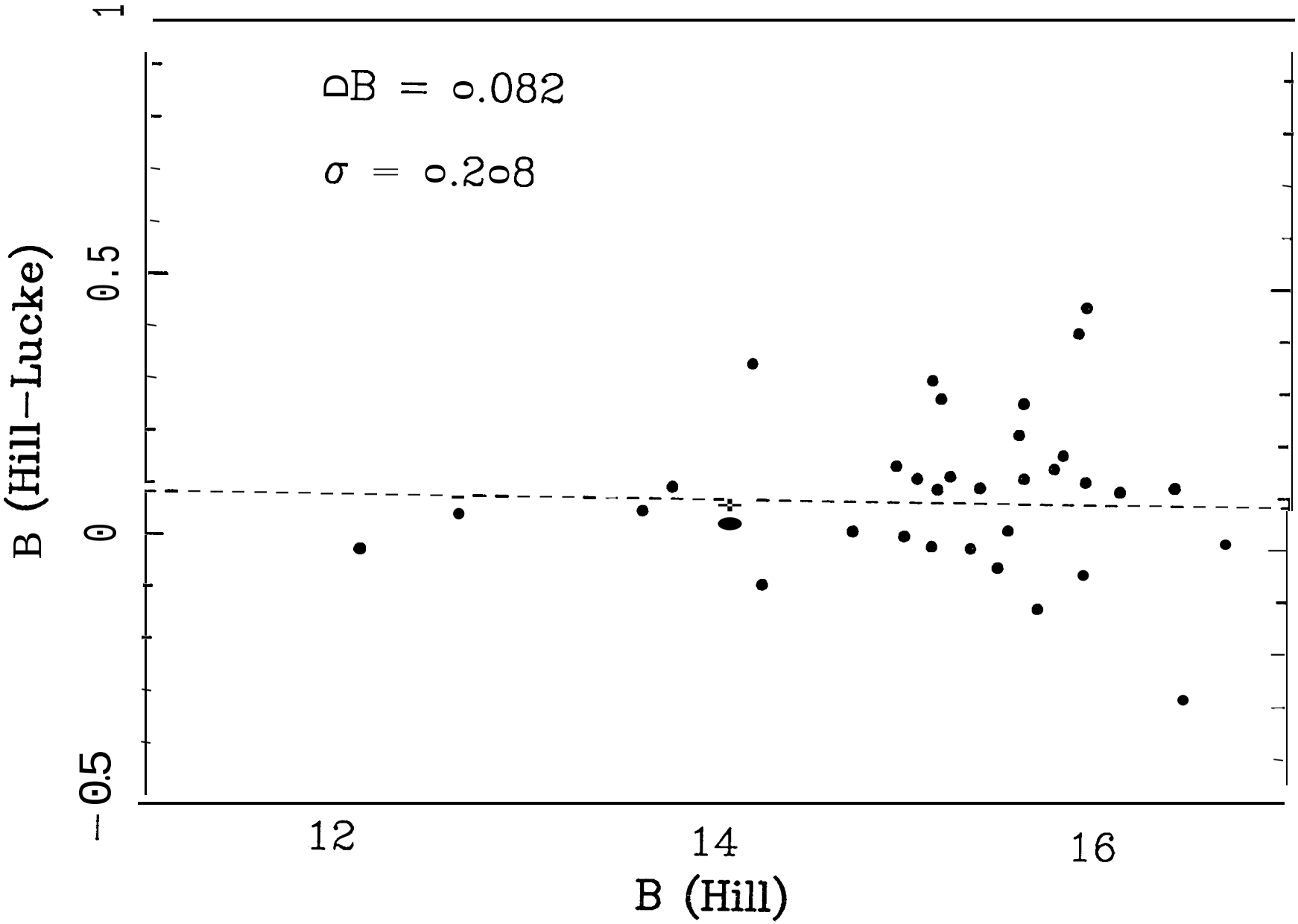

Figure 9

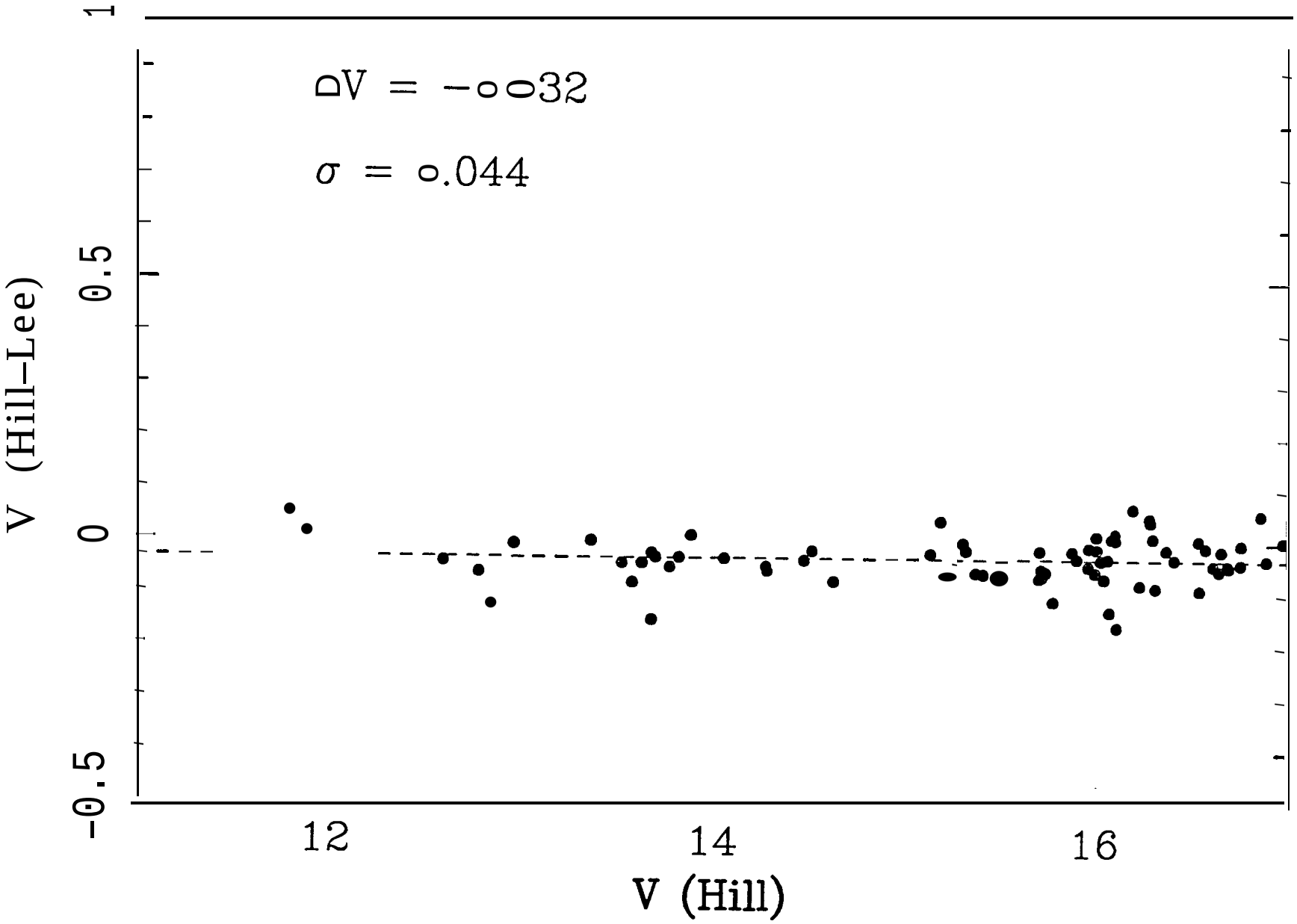

Figure 10

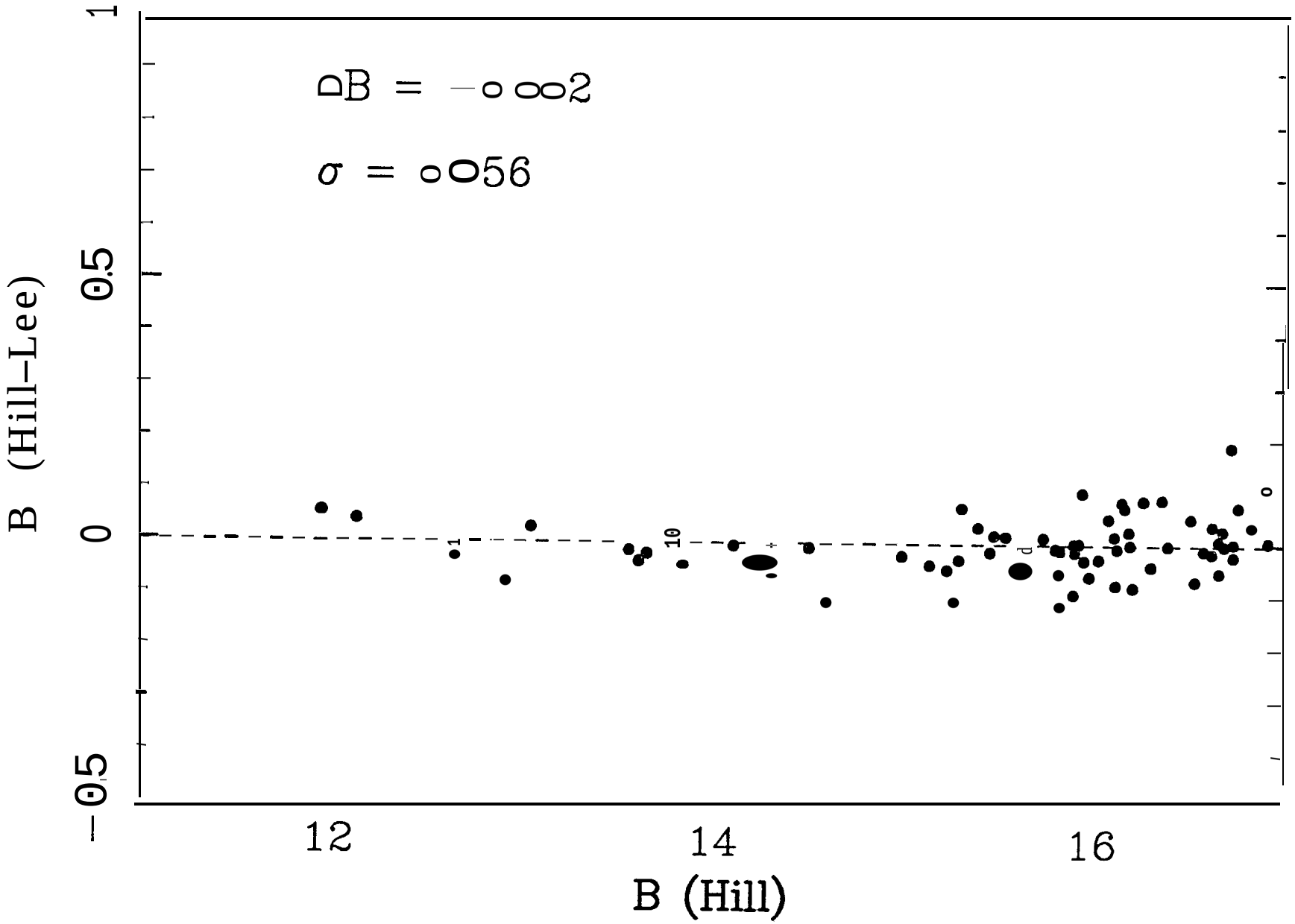

Figure -

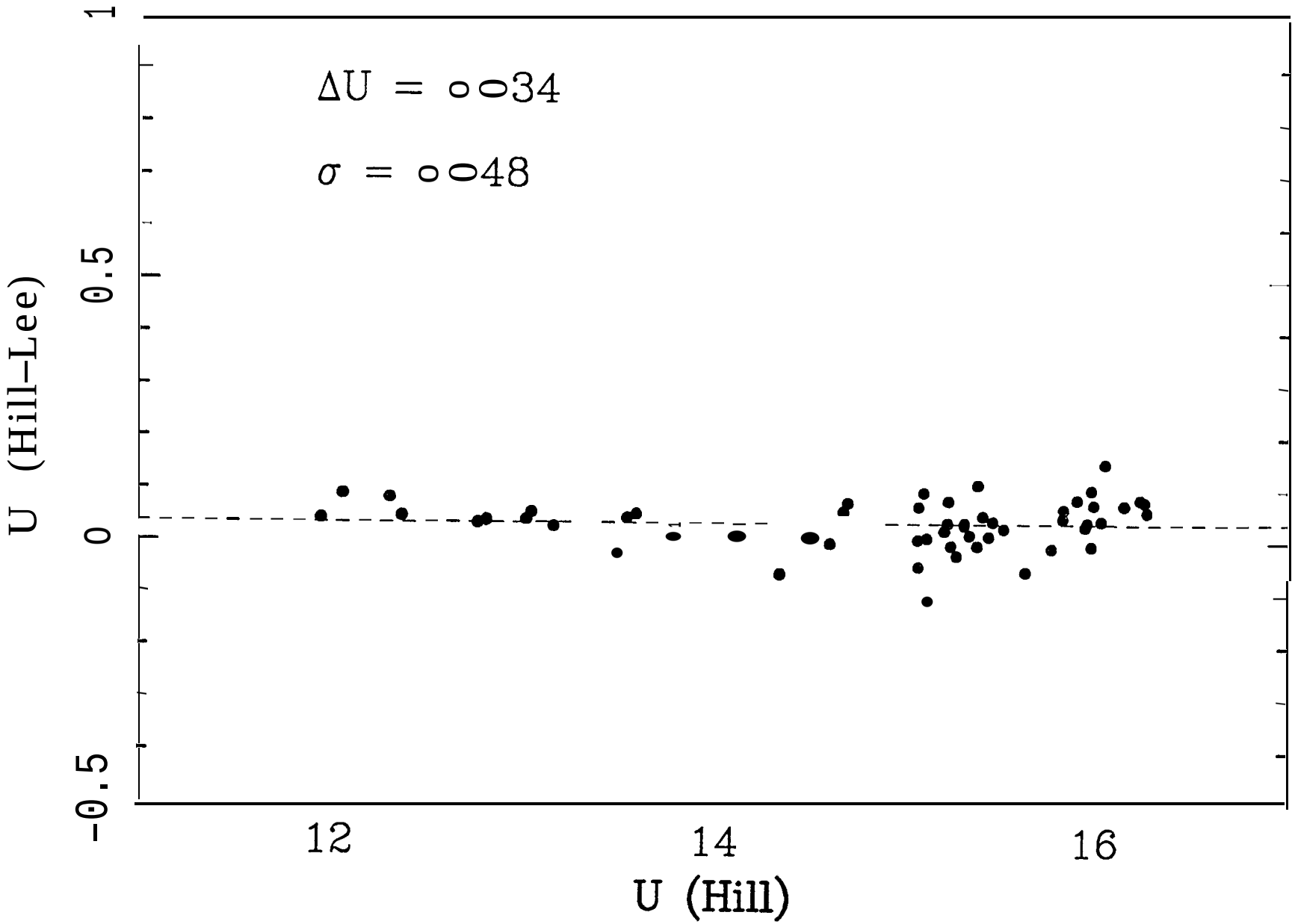

Figure 12

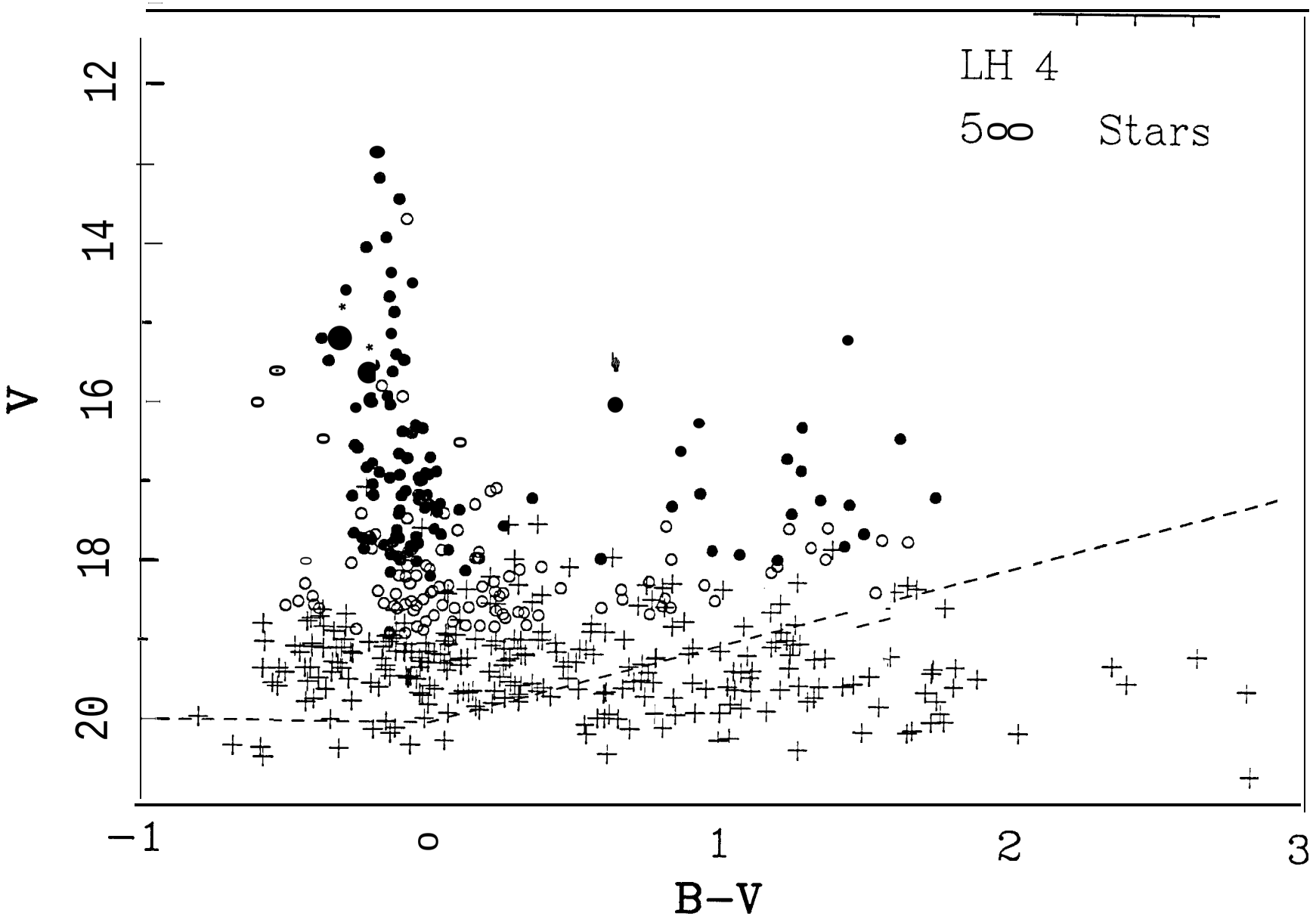

Figure 13

Figure 14

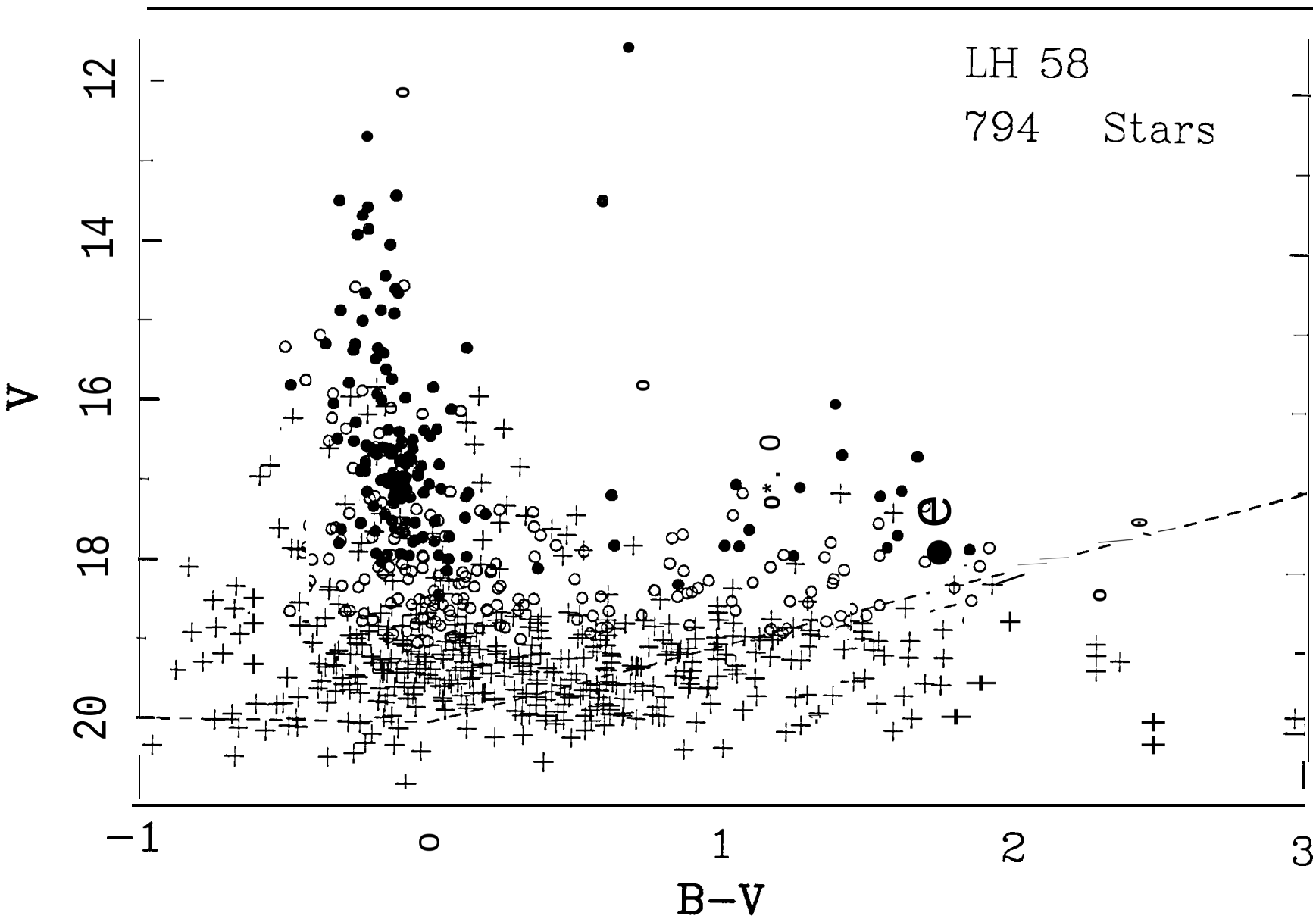

Figure 15

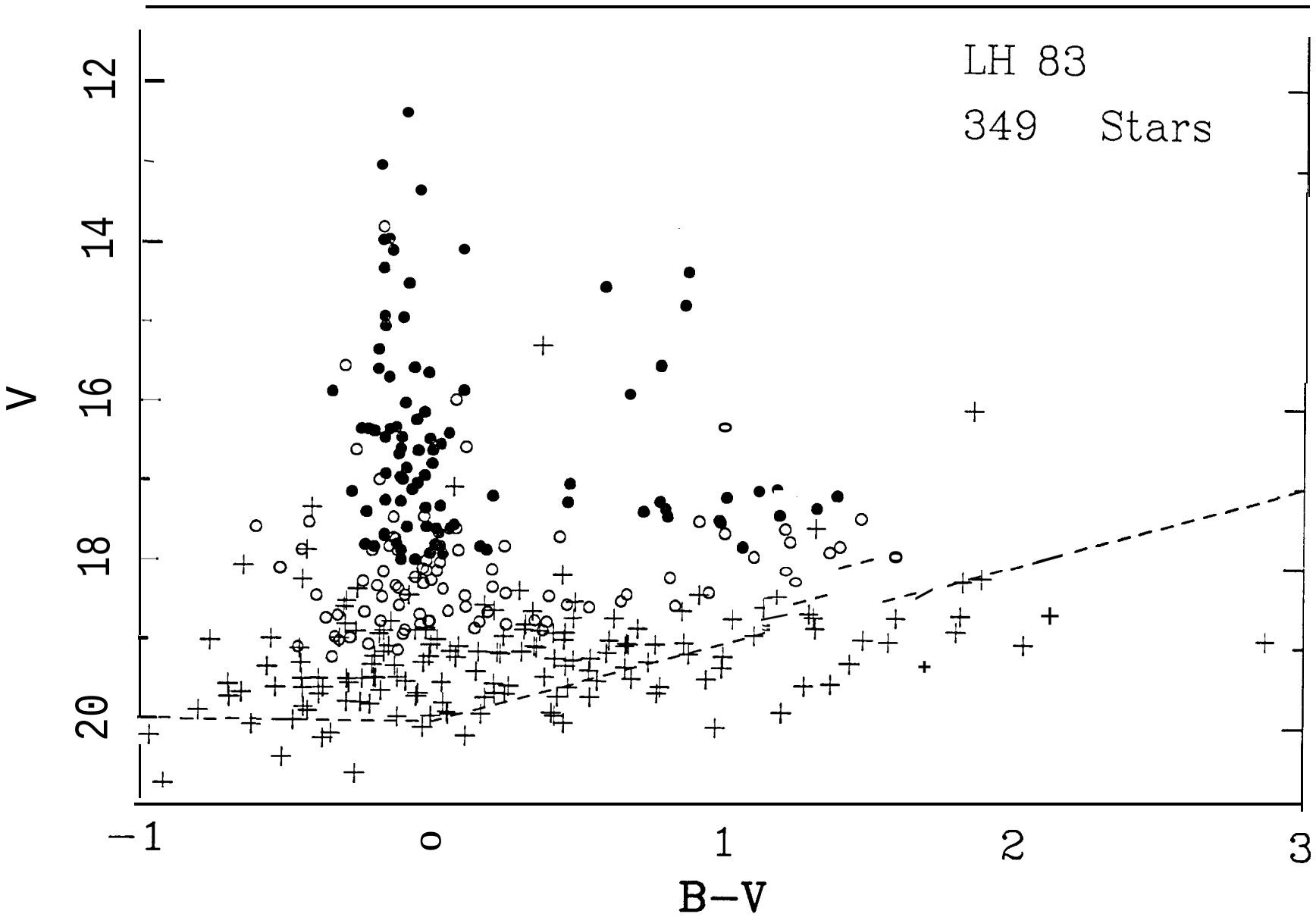

Figure 16

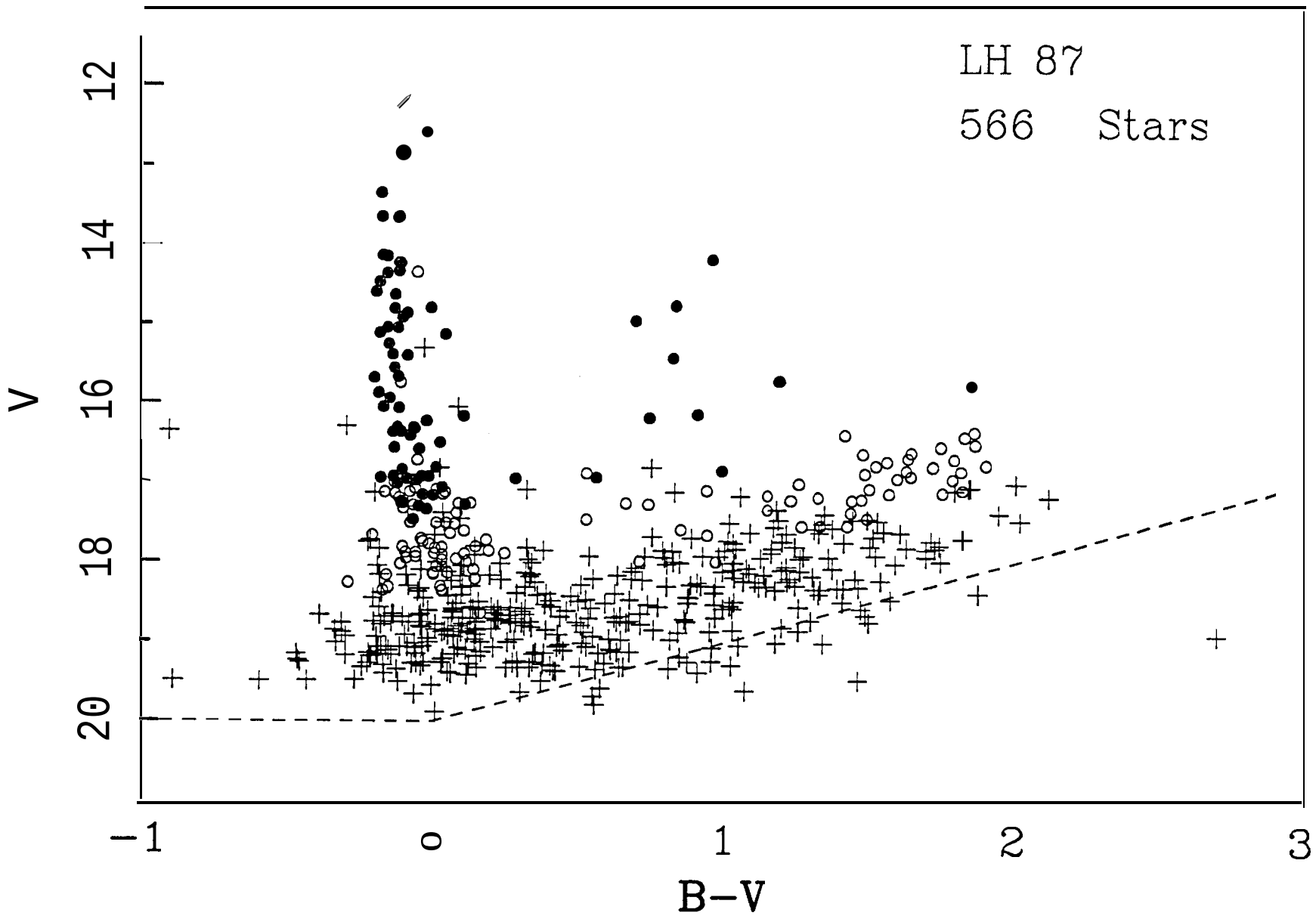

Figure

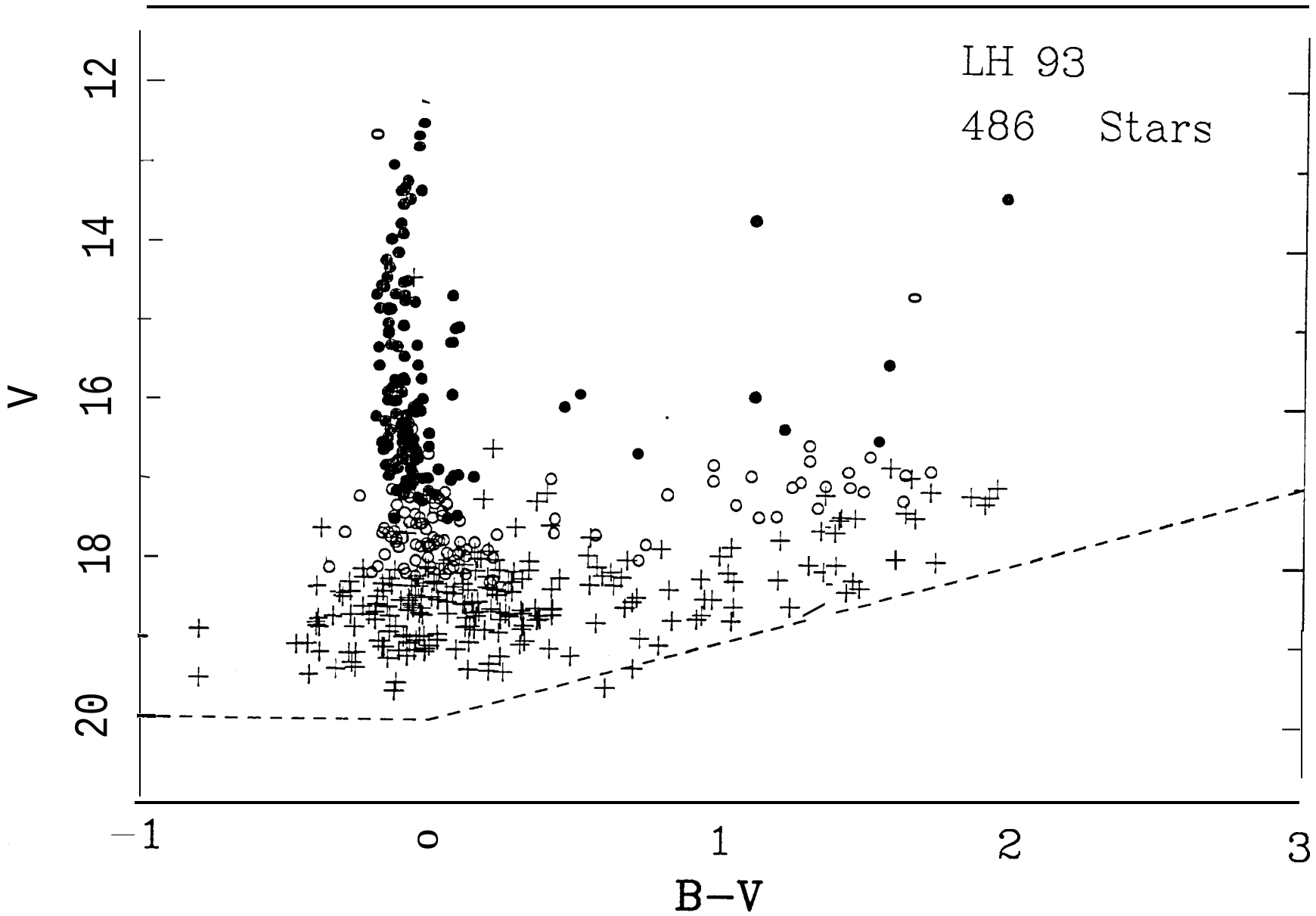

Figure 18

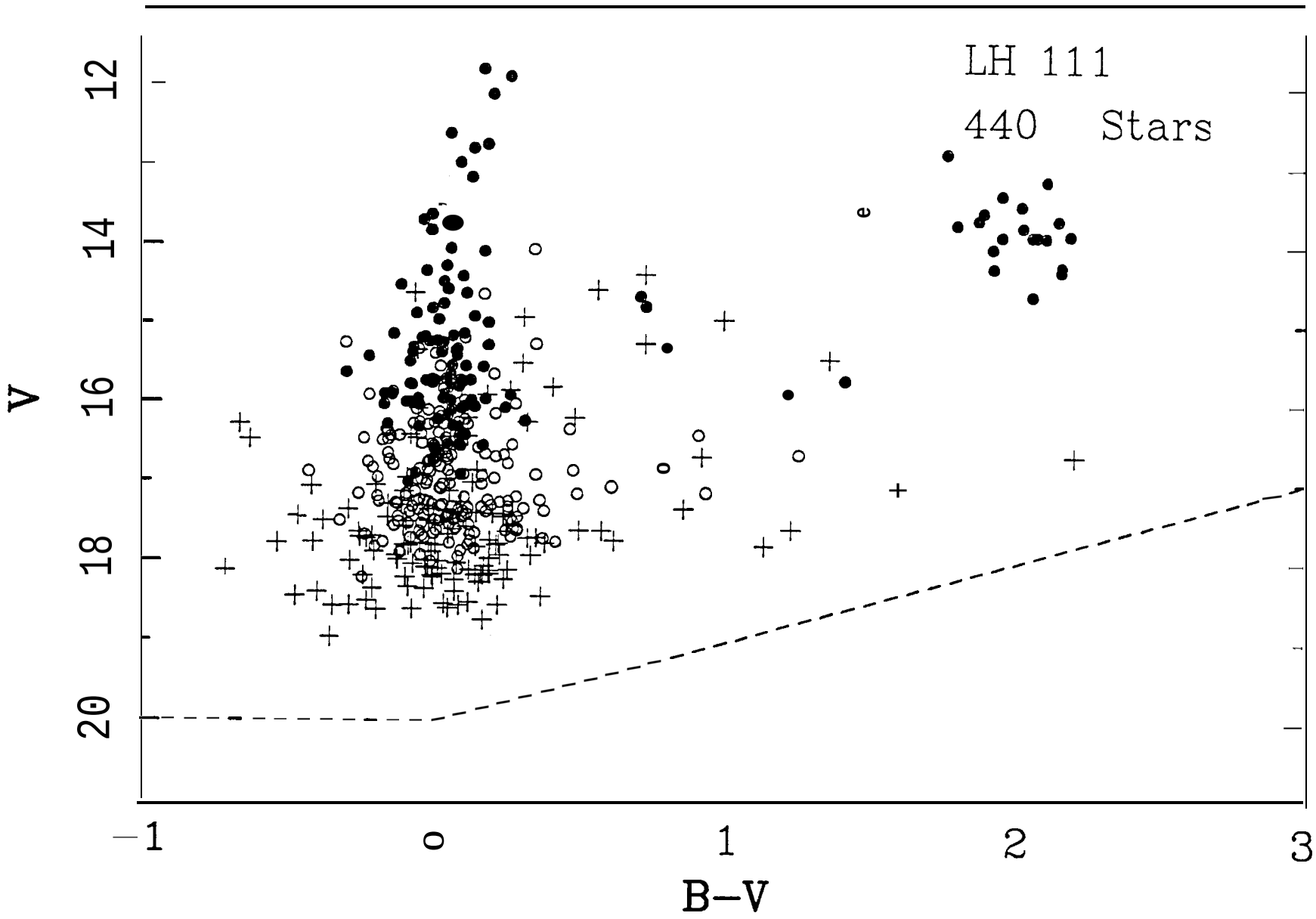

Figure 19

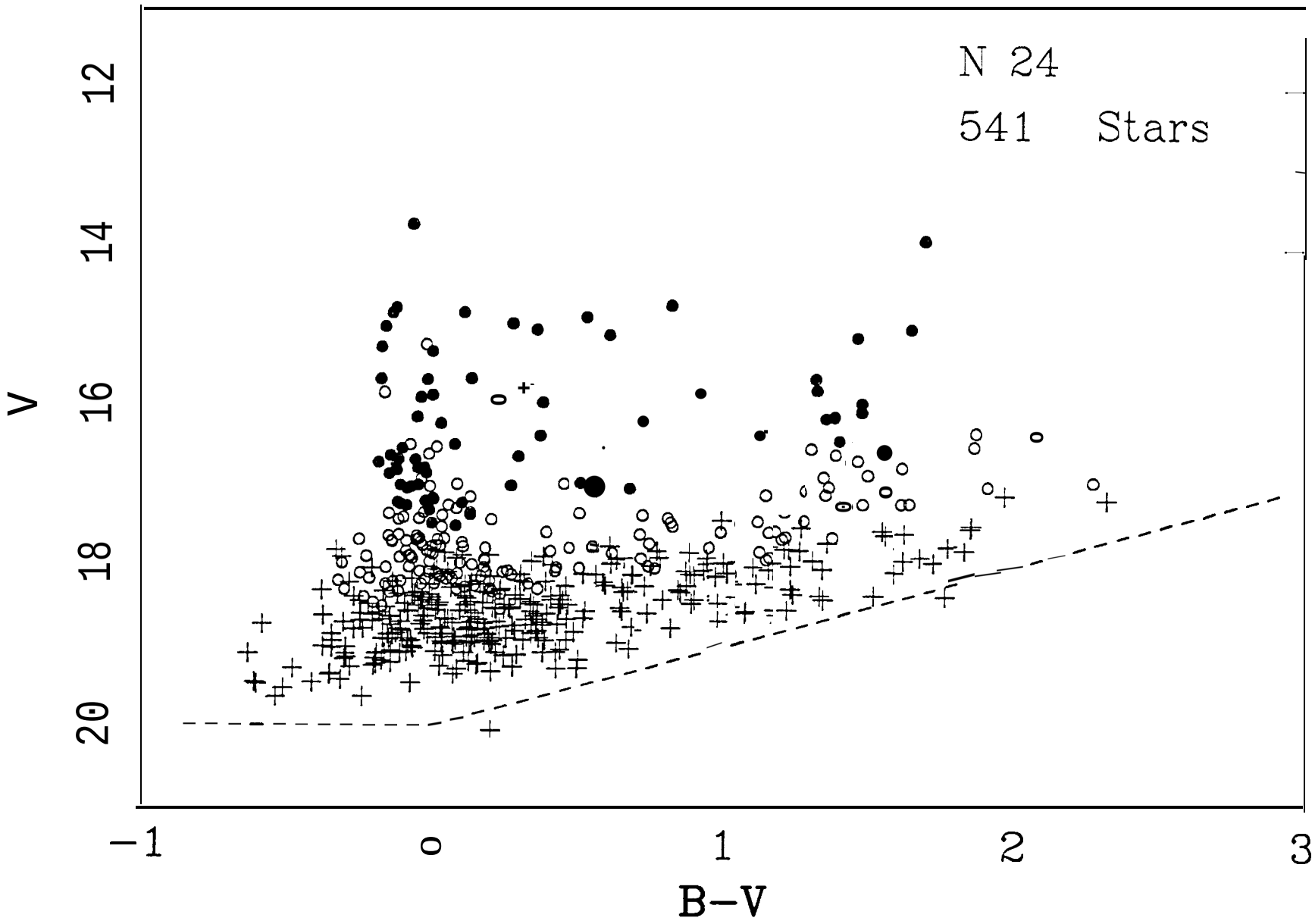

Figure 23

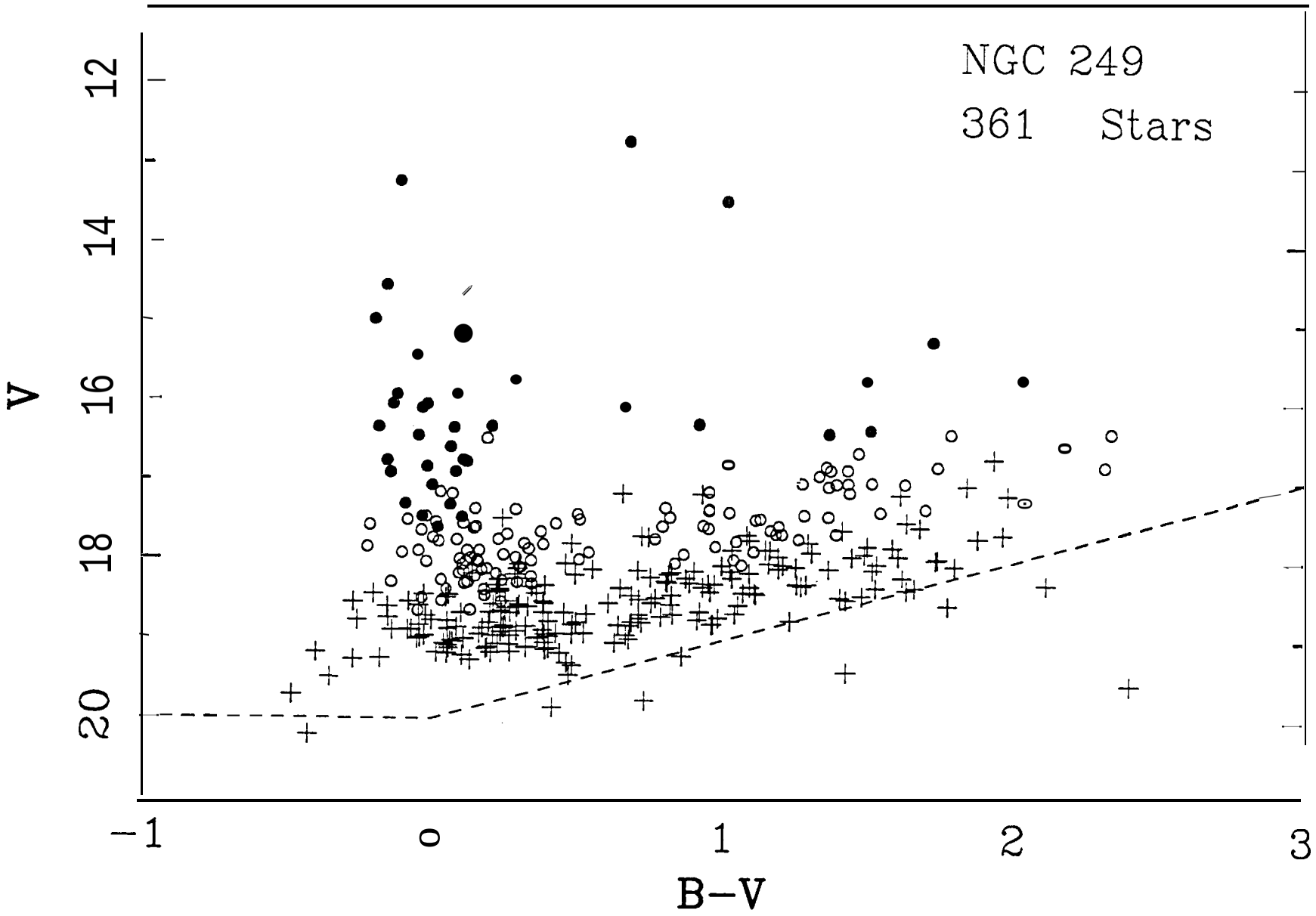

Figure 21

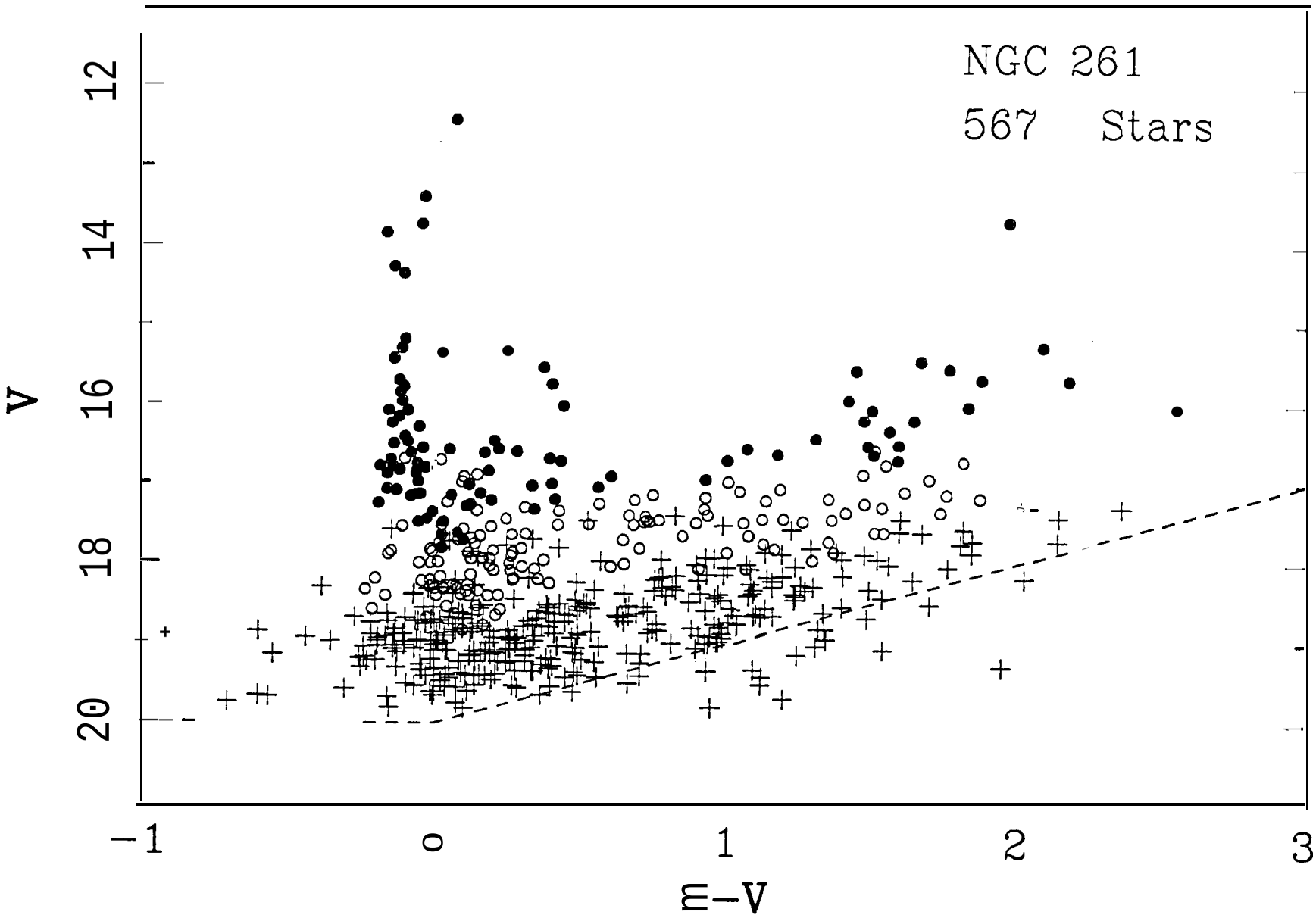

Figure 22

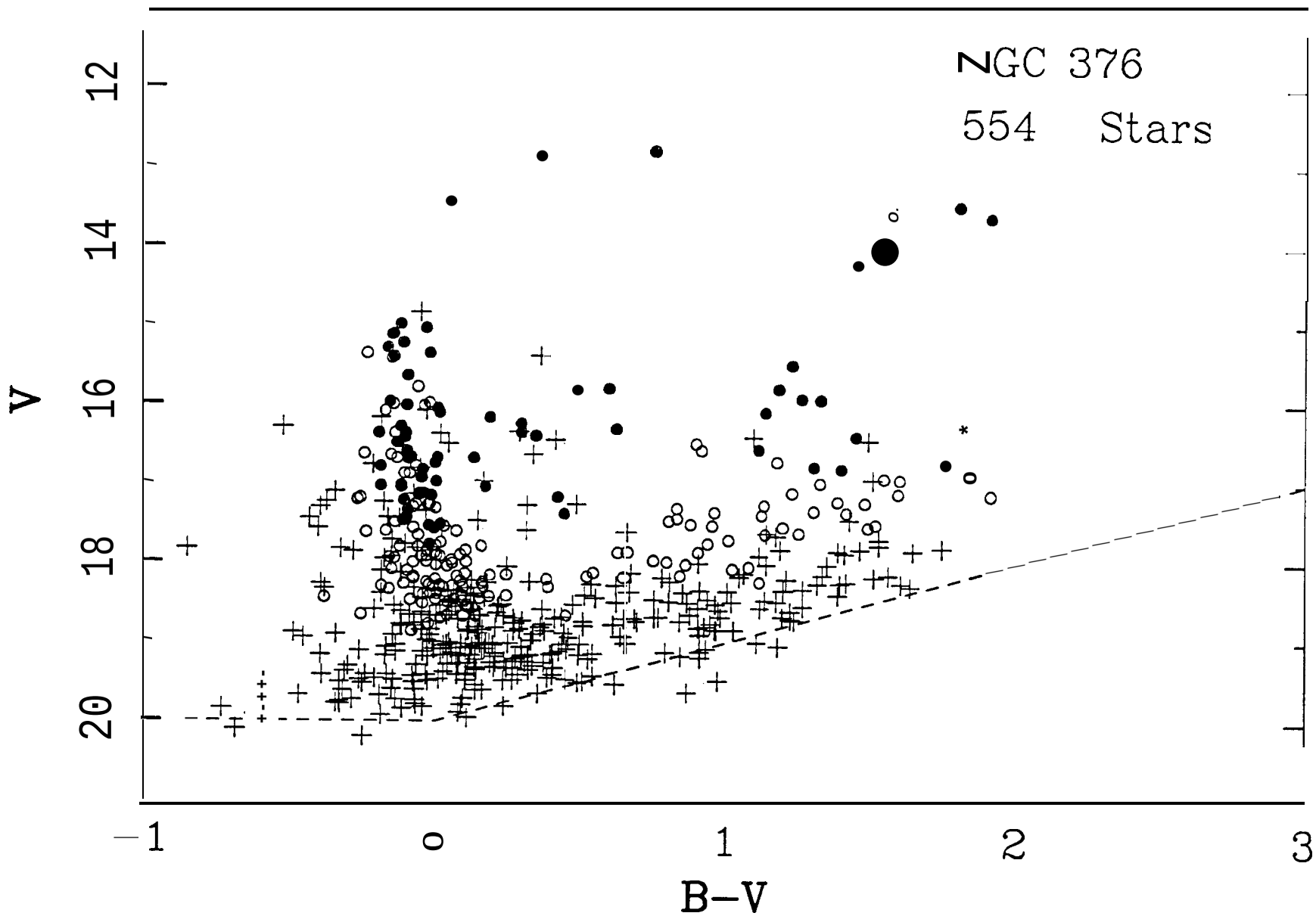

Figure 23

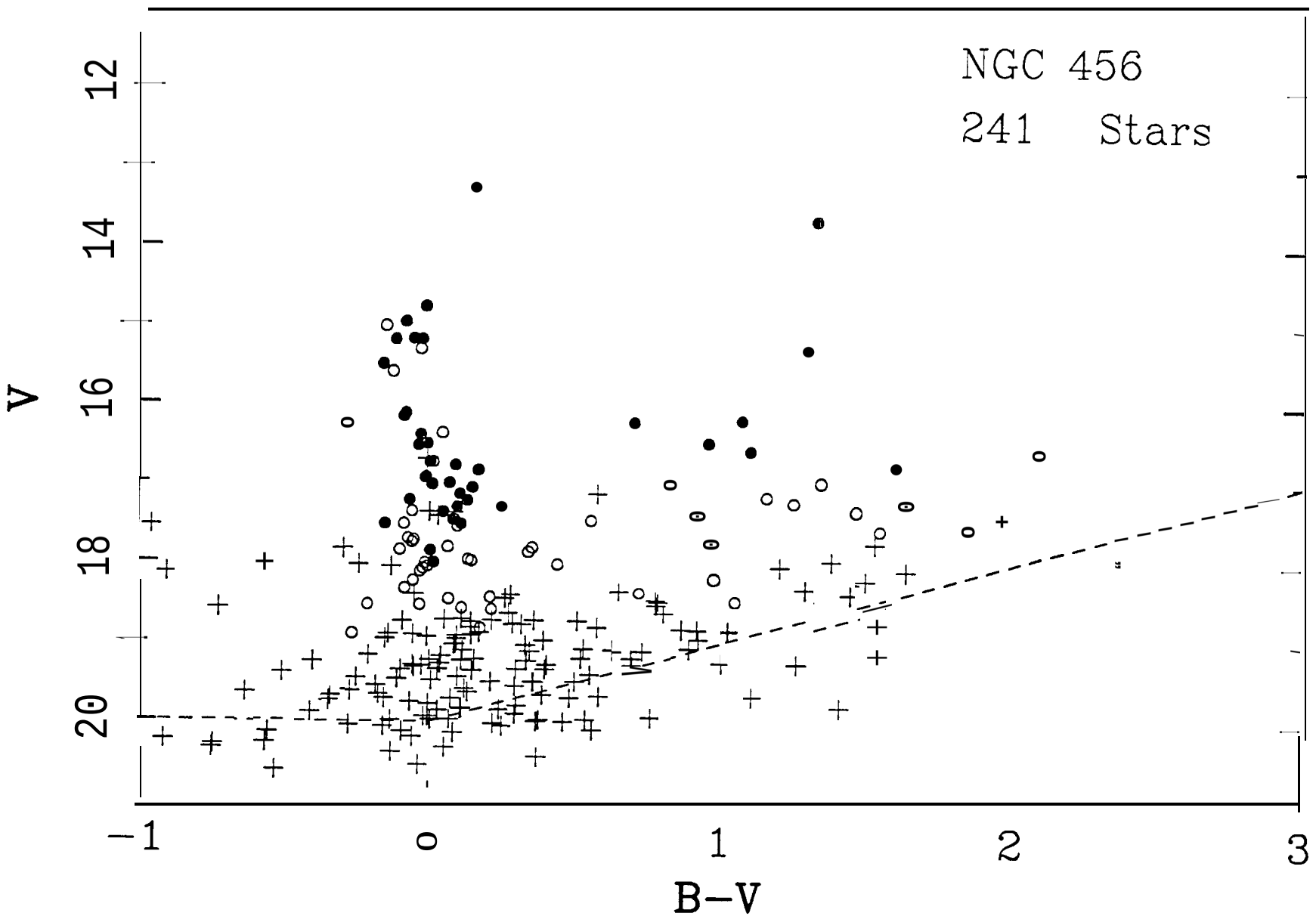

Figure 24

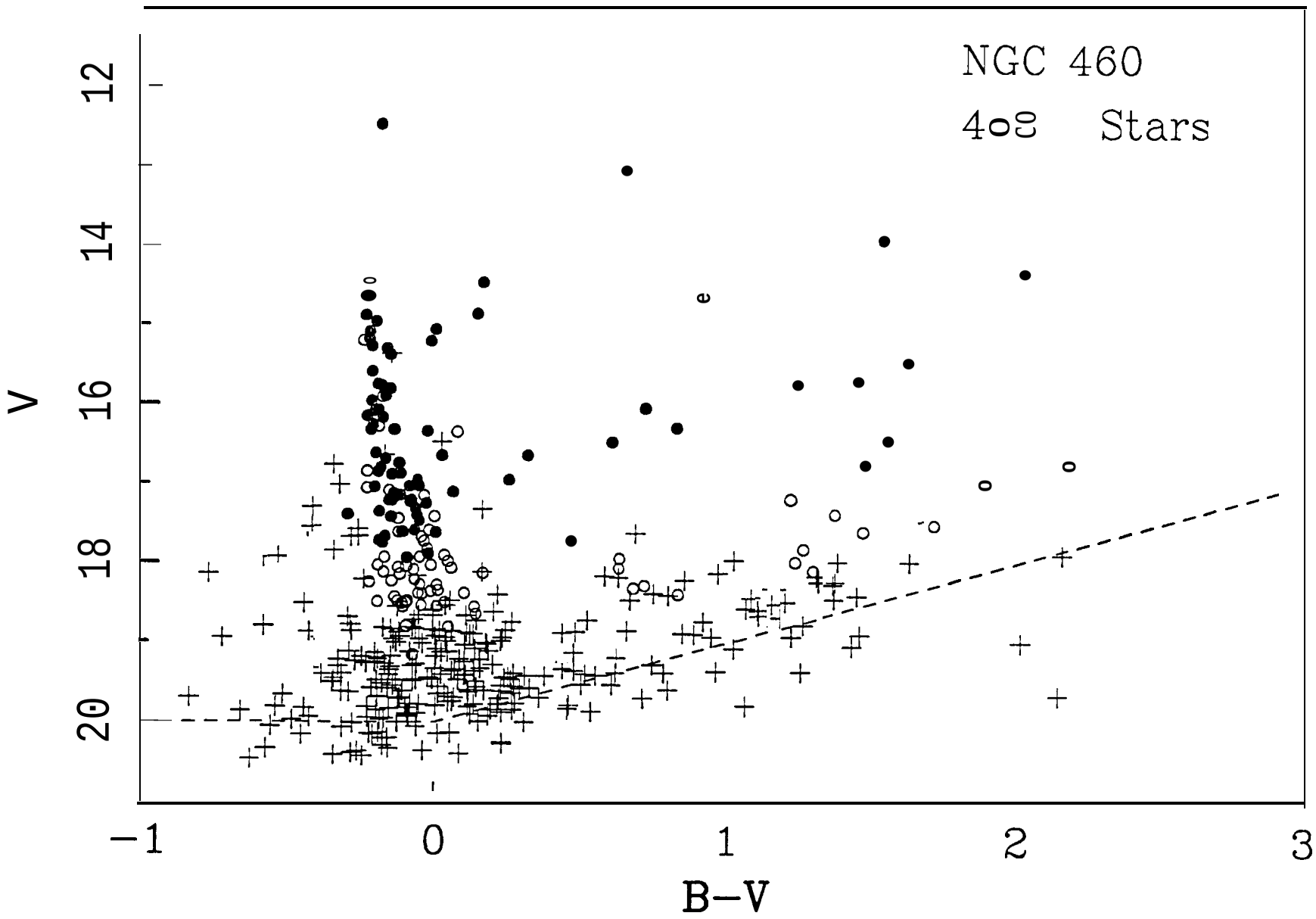

Figure 25

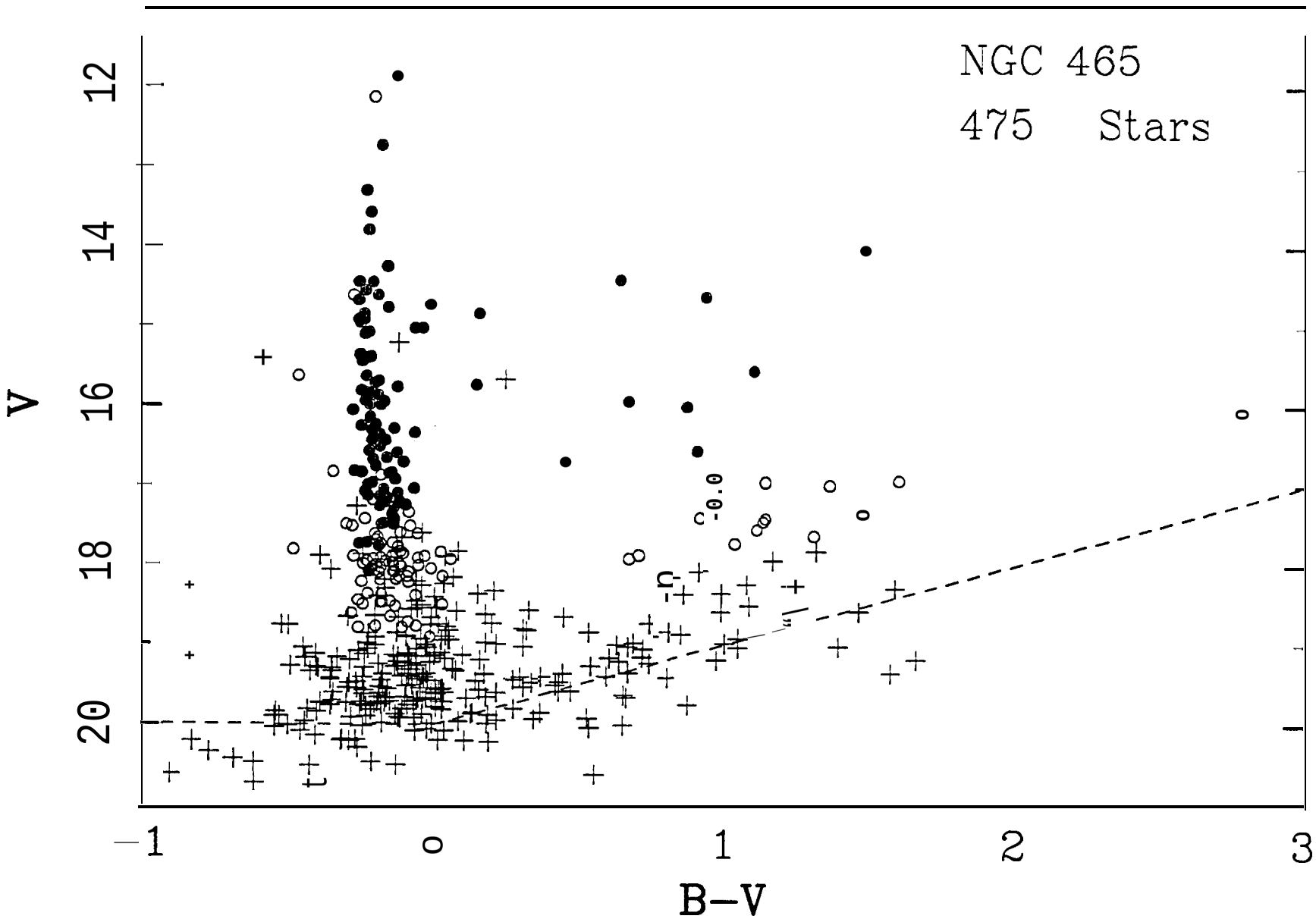

Table 5: UBV Photometry for LH 4

No.	x	y	V	σ_V	$B-V$	σ_{B-V}	$U-B$	σ_{U-B}	No.	x	y	V	σ_V	A-E?	O-B	$U-B$	σ_{U-B}
1	8.2	197.9	17.64	0.03	0.03	0.03	-0.03	[illegible]	48	50.5	360.5	19.10	[illegible]	1.24	0.14	.....	
3	10.1	438.2	15.37	0.01	0.64	0.01	-0.08	[illegible]	49	50.5	[illegible]	17.35	[illegible]	0.02	[illegible]	[illegible]	0.04
4	11.8	405.0	[illegible]	[illegible]	-0.11	[illegible]	-0.29	0.20	50	50.7	226.9	18.92	0.07	[illegible]	[illegible]	.....	
5	[illegible]	261.5	19.29	0.10	0.46	0.13	.....		51	51.1	485.7	19.15	[illegible]	3.56	0.66	.....	
6	12.7	241.3	19.63	0.13	-0.03	0.16	.....		52	51.2	60.5	18.55	[illegible]	-0.49	0.06	.....	
8	16.4	447.4	17.81	0.03	0.96	0.04	[illegible]	0.13	53	54.4	259.3	18.60	0.06	0.30	[illegible]	.....	
9	17.0	167.9	18.51	0.06	0.80	0.08	.....		54	56.4	239.4	19.59	0.13	0.37	0.17	.....	
12	17.4	[illegible]	19.50	0.09	1.42	0.20	.....		55	56.7	205.0	17.92	0.03	-0.11	0.03	[illegible]	0.06
13	17.5	216.6	17.74	[illegible]	-0.05	0.03	0.17	0.12	56	57.7	[illegible]	19.66	0.13	0.42	0.17	.....	
14	20.5	332.1	18.03	[illegible]	0.48	0.12	-0.33	0.22	57	58.8	223.6	17.63	0.03	-0.26	0.03	[illegible]	0.04
15	21.0	282.1	[illegible]	0.11	1.30	0.20	.....		58	60.4	419.9	20.58	0.14	2.82	1.60	.....	
16	21.2	180.3	19.11	[illegible]	-0.12	0.10	.....		59	60.7	395.8	18.40	0.04	0.24	0.07	.....	
17	21.7	168.8	18.03	0.03	[illegible]	0.06	.....		60	62.2	427.8	19.33	[illegible]	-0.42	0.12	.....	
19	23.5	439.2	18.94	0.06	0.67	0.10	.....		61	62.5	26.3	19.23	[illegible]	[illegible]	0.15	.....	
20	24.7	75.9	16.92	0.01	-0.05	[illegible]	[illegible]	[illegible]	62	63.5	317.6	18.59	[illegible]	-0.06	0.06	0.20	0.19
21	24.9	92.2	17.67	0.02	-0.05	0.03	[illegible]	[illegible]	63	63.7	436.7	20.16	0.13	0.03	[illegible]	.....	
22	26.3	193.6	18.61	0.05	0.32	[illegible]	.....		64	64.0	[illegible]	19.73	[illegible]	[illegible]	[illegible]	.....	
23	28.0	335.2	13.14	0.02	-0.19	[illegible]	-1.07	0.01	65	64.1	106.1	19.11	[illegible]	[illegible]	[illegible]	.....	
24	28.0	378.6	17.71	0.03	-0.20	0.03	-0.81	[illegible]	66	64.1	51.9	16.36	0.01	191	200	.....	
25	30.9	418.9	16.86	0.02	-0.18	[illegible]	-0.89	0.03	67	64.9	124.2	19.52	0.12	[illegible]	0.13	.....	
27	33.8	7.7	19.16	0.08	0.78	0.14	.....		68	65.2	463.0	[illegible]	0.09	-0.56	[illegible]	.....	
28	34.1	[illegible]	18.78	0.06	0.17	0.08	.....		69	65.9	209.9	15.97	0.01	[illegible]	0.01	[illegible]	0.01
29	34.9	275.5	19.62	0.16	[illegible]	0.20	.....		70	65.9	202.3	17.92	0.03	0.83	0.05	.....	
30	36.3	208.4	19.11	[illegible]	[illegible]	0.10	.....		71	[illegible]	246.8	19.20	[illegible]	0.11	[illegible]	.....	
31	36.7	237.4	17.56	[illegible]	-0.03	[illegible]	[illegible]	[illegible]	72	66.8	349.3	[illegible]	0.12	0.84	0.20	.....	
32	37.7	233.0	16.56	0.03	-0.25	0.03	-0.82	0.03	74	[illegible]	239.5	17.66	0.03	-0.12	0.03	[illegible]	[illegible]
33	38.7	201.5	18.50	[illegible]	-0.45	0.06	-0.65	0.09	75	68.1	6.1	18.73	0.07	1.25	0.10	.....	
34	40.7	426.0	19.53	[illegible]	0.31	0.15	.....		79	[illegible]	278.5	19.00	0.07	0.43	[illegible]	.....	
37	42.7	207.5	18.77	[illegible]	0.33	[illegible]	.....		80	71.6	213.1	18.29	[illegible]	0.18	0.07	-0.25	0.17
38	42.9	303.8	18.77	0.05	0.83	0.09	.....		81	71.6	[illegible]	18.68	[illegible]	-0.38	[illegible]	-1.13	[illegible]
41	44.5	237.2	18.52	[illegible]	0.04	0.06	-0.54	0.13	82	71.9	139.1	18.59	[illegible]	[illegible]	[illegible]	[illegible]	[illegible]
42	44.8	135.2	19.14	0.13	-0.44	0.14	.....		83	72.2	356.6	17.09	[illegible]	0.92	[illegible]	[illegible]	[illegible]
44	48.2	217.7	18.16	0.04	0.27	0.06	.....		84	74.7	418.0	21.01	0.37	1.45	1.00	.....	
45	48.8	83.8	19.34	0.08	1.07	0.15	.....		85	75.6	227.9	15.59	[illegible]	-0.14	[illegible]	[illegible]	0.02
46	49.3	245.3	19.06	[illegible]	-0.16	0.10	.....		86	75.7	85.1	18.44	0.05	[illegible]	0.06	-0.98	[illegible]

Table 6: UBV Photometry for LH 54

No.	x	y	V	σ_V	$B-V$	σ_{B-V}	$U-B$	σ_{U-B}	No.	x	y	V	σ_V	$B-V$	σ_{B-V}	$U-B$	σ_{U-B}
3	15.0	135.4	18.99	0.07	-0.59	0.09	...	...	43	51.3	132.2	19.12	0.08	0.17	0.11	...	...
4	19.2	37.5	19.41	0.11	-0.35	0.14	...	...	44	53.8	137.7	19.15	0.08	1.01	0.14	...	...
5	19.9	261.2	18.31	0.04	-0.23	0.05	-0.30	0.10	45	53.9	53.1	18.87	0.05	0.15	0.10	...	...
6	20.0	111.7	18.40	0.04	-0.03	0.05	-0.93	0.08	46	53.9	475.3	19.20	0.11	0.56	0.13	...	...
7	20.9	124.2	19.28	0.08	0.51	0.14	...	...	47	54.8	145.1	19.97	0.12	5.06	3.85	...	...
8	21.2	83.8	19.00	0.06	1.41	0.13	...	...	48	55.1	272.9	17.84	0.04	-0.03	0.04	-0.08	0.12
9	23.0	99.0	18.17	0.03	-0.06	0.04	-0.85	0.07	49	55.1	366.0	18.54	0.05	0.73	0.06	...	...
11	25.0	435.2	19.11	0.06	0.97	0.11	...	...	50	55.7	301.8	17.35	0.02	1.56	0.03	...	...
12	25.5	246.0	18.48	0.05	-0.20	0.06	-0.20	0.14	51	57.5	229.2	17.66	0.11	0.65	0.31	...	...
13	26.9	228.1	17.00	0.02	-0.28	0.02	-0.80	0.02	52	57.9	391.1	19.06	0.08	0.83	0.15	...	...
14	27.2	289.8	19.17	0.05	0.59	0.09	...	...	53	59.4	284.2	14.68	0.01	-0.27	0.02	-1.02	0.02
15	29.5	243.5	17.00	0.01	-0.28	0.02	0.90	0.03	56	62.1	373.4	19.24	0.06	0.55	0.12	...	...
17	31.0	272.3	19.30	0.12	-0.72	0.13	...	...	58	64.0	330.7	18.37	0.04	-0.32	0.04	-0.46	0.09
18	31.5	382.1	19.38	0.11	-0.14	0.14	...	...	59	64.8	113.5	19.34	0.07	0.41	0.12	...	...
21	34.0	43.7	20.11	0.17	0.62	0.31	...	...	60	67.9	258.5	18.90	0.06	-0.15	0.08		
23	36.3	235.1	19.11	0.06	0.54	0.10	...	...	61	68.0	198.8	19.06	0.07	0.04	0.10		
24	37.2	440.7	19.61	0.11	1.10	0.18	...	...	62	69.1	335.6	19.39	0.09	0.04	0.13	...	...
25	38.4	213.2	17.17	0.02	-0.29	0.03	-0.65	0.04	63	70.0	230.8	17.38	0.20	-0.33	0.29	1.09	1.59
26	40.0	329.4	17.60	0.26	-0.90	0.30	...	...	64	71.2	205.6	16.16	0.01	-0.09	0.03	-0.91	0.04
27	40.2	195.5	17.52	0.04	-0.41	0.06	-0.78	0.06	66	73.7	135.5	19.13	0.08	1.05	0.13	...	...
28	41.7	330.0	16.58	0.09	0.04	0.13	-1.30	0.10	67	75.3	280.9	17.67	0.04	1.55	0.28	...	...
29	42.2	363.1	17.74	0.02	-0.22	0.03	-0.77	0.04	69	76.1	93.6	19.38	0.11	0.62	0.16	...	...
30	42.6	47.4	16.44	0.01	-0.32	0.02	-1.02	0.02	70	76.2	301.8	15.28	0.01	-0.24	0.01	-0.97	0.01
31	43.3	190.3	18.58	0.07	0.05	0.11	...	...	71	76.7	257.0	18.96	0.08	-0.20	0.10	...	...
32	43.4	421.2	15.84	0.02	-0.10	0.02	-0.89	0.02	73	77.8	226.3	11.53	0.01	-0.19	0.01	-0.99	0.01
33	45.1	423.5	16.97	0.03	-0.23	0.07	-0.35	0.32	74	78.7	34.5	17.31	0.01	-0.15	0.02	-0.56	0.06
34	45.1	139.1	18.11	0.04	0.91	0.06	...	...	76	79.2	278.8	14.74	0.01	-0.30	0.02	-0.98	0.02
35	45.5	265.6	17.89	0.03	-0.15	0.04	-0.71	0.06	77	81.1	316.5	16.25	0.01	-0.22	0.02	-0.91	0.02
36	48.5	457.8	18.96	0.05	0.58	0.08	...	...	78	81.6	267.4	16.02	0.01	-0.23	0.01	-0.88	0.01
37	48.8	158.1	16.93	0.02	-0.09	0.02	-0.16	0.11	79	81.9	157.3	19.17	0.11	-0.53	0.13		
38	49.6	317.2	19.60	0.12	-0.11	0.15	...	...	80	82.3	99.3	19.19	0.07	0.72	0.10		
39	49.9	30.7	18.50	0.05	-0.44	0.06	...	...	81	82.5	259.8	19.60	0.15	-0.58	0.16		
40	50.1	247.8	17.95	0.02	-0.07	0.03	-0.34	0.08	83	82.7	79.6	19.49	0.08	1.08	0.20	...	...
41	50.9	83.7	16.35	0.01	-0.08	0.02	-0.36	0.04	84	83.7	321.2	15.85	0.01	-0.17	0.03	-0.95	0.03
42	51.2	306.0	18.92	0.08	0.13	0.10	...	...	86	85.4	230.7	17.61	0.29	-0.94	0.34		

Table 7: UBV Photometry for LH 58

No.	x	y	V	σ_V	$B-V$	σ_{B-V}	$U-B$	σ_{U-B}	No.	x	y	V	σ_V	$B-V$	σ_{B-V}	$U-B$	σ_{U-B}
4	7.9	113.3	14.40	0.01	-0.17	0.04	-0.83	0.04	55	25.1	192.7	19.61	0.14	-0.06	0.16	...	...
5	9.0	25.6	19.71	0.12	-0.08	0.24	...	...	56	25.5	78.8	19.24	0.10	0.62	0.15	...	...
8	9.2	77.1	18.24	0.09	-0.13	0.19	...	...	57	26.0	256.3	15.58	0.01	-0.16	0.00	-0.82	0.01
9	9.3	128.2	18.43	0.07	0.78	0.19	-1.54	0.21	58	26.0	97.8	17.70	0.02	-0.03	0.03	-0.80	0.05
11	9.9	207.3	18.70	0.04	-0.02	0.08	-0.40	0.17	59	26.9	87.1	19.47	0.10	0.60	0.14	...	...
12	10.2	56.7	19.76	0.12	-0.15	0.16	...	...	60	26.9	33.2	19.31	0.09	-0.32	0.11	...	...
13	11.5	296.0	16.85	0.02	-0.25	0.00	0.08	0.00	61	28.3	297.0	14.88	0.05	-0.14	0.03	-0.00	0.03
14	12.2	136.8	18.78	0.07	-0.44	0.08	...	...	62	28.5	74.0	17.96	0.03	1.88	0.07	...	...
15	12.6	368.1	18.74	0.06	-0.23	0.08	...	...	64	28.6	47.8	18.92	0.05	0.08	0.08	...	...
16	12.6	463.1	17.04	0.01	1.61	0.03	...	...	65	30.3	80.6	18.52	0.06	0.22	0.07	...	...
17	13.0	197.7	19.90	0.20	0.32	0.27	...	...	66	31.7	151.1	16.33	0.01	0.01	0.00	0.09	0.04
18	13.3	229.7	20.38	0.20	3.52	1.66	...	...	68	32.8	136.6	16.61	0.01	1.66	0.04	...	...
19	13.3	249.6	19.12	0.09	0.13	0.12	...	...	70	33.0	131.1	18.75	0.11	-0.04	0.15	...	...
21	13.4	378.4	19.04	0.07	0.00	0.10	...	...	72	33.3	28.0	19.09	0.09	0.08	0.11	...	...
22	13.5	450.3	19.75	0.13	0.59	0.19	...	...	73	33.3	13.8	19.15	0.06	0.62	0.14	...	...
23	13.7	445.2	20.08	0.23	0.13	0.27	...	...	75	35.3	461.8	18.00	0.03	-0.17	0.04	-0.98	0.06
24	13.8	331.8	16.98	0.01	-0.18	0.00	0.77	0.03	77	37.2	368.4	16.98	0.04	-0.11	0.06	-0.88	0.08
27	14.8	359.0	18.54	0.06	0.01	0.07	...	...	78	37.5	90.1	18.79	0.05	0.33	0.09	...	...
29	15.2	57.2	18.81	0.05	0.25	0.08	-1.52	0.08	82	41.1	288.6	18.92	0.09	-0.04	0.11	...	...
31	16.1	336.9	17.92	0.03	-0.08	0.04	-0.74	0.07	84	41.2	301.7	18.20	0.05	0.09	0.11	...	...
32	16.2	165.9	17.08	0.02	0.03	0.03	-0.93	0.04	85	41.2	50.6	19.21	0.08	0.89	0.15		
34	16.8	170.9	19.38	0.12	0.31	0.22	...	...	86	42.1	23.6	19.61	0.16	0.80	0.23	...	...
35	17.1	415.2	18.87	0.08	0.15	0.10	...	...	87	42.4	213.4	18.80	0.04	0.58	0.07	...	...
36	17.1	411.0	18.03	0.04	-0.10	0.05	-1.00	0.06	90	42.8	157.8	18.58	0.11	0.31	0.13	...	...
39	17.5	130.9	18.28	0.06	1.03	0.09	...	...	91	42.9	314.6	19.04	0.06	-0.23	0.09	...	...
40	18.6	271.1	15.38	0.01	-0.17	0.02	-1.01	0.00	93	43.2	35.1	18.93	0.05	1.12	0.10	...	...
42	19.2	143.4	19.63	0.10	0.18	0.15	...	...	94	43.9	220.9	16.75	0.00	-0.12	0.03	0.06	0.00
43	19.3	357.8	18.92	0.06	-0.15	0.08	...	...	96	45.0	109.7	19.28	0.10	0.18	0.13	...	...
44	19.5	100.9	18.62	0.05	0.00	0.08	...	...	97	45.2	365.5	16.55	0.00	-0.23	0.02	0.82	0.00
45	19.9	137.7	19.67	0.11	-0.14	0.15	...	...	98	45.7	382.8	18.33	0.04	0.89	0.06	...	...
48	21.4	219.9	18.80	0.07	-0.10	0.10	0.70	0.12	100	46.7	80.3	18.67	0.04	1.39	0.12	...	...
49	22.2	36.0	19.51	0.10	-0.02	0.14	...	...	101	46.9	349.8	19.57	0.12	-0.05	0.12	...	...
50	22.6	157.0	18.18	0.04	0.49	0.08	...	...	102	47.6	59.3	20.10	0.14	-0.60	0.17	...	...
51	22.9	21.1	19.70	0.12	0.39	0.17	...	...	104	48.0	260.4	15.90	0.01	-0.19	0.02	0.56	0.00
52	22.9	152.7	19.88	0.11	1.65	0.60	...	...	106	49.0	112.1	18.89	0.06	0.60	0.09	...	...

Table 8: UBV Photometry for LH 83

No.	x	y	V	σ_V	$B-V$	σ_{B-V}	$U-B$	σ_{U-B}	No.	x	y	V	σ_V	$B-V$	σ_{B-V}	$U-B$	σ_{U-B}
1	4.9	165.6	16.04	0.12	1.85	0.13	...	...	44	49.9	67.5	18.78	0.04	0.25	0.07	...	...
4	12.4	4.3	18.62	0.07	0.34	0.13	...	...	45	50.7	197.6	19.10	0.11	-0.45	0.12	...	...
5	13.1	405.3	19.77	0.10	0.04	0.15	...	...	46	54.6	235.2	19.01	0.08	0.18	0.14	...	...
6	13.2	14.4	14.52	0.01	0.50	0.20	-0.02	0.02	49	56.7	242.1	17.61	0.03	1.00	0.04	...	...
7	13.4	383.3	18.97	0.07	-0.03	0.09	...	...	53	63.5	162.8	18.99	0.06	2.03	0.29	...	...
10	16.0	187.7	18.68	0.08	-0.12	0.09	...	...	54	63.6	277.4	18.81	0.06	0.96	0.11	...	...
11	16.6	247.8	15.85	0.01	0.10	0.10	-0.09	0.10	55	63.8	70.5	19.48	0.08	-0.29	0.10	...	...
12	17.4	379.9	19.88	0.15	-0.17	0.18	...	...	57	65.7	85.3	17.97	0.03	-0.11	0.03	-1.12	0.08
14	18.6	231.2	19.04	0.05	-0.22	0.07	...	...	58	68.2	357.2	19.31	0.07	0.66	0.17	...	...
15	18.6	47.2	17.09	0.01	-0.07	0.02	-0.10	0.05	59	68.5	56.4	18.86	0.08	-0.02	0.09	...	...
16	20.9	312.3	18.10	0.03	1.21	0.08	...	...	60	68.0	293.8	19.05	0.08	1.32	0.20	..	...
17	23.5	213.2	18.18	0.03	0.81	0.07	...	...	63	68.9	40.7	17.90	0.03	0.07	0.07		...
18	24.6	412.0	19.47	0.09	-0.24	0.13	...	...	65	69.7	237.1	19.36	0.08	0.53	0.15		...
20	27.0	351.9	19.67	0.11	-0.38	0.14	...	...	68	70.8	198.9	19.46	0.11	-0.19	0.13		...
21	27.3	426.8	20.22	0.17	-0.37	0.20	...	...	69	71.8	226.9	19.14	0.08	0.88	0.14	...	...
22	29.1	315.5	18.48	0.05	0.64	0.08	...	...	68	71.9	289.0	17.37	0.07	1.12	0.04	..	
23	30.1	465.1	17.56	0.02	-0.02	0.03	-1.24	0.04	69	73.8	39.1	18.13	0.03	-0.17	0.05	...	...
24	31.3	13.7	18.42	0.04	0.48%	0.07	...	...	73	76.9	152.4	14.31	0.01	-0.18	0.00	-1.17	0.01
25	32.8	210.5	18.75	0.07	-0.14	0.08	...	...	75	77.6	395.3	16.76	0.00	-0.00	0.02	-0.87	0.04
26	36.5	125.4	19.53	0.12	-0.28	0.16	...	...	76	78.3	268.5	19.02	0.08	0.67	0.12	...	...
27	37.9	28.3	18.75	0.05	0.38	0.08	...	...	77	78.5	37.2	18.81	0.09	0.41	0.11	..	...
28	38.8	163.2	19.57	0.12	0.46	0.20	...	...	78	80.7	353.5	20.27	0.01	-0.15	0.13	...	...
29	39.3	294.2	19.28	0.09	-0.45	0.11	...	...	80	81.6	387.0	19.91	0.00	-0.05	0.00	0.67	0.03
30	41.0	284.3	19.00	0.06	-0.32	0.07	-0.55	0.09	81	82.2	68.8	16.22	0.01	-0.06	0.01	-0.02	0.03
31	42.4	415.2	19.49	0.11	0.95	0.20	...	...	84	84.3	46.9	17.48	0.00	0.98	bono	...	...
32	42.7	177.4	18.79	0.05	-0.04	0.08	...	...	85	85.8	273.2	18.92	0.00	1.32	0.17	...	...
33	43.4	237.9	20.80	0.30	-0.16	0.34	...	...	86	86.8	155.8	18.91	0.07	-0.18	0.09	-0.25	0.09
34	43.5	134.1	19.53	0.08	0.12	0.13	...	...	89	91.7	1008	17.85	0.03	0.18	0.04	3.68	3.03
35	44.2	186.9	19.59	0.09	-0.37	0.12	...	...	90	94.1	75.7	18.73	0.05	0.34	0.09	...	...
36	45.1	91.5	17.53	0.03	0.10	0.00	0.48%	0.21	91	94.7	226.9	16.94	0.01	-0.11	0.00	-0.03	0.03
38	45.5	51.5	19.88	0.14	-0.46	0.91	...	...	94	96.3	175.4	17.29	0.00	0.00	0.00	1.00	0.24
39	46.3	298.1	17.83	0.03	1.40	0.06	...	...	98	990	118.4	19.55	0.13	0.26	0.22	...	...
40	47.1	172.9	18.97	0.07	0.95	0.22	...	...	99	102.1	163.6	18.98	0.00	-0.55	0.09	...	...
41	48.6	288.6	18.75	0.06	0.91	0.08	...	...	100	102.6	368.2	18.61	0.05	1.82	0.19	...	...
43	49.4	44.8	19.46	0.09	-0.02	0.12	...	...	101	104.7	277.1	17.54	0.03	1.24	0.06	...	...

Table 9: UBV Photometry for LH 87

No.	x	y	V	σ_V	$B-V$	σ_{B-V}	$U-B$	σ_{U-B}	No.	x	y	V	σ_V	$B-V$	σ_{B-V}	$U-B$	σ_{U-B}
2	86.3	8.5	18.69	0.10	0.43	0.20	...	...	71	120.3	25.3	17.52	0.03	0.04	0.05	-0.10	0.08
5	204.4	6.3	18.40	0.06	1.33	0.26	...	...	73	237.4	25.8	17.09	0.02	0.01	0.04	-0.63	0.05
6	178.6	7.5	18.14	0.05	1.08	0.16	...	...	74	271.0	26.0	18.63	0.07	0.30	0.16	...	...
10	107.5	7.7	18.16	0.06	0.34	0.11	0.03	0.21	75	288.1	26.2	19.42	0.15	0.12	0.22	...	...
12	71.8	7.8	18.97	0.10	0.28	0.19	...	...	78	4.1	26.9	19.31	0.12	-0.04	0.20	...	...
17	359.2	8.6	18.51	0.05	0.87	0.22	...	...	79	64.2	28.1	17.09	0.02	1.80	0.12	...	...
18	83.8	8.7	17.68	0.05	0.75	0.10	...	...	80	86.4	28.2	18.50	0.04	1.03	0.13	...	...
20	194.5	9.2	17.13	0.03	1.57	0.10	...	...	86	112.0	29.1	19.18	0.10	-0.21	0.14	...	...
22	336.3	9.6	16.94	0.02	1.60	0.06	...	...	89	134.6	29.6	19.17	0.12	-0.14	0.17	...	...
23	305.1	10.3	19.16	0.11	0.61	0.18	...	...	91	235.9	29.8	17.89	0.03	1.16	0.14	...	...
25	227.6	10.7	18.74	0.08	0.22	0.12	0.70	0.19	93	198.5	29.9	17.47	0.04	0.09	0.13	-0.58	0.13
27	135.3	10.9	18.26	0.05	-0.29	0.08	-0.79	0.10	103	230.8	33.9	18.66	0.08	1.49	0.22	...	...
29	308.9	12.3	18.88	0.08	-0.31	0.14	...	...	104	273.0	34.2	16.84	0.02	0.99	0.04	0.78	0.16
32	130.7	12.9	17.29	0.03	-0.07	0.04	-0.87	0.05	113	247.8	37.0	19.07	0.10	-0.16	0.16	...	...
35	99.4	13.4	17.67	0.06	0.01	0.09	-0.56	0.09	114	222.9	37.3	16.78	0.03	1.52	0.07	0.97	0.29
37	350.9	13.9	17.01	0.03	-0.13	0.04	-0.95	0.04	117	283.9	38.0	16.97	0.03	-0.07	0.04	-0.70	0.04
38	206.2	14.0	18.75	0.09	-0.20	0.12	...	...	118	372.8	38.6	18.30	0.05	1.15	0.14	...	...
42	56.7	16.0	18.10	0.09	-0.04	0.11	-0.96	0.10	119	123.7	39.0	18.97	0.06	-0.02	0.15	-0.38	0.23
44	46.6	16.3	19.07	0.09	-0.19	0.14	...	...	121	207.8	39.6	16.58	0.02	-0.05	0.03	-0.94	0.03
45	233.0	16.4	18.06	0.06	-0.19	0.10	-0.62	0.11	122	288.2	40.8	18.81	0.05	0.-w	0.11		...
46	309	17.6	18.32	0.08	0.10	0.13	-0.78	0.13	124	230.6	41.2	19.47	0.12	-1.49	0.67		
47	194.4	17.9	19.08	0.11	-0.06	0.16	...	...	126	238.0	41.2	18.75	0.08	0.63	0.19	...	...
49	259.4	18.1	19.50	0.14	-0.12	0.21	...	...	128	349.6	41.8	17.70	0.06	0.89	0.10	...	...
50	369.9	18.7	18.71	0.11	0.53	0.19	...	...	135	65.2	45.7	16.41	0.02	-0.08	0.03	-1.00	0.03
53	386	19.5	18.86	0.09	-0.34	0.13	...	...	137	367.3	46.5	17.13	0.03	-0.16	0.05	-0.74	0.05
55	330.9	20.8	18.54	0.12	0.9	0.21	...	...	139	68.1	47.0	17.10	0.02	0.94	0.06	...	
58	345.7	21.5	15.70	0.01	1.19	0.03	0.82	0.06	142	316.9	47.8	18.81	0.08	-0.02	0.13	...	...
59	312.1	21.9	16.96	0.15	1.07	0.49	...	...	143	348.5	47.8	18.34	0.06	1.33	0.20	...	...
60	204.0	22.1	16.63	0.02	1.48	0.05	...	...	144	375.2	47.9	17.08	0.03	-0.06	0.05	-0.16	0.05
61	43.2	22.1	16.84	0.02	1.82	0.08	...	...	145	353.7	48.1	18.58	0.07	1.02	0.24	...	...
62	2066	22.3	15.05	0.01	-0.12	0.01	-0.75	0.01	147	235.0	48.8	17.92	0.04	1.27	0.13	...	...
64	268.8	23.0	18.05	0.05	0.10	0.09	...	...	149	371.3	49.0	1650	0.02	1.86	0.07	...	...
65	34.8	23.1	18.69	0.06	-0.10	0.10	...	...	154	287.2	51.1	12.15	0.00	-0.10	0.01	-1.05	0.01
66	130.3	23.1	15.87	0.01	-0.19	0.02	-0.77	0.02	164	172.4	53.6	19.16	0.11	0.08	0.19	...	...
68	244.2	23.8	16.32	0.02	-0.06	0.02	-1.01	0.02	165	207.9	54.0	17.44	0.03	1.49	008	...	...

Table 10: UBV Photometry for LH 93

No.	x	y	V	σ_V	$B-V$	σ_{B-V}	$U-B$	σ_{U-B}	No.	x	y	V	σ_V	$B-V$	σ_{B-V}	$U-B$	σ_{U-B}
1	204.2	3.3	13.76	0.10	-0.11	0.01	-0.08	0.21	134	101.9	80.8	18.90	0.10	-0.79	0.12	.....	
2	278.7	3.7	17.61	0.30	-0.37	0.30	...	...	139	297.9	63.5	14.44	0.01	-0.16	0.01	-1.15	0.10
14	173.6	8.2	17.50	0.05	1.40	0.10	...	...	144	1008	65.4	17.81	0.04	-0.05	0.07	-0.80	0.18
15	210.1	8.2	16.03	0.02	-0.05	0.03	-1.11	0.09	146	1611	66.5	16.01	0.04	0.92	0.04	-1.00	0.02
23	53.7	11.3	18.18	0.05	-0.06	0.09	-0.58	0.12	152	234.0	67.7	16.59	0.08	0.21	0.09	-0.83	0.04
29	183.4	14.9	18.70	0.06	0.91	0.11	-0.23	0.19	155	1052	69.8	18.81	0.09	0.32	0.14	.....	
35	294.5	18.7	16.74	0.02	-0.08	0.03	-1.03	0.03	157	140.7	69.7	16.67	0.03	-0.01	0.04	-1.01	0.04
39	1.86	21.1	18.95	0.08	-0.02	0.14	...	...	158	30.8	69.9	18.35	0.08	0.21	0.13	-0.81	0.13
42	235.2	21.9	18.34	0.04	0.92	0.08	-1.11	0.10	161	218.8	71.0	17.25	0.14	0.36	0.15	-0.70	0.08
47	271.7	22.9	18.09	bono	0.08	0.08	-0.54	0.10	162	239.3	71.5	17.23	0.10	0.81	0.09	-0.78	0.06
58	192.0	29.1	15.14	0.10	-0.15	0.01	-1.02	0.10	164	102.3	72.1	16.85	0.02	1.43	0.08	.....	
60	1.011	30.6	16.48	0.02	-0.10	0.03	-0.98	0.03	167	38.8	72.5	16.65	0.01	-0.10	0.03	-0.58	0.03
69	192.2	33.9	20.12	0.62	-1.53	0.32	...	...	171	210.2	74.1	14.48	0.03	-0.09	0.04	-1.08	0.03
70	1881	35.4	19.02	0.10	-0.17	0.18	...	...	176	197.0	75.1	14.62	0.10	1.65	0.07	.....	
72	115.4	36.4	17.11	0.02	1.48	0.00	...	...	180	130.1	77.0	17.29	0.00	0.56	0.09	0.03	0.02
73	291.2	36.8	17.53	0.03	-0.07	0.08	-0.57	0.10	182	195.2	77.1	17.67	0.00	Soon	0.62	-1.22	0.28
76	82.7	38.0	17.85	0.04	-0.01	0.06	-0.71	0.00	183	227.9	77.2	10.94	0.02	1.71	0.02	1.99	0.00
78	58.2	39.4	16.77	0.04	0.96	0.05	...	...	184	1-112	77.3	17.55	0.10	0.41	0.20	.....	
79	285.7	39.5	18.46	0.08	0.10	0.14	...	...	185	0.76	77.6	12.64	0.04	-0.19	0.05	-1.08	0.08
80	906	65.8	16.12	0.01	bono	0.02	-0.66	0.20	189	92.1	79.8	16.51	0.02	-0.08	0.03	-0.86	0.20
84	64.8	40.1	18.12	0.00	-0.23	0.08	-0.68	0.09	198	23.2	84.1	18.50	0.08	0.03	0.11	-0.57	0.12
90	203.1	42.9	18.11	0.04	-0.34	0.08	-0.92	0.09	200	193.8	84.5	18.24	0.10	-0.14	0.13	-0.77	0.12
92	284.4	43.3	18.14	0.05	0.62	0.13	...	...	204	274.1	85.4	1806	0.09	0.00	0.61	.....	
96	172.5	45.8	17.65	0.05	0.42	0.07	-0.75	0.08	208	177.9	88.5	19.04	0.11	0.70	0.91	.....	
101	115.6	48.6	18.56	0.09	-0.18	0.12	...		216	62.2	91.1	18.90	0.09	0.23	0.16	.....	
106	160.3	50.1	12.77	0.10	-0.05	0.01	-1.02	0.00	221	228.3	92.8	17.58	0.13	0.29	0.12	-0.96	0.12
109	166.0	51.6	18.72	0.00	0.12	0.18	...	...	224	84.1	93.2	19.34	0.12	0.69	0.39	.....	
116	198.1	53.9	17.67	0.20	-0.16	0.04	-1.70	0.05	229	183.3	95.0	17.47	0.03	1.46	0.11	.....	
119	79.2	54.5	15.92	0.00	0.02	0.00	-0.90	0.02	231	166.6	96.0	18.71	0.09	-0.13	0.14	-0.69	0.14
120	174.6	55.3	18.22	0.03	0.93	0.12	...		234	156.3	96.5	17.55	0.03	-0.03	0.06	-0.88	0.06
121	125.8	56.3	17.15	0.12	0.39	0.14	-0.56	0.12	236	115.5	97.0	14.31	0.01	-0.15	0.10	-1.12	0.01
123	296.5	57.5	17.54	0.03	-0.03	0.05			238	164.7	97.6	17.67	0.03	1.39	0.09	.....	
124	291.1	57.6	18.21	0.05	0.19	0.10	-0.58	0.17	242	172.7	99.1	16.49	0.02	-0.08	0.03	-0.26	0.03
127	152.3	58.6	18.00	0.06	0.34	0.09	-0.66	0.09	245	1.69	100.3	16.38	0.02	-0.08	0.02	-0.94	0.02
128	234.6	60.5	16.71	0.02	1.30	0.06	...	...	246	216.9	100.5	16.93	0.03	-0.06	0.04	-1.00	bono

Table 11: UBV Photometry for LH 111

No.	x	y	V	σ_V	$B-V$	σ_{B-V}	$U-B$	σ_{U-B}	No.	x	y	V	σ_V	$B-V$	σ_{B-V}	$U-B$	σ_{U-B}
1	141.2	3.5	15.84	.007	0.25	0.11	-0.74	0.10	71	9.951	65.3	17.24	0.03	0.25	.007	-0.74	.010
4	361.8	9.5	17.26	0.12	0.09	0.13	-0.85	0.12	72	243.8	5.59	17.89	0.04	0.20	.008	-0.77	0.05
7	235.0	8.8	17.46	.006	-0.16	.008	...	...	77	143.9	67.4	17.53	0.04	-.009	0.06	-0.56	0.06
8	321.4	8.9	16.52	0.03	-0.05	0.05	.009	0.05	78	169.6	69.6	16.27	0.04	0.11	0.05	-0.78	0.04
10	277.3	9.2	17.36	0.05	0.36	.008	...	...	79	84.0	68.0	13.86	.010	2.18	0.02	.....	
12	305.6	9.5	15.97	0.03	.010	0.04	-.059	0.04	82	82.6	73.2	15.27	.002	0.17	0.02	-.019	.001
15	358.5	11.5	17.32	.005	0.16	.007	-0.63	-.060	85	359.9	74.5	16.18	0.03	0.02	.008	-.010	.006
17	179.1	14.5	16.93	.005	.010	-.008	-0.57	0.05	88	355.3	74.8	17.32	.005	0.05	.008	-.058	.009
22	124.4	17.7	16.25	0.03	.008	0.04	-0.63	0.05	88	196.1	78.4	17.03	0.05	-.005	.006	-.050	0.07
23	49.2	19.3	14.08	.002	0.16	0.03	-0.80	.002	90	85.4	80.3	15.86	0.03	0.05	0.03	-0.62	0.03
92	149.3	28.6	.041-.060	0.03	0.02	.005	-0.56	.006	16	266.5	85.8	16.12	0.03	.001	0.04	-0.61	0.03
27	146.7	30.8	14.77	0.02	0.71	0.02	0.33	0.04	96	181.2	88.8	17.80	.007	-0.11	0.09	-0.39	0.12
28	144.7	30.9	1691	0.03	0.34	.006	-0.59	.008	98	361.2	89.4	17.61	0.04	0.48	0.10	.....	
29	252.9	30.9	17.34	0.03	-.080	.006	-0.71	.007	101	64.1	93.5	16.82	0.03	.006	0.38	0.24	
31	369.9	32.6	16.39	.006	.010	0.05	-0.69	.006	104	113.2	96.0	14.98	0.03	0.17	0.03	-0.70	.006
33	132.9	36.2	17.27	.005	-.017	.006	-0.67	.007	105	353.4	96.4	17.90	0.05	-0.12	0.08	-0.66	.008
34	160.2	36.7	18.11	0.06	0.24	0.14	-0.59	0.20	107	360.0	97.8	17.29	0.03	.006	.007	-.010	.008
35	1251	37.9	13.87	.001	2.05	.002	...	...	108	249.4	98.2	17.38	0.03	0.17	.008	.....	
37	194.7	41.4	17.59	.005	0.28	.006	-.059	0.13	109	297.3	98.8	17.62	0.04	0.28	.009	-.009	0.10
39	94.0	41.9	16.85	.002	0.46	0.05	...	...	110	287.1	99.1	16.02	0.03	-.018	.006	-0.82	.002
42	281 V	46.2	15.54	.002	.019	0.03	.051	0.03	112	374.8	103.6	15.75	.002	-0.01	.002	-.018	0.03
44	318.4	47.0	17.87	0.04	.008	.008	-0.71	0.10	113	178.6	103.9	14.31	.001	2.15	0.02	.....	
48	175.8	47.9	16.82	.008	0.01	.018	-0.65	.006	114	275.1	104.0	17.61	.008	.006	.009	.008	0.09
49	203.0	48.2	16.53	0.03	.009	0.04	-0.62	0.05	116	6589	.801	14.87	0.01	-.004	.002	-0.73	.002
50	145.5	49.5	17.62	.006	0.24	.006	...		117	224.9	107.8	16.45	0.03	0.03	.008	-0.76	.009
52	1610	52.5	17.82	0.05	0.14	0.10	...		118	357.7	108.2	17.50	0.05	.017-	0.06	-.010	.006
53	290.3	52.9	16.04	.002	.010	0.03	.006	0.03	120	222.1	111.1	17.12	.005	.010	.009	-.010	
54	371.1	53.5	16.52	.002	-.007	0.04	-0.39	0.19	121	307.1	115.0	16.73	0.02	-.010	0.04	.006	
56	184.2	55.7	15.15	0.02	0.05	.002	-0.76	.002	125	280.3	118.3	16.07	0.03	.006	0.03	-.006	0.03
57	285.5	.095	17.77	.009	0.37	.011	...		127	381.0	9021	17.63	0.05	-0.05	.006	.....	
59	107.1	57.0	17.19	0.05	.007	.008	-.059	.006	128	128.7	120.7	16.23	0.02	0.30	0.03	-.050	0.05
60	183.7	63.2	17.93	0.05	0.32	0.12	...	...	129	286.0	120.7	16.41	0.02	.010	0.04	-0.68	0.05
61	.609	63.2	16.40	0.03	.006	0.05	...	...	131	299.0	121.9	16.09	0.01	0.05	0.03	-0.71	0.03
62	123.3	63.7	15.53	.002	0.05	.002	-.061	.002	132	348.1	122.5	17.29	0.03	-0.13	0.04	-0.60	0.06
63	172.8	64.1	13.18	.010	.012	0.02	...	...	138	120.6	128.0	17.23	0.03	0.35	0.08	-0.65	.010

Table 12: UBV Photometry for N 24

No.	x	y	V	σ_V	$B-V$	σ_{B-V}	$U-B$	σ_{U-B}	No.	x	y	V	σ_V	$B-V$	σ_{B-V}	$U-B$	σ_{U-B}
1	77.8	4.8	18.60	0.25	-1.01	0.30	...	...	92	241.0	34.7	19.37	0.10	-0.35	0.14	.....	
3	250.9	5.3	18.94	0.16	-0.07	0.27	088	0.26	9S	353.5	35.0	19.10	0.12	-0.19	0.17	.....	
4	160.5	5.3	17.81	009	-0.33	0.12	-0.72	0-09	98	359.5	35.9	18.60	007	0.36	0.14	.....	
8	286.3	7.1	17.96	007	190	0.11	...	...	97	70.9	36.1	18.67	0.06	0.35	0.13	.....	
10	190.7	7.2	18.11	0.09	0.01	0.11	-0.17	0.10	99	174.3	36.7	19.65	0.13	-0.54	0.18	.....	
15	356.2	7.7	15.91	002	0.23	0.05	-0.06	0.11	101	77.3	37.3	18.87	0.08	0.14	0.17	.....	
16	374.5	8.2	17.81	0.06	-0.01	0-09	-0.77	0.09	103	104.0	37.4	18.16	005	-0.22	007	-0.17	008
22	169.7	8.7	16.49	0.03	-0.05	0.04	-0.92	0.03	106	165.1	37.8	18.95	0.10	0.03	0.14	.....	
25	261	9.1	18.33	0.07	0.17	0.09	-0.74	0.11	108	20.0	38.5	15.01	001	1.64	0.02	2.13	0.18
31	126.0	9.8	17.91	0.11	0.08	0.12	-0.73	0.09	111	349.9	40.3	17.25	0.05	0.05	0.06	-0.65	0.08
38	271.9	11.7	16.41	002	1.41	0.04	...	...	113	240.0	41.0	17.95	0.04	-0.01	0.06	-0.98	0.08
41	373.6	12.8	18.36	009	-0.12	0.13	0.51	0.12	114	341.4	41.1	17.56	0.03	1.18	0.08	.....	
43	291.3	13.8	18.19	0.09	0.38	0.14	...	...	117	318.5	43.4	16.53	002	-0.11	0.03	-0.16	0.03
44	312.6	13.9	18.59	0.09	-0.18	0.12	...	...	124	364.6	45.1	16.96	002	0.50	0.02	0.12	0-09
46	117.4	14.3	16.05	001	1.47	005	...	...	126	277.8	46.0	17.42	0.03	1.27	0-08	.....	
47	238.7	14.4	18.45	0.11	0.34	0.14	...	...	129	244.2	46.7	17.88	0.04	1.68	0.15	.....	
49	30.6	15.5	17.78	005	0.18	0.07	-190	008	131	309.3	47.3	18-51	001	-0.02	002	-0.82	002
50	368.2	15.9	17.42	0.04	-0.05	0.06	-0.79	0.05	133	98.4	49.3	18.67	007	0.05	0.21	.....	
51	180.4	16.4	18.67	008	0.6	0.12	...	...	135	90.3	49.6	18.85	0.06	0.04	0.12	-0.14	
52	149.8	16.9	15.61	0.05	1	0.10	...	...	139	83.7	51.0	18.77	0.08	0.03	0.21	-0.97	0.12
53	119.2	16.9	18.38	0.09	-0.06	0.10	0.57	0.10	141	346.1	51.7	16.10	001	1.40	0.04	.....	
56	209.1	17.7	18.32	0.05	-0.11	0.07	-0.61	009	145	97.2	53.8	17.68	0.03	002	0.05	0.19	0.08
59	247.6	19.8	17.67	0.04	0.04	0.06	-0.85	0.06	150	160.7	55.3	17.34	0.03	0.50	0.05	0.23	0.09
62	311.3	20.1	19.03	0.12	-0.07	0.16	-0.68	0.19	153	278.3	56.9	18.07	0.03	1.59	0.13	.....	
63	324.6	21.3	18.41	0.04	0.12	0.10	-0.57	0.12	154	32.8	57.3	19.05	008	0.43	0.18	.....	
67	335.0	22.8	18.63	008	-0.37	0.10	-0.46	009	156	326.8	57.5	18.79	0.06	-0.24	0.10	-1.17	0.13
70	27.2	25.2	18.23	008	0.16	0.10	...	...	157	85.8	58.2	17.75	0.03	0.10	0.06	-0.88	0.07
71	283.7	25.7	16.32	001	1.87	006	...	...	159	53.3	59.2	18.48	0.06	0.46	0.11	.....	
73	276.7	27.6	18.66	0.10	0.04	0.14	-0.68	0.13	164	29.1	60.9	19.17	009	0.50	0.17	.....	
74	312.8	28.1	15.63	001	1.33	0.04	1.29	0.15	165	181.1	609	17.75	0.06	060	0.10	-1.55	0.10
75	188.2	28.5	19.12	008	0.24	0.15	...	...	168	124.2	62.7	17.82	0.04	0.40	0.07	-1.56	0.10
79	113.8	30.0	18.53	0.05	0.21	0.09	-0.66	0.13	177	328.4	69.1	18.18	0.10	0.30	0.16	.....	
86	231.6	33.2	17.81	0-08	0.77	0.10		...	178	248.6	69.1	17.31	0.03	-0.01	0.04	-190	0.04
87	40.5	33.4	19.08	009	0.01	0.16		...	180	341.7	70.0	18.39	007	-0.27	0.10	.....	
89	2900	33.9	18.10	0.05	0.90	0.13		...	187	360.2	71.1	18.31	0.16	-0.38	0.09	-0.70	0.09

Table 13: UBV Photometry for NGC 249

No.	x	y	V	σ_V	B − V	σ_{B-V}	U − B	σ_{U-B}	No.	x	y	V	σ_V	B − V	σ_{B-V}	U − B	σ_{U-B}
4	180.2	6.9	18.14	0.07	0.70	0.12	...		107	351.5	19.2	18.30	0.03	1.28	0.14	...	...
9	244.6	10.1	17.45	0.03	1.36	0.08	...	...	109	267.9	61.5	18.88	0.07	0.90	0.14	...	...
11	47.4	10.1	18.53	0.07	0.25	0.13	...	...	115	47.7	65.9	16.94	0.03	1.32	0.05	0.07	0.09
12	266	11.3	18.61	0.07	0.49	0.12	...	...	117	170.0	65.2	18.81	0.05	0.95	0.21	...	...
14	254.8	11.9	17.83	0.02	0.97	0.08		...	118	195.7	65.3	18.54	0.05	0.23	0.08	-0.26	0.12
18	264.1	13.7	18.27	0.08	0.80	0.13	...	...	120	293.9	66.3	17.54	0.02	0.10	0.05	-0.05	0.07
19	86	14.3	17.34	0.03	0.80	0.08	...	...	121	29.6	66.4	14.46	0.00	0.21	0.00	-0.16	0.00
25	918S	20.1	17.51	0.00	1.63	0.11	...	...	123	137.2	67.5	18.30	0.03	0.11	0.33	...	...
32	319.9	21.5	19.16	0.06	0.07	0.16	...	...	124	67.2	67.5	18.49	0.05	1.42	0.15	...	...
39	230.7	24.7	19.00	0.06	-0.05	0.12	...	...	126	237.6	69.1	18.46	0.04	1.40	0.17		...
41	275.3	252	18.68	0.05	0.10	0.09	-0.86	0.10	136	0.10	72.7	16.40	0.00	1.78	0.05		
46	120.6	28.9	13.46	0.00	1.00	0.00	0.54	0.00	137	161.4	72.7	19.30	0.10	0.46	0.18		...
47	352.3	29.5	18.82	0.05	0.48	0.12	...	...	140	5.3	74.8	19.86	0.02	1.36	0.05		...
49	68.6	30.4	18.67	0.06	0.23	0.13	...	...	146	89.5	77.4	19.04	0.10	0.07	0.15		...
54	252.8	34.1	18.38	0.06	0.23	0.09	-1.02	0.09	148	225.3	79.3	18.73	0.05	0.98	0.17		...
55	621.5	35.5	16.71	0.12	1.93	0.14	...	...	150	35.9	82.5	18.25	0.05	0.29	0.09	-0.72	0.09
56	148.4	35.5	17.50	0.05	0.50	0.08	-0.35	0.08	151	133.0	83.4	18.12	0.06	0.55	0.10	-0.65	0.10
57	51.0	35.7	17.73	0.03	1.92	0.09	...	...	154	92.5	85.1	18.86	0.06	0.25	0.13	...	...
58	104.1	35.9	17.17	0.30	2.60	0.70	...	...	155	17.0	85.2	18.19	0.05	0.22	0.08	-0.-%	0.08
63	293.5	37.0	19.12	0.07	0.-0F	0.18	...	...	156	148.8	85.6	18.79	0.06	0.72	0.16	...	...
68	811.5	37.5	12.71	0.10	0.69	0.01	0.60	0.01	157	221.3	85.8	17.98	0.00	0.28	0.06	0.76	0.07
78	285.2	44.3	17.85	0.03	-0.22	0.05	-0.25	0.05	160	141.3	87.4	17.03	0.00	1.62	0.07	...	...
79	208.5	45.1	17.89	0.03	0.91	0.07	-0.66	0.08	162	293.8	88.3	18.94	0.09	0.16	0.15	...	...
80	72.0	46.0	18.93	0.04	0.42	0.15	...	...	163	366.2	88.6	17.82	0.02	1.49	0.10	...	...
84	288.9	49.5	16.85	0.00	1.42	0.05		...	164	46.9	88.9	18.37	0.04	1.63	0.21	...	...
86	257.4	51.2	18.14	0.04	0.-06	0.10		...	168	274.2	90.8	18.16	0.04	1.09	0.13		
87	328.5	51.3	16.59	0.10	0.06	0.05	-0.78	0.03	170	210.2	92.1	16.81	0.00	1.73	0.07	...	...
90	305.5	52.5	19.00	0.05	0.67	0.19		...	172	96.6	92.7	16.75	0.-10	0.11	0.03	0.18	0.03
91	37.6	52.1	18.76	0.06	1.23	0.12		...	178	167.4	98.1	18.68	0.06	0.82	0.16	...	...
93	84.8	62.5	16.35	0.10	0.51	0.03		...	180	355.1	98.8	17.61	0.02	0.14	0.05	0.80	0.06
96	344.5	53.7	17.87	0.03	1.03	0.10	...	...	183	273.2	100.4	18.22	0.03	0.15	0.08		
97	278.2	54.7	18.18	0.04	0.09	0.00	0.75	0.09	185	286.2	102.7	18.81	0.02	0.18	0.13	...	
100	284.8	55.5	18.05	0.03	1.15	0.11	...	...	188	89.4	104.0	17.95	0.03	0.24	0.-06	0.28	0.08
101	605.6	55.7	16.32	0.00	0.20	0.02	0.07	0.03	192	175.9	106.1	18.32	0.05	1.27	0.15	...	...
105	361.5	61.2	17.65	0.04	0.37	0.6%	-0.14	0.17	193	142.5	106.9	18.41	0.04	0.12	0.14	...	...

Table 14: UBV Photometry for NGC 261

No.	x	y	V	σ_V	$B-V$	σ_{B-V}	$U-B$	σ_{U-B}	No.	x	y	V	σ_V	$B-V$	σ_{B-V}	$U-B$	σ_{U-B}
1	361.5	4.0	18.81	0.32	-0.52	0.34	...	...	96	45.0	39.2	17.82	0.02	0.02	0.04	-0.26	0.06
3	236.5	6.1	17.79	0.08	0.24	0.11	-0.60	0.10	97	356.5	40.1	17.36	0.03	1.41	0.09	...	...
6	88.8	5.1	18.17	0.06	0.18	0.11	...	...	98	349.5	40.2	17.55	0.04	-0.11	0.06	-0.02	0.06
9	244.6	7.9	18.66	0.09	0.46	0.12	-0.52	0.17	101	84.8	41.6	18.88	0.05	-0.14	0.11	...	...
13	268.4	8.6	17.88	0.03	0.12	0.00	-0.57	0.08	105	60.6	42.7	17.14	0.02	-0.07	0.03	-0.05	0.03
15	29.2	9.3	18.83	0.09	0.10	0.13	-0.83	0.14	107	122.1	43.3	18.59	0.05	0.22	0.08	...	...
19	14.1	10.3	17.94	0.08	0.15	0.10	-0.60	0.06	111	130.3	44.1	19.07	0.07	0.33	0.15	...	...
20	361.5	15.0	17.47	0.06	0.52	0.11	-0.07	0.11	112	49.5	45.0	18.58	0.04	0.00	0.08	...	...
22	332.5	11.1	17.26	0.03	0.52	0.08	-0.19	0.08	114	296.6	45.7	18.33	0.03	0.82	0.12	...	...
29	289.9	15.3	19.04	0.07	0.46	0.12	-0.67	0.13	115	196.3	46.1	19.16	0.09	0.09	0.14	...	...
31	252.8	19.1	19.03	0.07	0.00	0.12	...	...	117	301.4	46.1	17.21	0.02	1.14	0.05	...	...
32	23.5	16.2	18.81	0.04	0.77	0.10	...	...	119	226.4	47.2	19.82	0.17	0.10	0.25	...	...
41	353.2	20.7	18.15	0.04	0.66	0.10	...	...	122	252.8	48.0	18.01	0.04	0.01	0.11	...	...
43	0.80	20.8	18.70	0.04	0.10	0.10		...	127	77.3	51.6	18.73	0.06	-0.06	0.09	...	...
46	254.2	21.5	18.98	0.00	1.00	0.11		...	129	376.0	52.3	18.57	0.04	-0.03	0.11	...	...
47	323.6	21.6	19.61	0.12	0.00	0.22	...	...	130	290.8	52.4	18.12	0.08	0.47	0.16	...	...
48	205.6	22.5	18.06	0.05	0.30	0.00	-0.04	0.08	131	104.7	52.5	19.00	0.06	0.92	0.18	...	...
50	298.1	22.8	17.04	0.02	0.52	0.04	0.36	0.08	133	121.1	54.2	18.70	0.05	-0.10	0.09	...	...
53	5.861	23.4	19.67	0.42	-0.16	0.45	...	...	134	15.3	54.2	18.32	0.03	0.03	0.00	-0.12	0.10
54	125.7	23.5	17.72	0.03	1.85	0.11	...	...	135	189.9	54.5	18.34	0.05	1.27	0.14	...	...
56	88.6	24.0	19.40	0.08	0.04	0.14	...	...	137	336.9	54.9	18.31	0.04	-0.01	0.09	...	...
58	171.8	25.0	19.31	0.08	-0.25	0.12	...	...	139	236.9	55.1	18.05	0.04	1.00	0.10	...	...
59	133.3	25.1	18.18	0.04	1.14	0.09	...	...	140	286.8	55.7	19.43	0.09	0.55	0.26	...	...
61	224.3	25.3	18.08	0.02	0.34	0.06	-0.12	0.10	141	272.5	56.1	16.43	0.01	1.30	0.00	...	...
65	69.1	27.0	19.54	0.06	0.00	0.15	...	...	142	351.6	56.2	17.96	0.03	0.10	0.10	...	...
66	186.7	27.3	18.05	0.02	1.16	0.12	...	...	143	317.0	56.4	19.10	0.01	0.04	0.14	...	...
75	12.7	29.6	19.60	0.10	0.11	0.18	...	...	147	105.1	58.5	17.61	0.02	1.54	0.09	...	...
76	156.0	30.4	16.83	0.10	-0.12	0.03	-0.60	0.03	151	271.6	62.5	19.06	0.08	0.48	0.14	...	...
78	211.8	32.4	15.42	0.10	-0.14	0.01	-0.98	0.00	157	378.8	62.5	17.96	0.03	1.30	0.09	...	...
79	316	33.5	19.36	0.00	0.47	0.12	...	...	159	204.6	63.9	19.58	0.01	-0.30	0.15	...	...
81	363.6	34.0	18.29	0.03	0.11	0.07	-0.82	0.10	163	264.4	65.3	16.52	0.10	1.49	0.04	...	...
82	293.0	34.1	17.45	0.02	-0.03	0.04	-0.63	0.04	164	37.2	65.4	18.32	0.05	0.03	0.09	-0.28	0.10
89	262.6	36.6	17.76	0.00	0.02	0.06	-0.97	0.05	165	21.1	65.5	19.41	0.11	0.11	0.17	...	...
91	368.7	37.3	19.07	0.06	0.54	0.36	...	...	171	299.2	68.1	18.76	0.05	0.96	0.21	...	...
95	299.4	39.0	17.61	0.02	1.67	0.11	...	...	174	218.9	69.6	16.70	0.01	-0.15	0.02	0.09	0.02

Table 15: UBV Photometry for NGC 376

No.	x	y	V	σ_V	$B-V$	σ_{B-V}	$U-B$	σ_{U-B}	No.	x	y	V	σ_V	$B-V$	σ_{B-V}	$U-B$	σ_{U-B}
4	115.5	5.7	18.79	0.11	-0.12	0.16	-0.81	0.13	125	144.6	43.7	17.87	0.03	0.62	0.08	-0.15	0.11
20	341.1	7.7	17.46	0.04	1.42	0.10	.....		126	136.3	43.7	19.12	0.06	0.42	0.16	.....	
35	294.9	12.1	14.21	0.01	1.45	0.02	1.32	0.04	127	277.1	44.8	18.51	0.08	0.02	0.12	-0.10	0.26
36	383.0	12.3	18.96	0.06	-0.45	0.12	.....		131	34.3	46.9	18.68	0.05	0.04	0.09	-0.86	0.10
37	266.9	12.9	18.41	0.05	0.00	0.08	-0.12	0.12	132	137.0	47.6	17.85	0.02	1.39	0.11	.....	
44	272.8	15.7	17.63	0.03	1.14	0.11	.....		135	184.2	49.0	17.03	0.20	-0.12	0.04	-0.11	0.05
46	21.8	17.2	19.33	0.06	0.40	0.14	.....		136	218.4	49.0	18.45	0.04	0.09	0.07	-0.73	0.08
47	210.6	17.2	16.98	0.02	0.00	0.04	-0.90	0.06	137	212.3	49.1	18.79	0.08	0.36	0.13	-1.10	0.13
54	164.9	20.5	19.73	0.15	-0.13	0.22	.....		138	229.9	50.7	20.19	0.13	-0.24	0.28	.....	
55	262.1	20.7	19.51	0.17	-0.58	0.20	.....		140	365.8	51.0	18.77	0.05	0.94	0.14	.....	
63	270	24.3	19.47	0.07	-0.20	0.16	.....		142	124.8	51.3	17.27	0.02	-0.02	0.05	-0.62	0.06
68	618	25.3	19.53	0.09	0.61	0.19	.....		144	298.8	52.2	17.34	0.02	1.30	0.06	.....	
69	262.8	25.7	19.09	0.07	0.00	0.12	.....		145	305.5	52.2	16.81	0.02	1.40	0.04	.....	
70	219.2	27.0	16.25	0.02	0.29	0.03	0.08	0.05	149	188.4	53.8	17.83	0.04	1.19	0.12	.....	
71	10.2	27.4	18.26	0.03	1.31	0.12	.....		150	42.0	53.8	19.36	0.09	0.32	0.20	.....	
75	292.7	28.8	18.31	0.05	-0.18	0.07	-0.52	0.10	151	378.0	53.9	18.82	0.08	0.90	0.18	.....	
80	1826	30.4	19.75	0.13	-0.32	0.17	.....		152	698	54.6	19.17	0.06	0.70	0.12	.....	
86	164.7	33.0	18.18	0.05	1.04	0.16	.....		156	292.0	60.5	18.35	0.03	1.20	0.14	.....	
87	78.4	33.1	18.99	0.07	-0.03	0.12	-0.62	0.13	160	271.7	57.6	18.85	0.04	1.02	0.14	.....	
88	110.8	34.1	1803	0.01	1.18	0.03	0.80	0.07	164	308.6	59.5	17.37	0.02	1.41	0.06	.....	
93	289.7	34.7	17.24	0.02	1.48	0.05	.....		169	177.1	63.8	19.84	0.10	-0.11	0.26	.....	
96	167.4	36.2	17.52	0.03	0.87	0.09	-0.06	0.13	172	290.2	65.0	19.08	0.06	0.10	0.13	-0.80	0.14
100	81.1	36.7	18.91	0.07	0.91	0.24	.....		173	76.5	65.2	18.56	0.05	0.10	0.08	-0.99	0.09
105	68.8	38.1	19.23	0.06	0.13	0.12	.....		174	162.3	65.3	18.05	0.04	-0.51	0.08	.....	
106	103.7	38.4	19.12	0.06	1.60	0.16	.....		175	251.6	65.7	17.93	0.03	-0.03	0.05	-0.82	0.07
108	26.9	38.5	19.02	0.05	0.05	0.11	.....		176	64.5	65.8	17.83	0.10	1.46	0.12	.....	
109	177.2	39.2	17.44	0.03	0.83	0.05	-0.72	0.11	177	294.2	65.9	19.34	0.07	0.92	0.15	.....	
113	292.3	40.2	18.31	0.04	0.01	0.07	-0.58	0.08	178	26.4	66.3	19.49	0.08	0.05	0.22	.....	
115	62.9	40.8	19.42	0.05	0.54	0.17	.....		180	315.7	68.7	15.98	0.02	-0.12	0.02	-0.62	0.20
116	125.4	40.9	19.48	0.09	0.97	0.45	.....		182	250.3	69.3	18.65	0.06	0.21	0.14	-0.86	0.15
117	250	41.5	18.18	0.04	0.52	0.09	.....		183	189.3	69.5	1698	0.05	0.43	0.06	-0.69	0.13
119	244.6	41.7	18.16	0.02	0.84	0.09	.....		184	335.5	69.8	19.17	0.09	0.84	0.16	.....	
121	159.6	42.3	18.32	0.04	0.09	0.07	-0.67	0.10	188	342.1	70.9	19.32	0.07	0.20	0.12	.....	
123	175.9	43.2	18.53	0.05	0.47	0.11	.....		189	360.5	71.2	18.01	0.03	0.90	0.11	.....	
124	34.1	43.4	19.05	0.16	0.14	0.12	.....		193	91.5	73.9	19.16	0.05	0.07	0.14	.....	

Table 16: UBV Photometry for NGC 456

No.	x	y	V	σ_V	$B-V$	σ_{B-V}	$U-B$	σ_{U-B}	No.	x	y	V	σ_V	$B-V$	σ_{B-V}	$U-B$	σ_{U-B}
25	262.2	7.9	18.40	0.05	-0.05	0.09	-0.68	0.19	151	117.8	102.8	17.00	0.02	0.82	0.05	0.15	0.08
39	245.0	11.4	18.23	0.04	-0.06	0.02	-1.10	0.07	155	366.2	105.9	20.12	0.15	-0.09	0.26	...	...
44	122.2	15.8	18.48	0.03	1.06	0.10	.....		157	287.0	107.1	20.27	0.19	-0.56	0.25	...	...
46	11.7	18.3	19.61	0.06	0.62	0.17	.....		162	376.2	108.2	18.81	0.05	0.14	0.10	-0.78	0.13
48	22.3	18.7	18.81	0.05	0.17	0.10	-0.78	0.12	164	189.4	110.1	19.68	0.13	-0.19	0.18	...	...
80	1815	27.2	17.24	0.01	1.25	0.06	0.70	0.18	168	80.3	111.0	17.14	0.02	0.03	0.10	-0.10	0.04
19	210.2	27.8	19.31	0.05	-0.05	0.11	.....		169	323.8	111.3	18-19	0.18	0.12	0.21	-0.40	0.29
62	31.6	28.3	20.38	0.18	-0.13	0.33	.....		176	100.9	113.6	18.25	0.02	1.44	0.16	...	...
63	0781	28.3	19.67	0.06	1.11	0.47	.....		177	38.3	114.6	17.87	0.02	0.33	0.05	-0.96	0.08
64	92.4	28.3	18.09	0.03	1.63	0.15	.....		180	102.2	118.5	20.53	0.20	-0.04	0.40	...	...
69	289.9	31.1	19.80	0.10	0.30	0.21	.....		182	231.5	120.3	17.52	0.02	-0.16	0.04	-0.58	0.04
88	354.7	31.9	17.17	0.02	1.16	0.02	.....		183	123.1	121.0	19.23	0.09	0.11	0.17	-0.53	0.21
73	58.1	37.3	19.10	0.09	0.11	0.12	-1.01	0.09	187	132.7	128.8	22.11	1.56	-0.94	1.74	...	...
76	356.4	39.3	19.13	0.05	1.55	0.40	.....		189	98.7	133.9	18.84	0.05	0.92	0.17	...	...
77	337.3	40.1	18.92	0.07	0.09	0.12	-0.95	0.12	195	106.6	140.2	19.21	0.08	0.15	0.14	-1.18	0.15
79	168.2	41.7	17.47	0.03	0.55	0.05	0.37	0.10	196	335.4	141.4	16.20	0.01	1.07	0.03	0.65	0.08
81	20.5	43.3	19.35	0.04	0.15	0.12	.....		199	343.9	148.6	19.22	0.02	0.00	0.16	-0.51	0.19
83	126.4	44.7	18.93	0.06	-0.01	0.09	0.29	0.15	200	114.9	148.8	18.82	0.04	0.17	0.09	...	...
84	2958	44.8	20.13	0.16	0.08	0.28	.....		204	50.2	153.8	19.93	0.11	0.00	0.21	...	...
88	246.4	47.3	16.22	0.01	0.96	0.03	0.62	0.04	205	317.7	154.7	19.62	0.11	-0.27	0.17	-0.12	0.21
16	242.7	50.4	17.74	0.03	0.97	0.09	1.17	0.34	206	1.69	155.1	19.07	0.04	0.89	0.56	...	...
94	100.2	52.3	19.94	0.14	0.79	0.45	.....		209	349.0	156.2	18.61	0.08	0.52	0.16	...	...
100	376.9	63.5	17.06	0.01	0.14	0.04	-0.12	0.05	211	202.3	157.1	18.85	0.14	1.03	0.23	...	...
102	309.3	65.3	19.11	0.05	0.34	0.17	-0.86	0.16	214	46.0	160.7	16.77	0.02	0.08	0.03	-0.10	0.03
105	0.55	70.0	19.63	0.06	0.13	0.17	.....		222	174.8	163.8	18.90	0.07	-0.13	0.09	-0.51	0.06
106	111.6	71.3	18.83	0.05	0.86	0.13	.....		221	149.2	164.5	16.84	0.03	0.16	0.03	-0.03	0.04
109	122.2	73.2	20.04	0.14	-0.27	0.21	.....		224	299.8	1651	18.98	0.04	0.09	0.11	-0.83	0.12
111	6.09	74.7	19.93	0.10	-0.02	0.23	.....		225	134.2	1656	19.64	0.11	-0.63	0.14	0.05	0.20
113	329.1	75.7	18.56	0.05	0.77	0.12	.....		227	255.9	171.9	16.12	0.10	-0.09	0.02	-0.83	0.02
117	55.7	77.6	18.59	0.05	0.21	0.46	-1.51	0.11	234	157.3	183.3	17.98	0.04	0.14	0.05	-0.79	0.08
123	192.6	81.5	17.13	0.05	0.57	0.48	-0.62	0.09	235	121.9	184.6	16.74	0.02	0.00	0.03	-0.86	0.03
124	190.5	82.8	13.66	0.01	1.32	0.02	1.24	0.04	236	40.5	1858	17.46	0.03	0.08	0.05	-0.73	0.04
139	212.7	6926	19.29	0.10	-0.03	0.16	-0.39	0.20	237	248.8	185.6	17.75	0.05	-0.06	0.06	-0.54	0.07
142	190.7	1.56	20.29	0.25	0.07	0.32	.....		239	226.8	187.0	19.78	0.10	0.07	0.18	...	...
147	305.9	99.1	18.98	0.05	0.59	0.12	-0.12	0.22	240	192.1	187.1	17.00	0.03	0.06	0.03	-1.90	0.03

Table 17: UBV Photometry for NGC 460

No.	x	y	V	σ_V	$B-V$	σ_{B-V}	$U-B$	σ_{U-B}	No.	x	y	V	σ_V	$B-V$	σ_{B-V}	$U-B$	σ_{U-B}
1	242.5	65	18.75	0.11	0.26	0.14	-1.07	0.12	188	163.0	126.6	16.65	0.01	0.03	0.03	-0.65	0.03
38	27.6	16.5	16.29	0.01	0.82	0.04	0.47	0.07	143	301.1	131.0	16.47	0.01	0.60	0.03	0.03	0.04
46	43.8	26.4	19.18	0.07	0.01	0.14	-0.47	0.17	145	99.7	135.0	18.27	0.03	1.36	0.13	...	...
48	219.7	28.3	18.25	0.04	1.30	0.20	...	...	153	26.4	148.4	18.50	0.05	1.18	0.17	...	...
51	6.3	37.0	18.69	0.19	-0.29	0.11	-1.80	0.11	163	56.3	158.2	18.38	0.04	0.75	0.10	...	...
53	150.4	37.3	14.32	0.00	2.02	0.00	2.57	0.19	168	106.2	163.4	19.49	0.10	0.14	0.21	...	...
54	198.1	39.8	15.47	0.01	1.62	0.00	1.67	0.19	169	85.0	163.9	18.65	0.05	0.14	0.09	-1.20	0.14
61	304.0	44.3	19.04	0.05	1.43	0.28	...	...	174	331.2	172.1	18.46	0.03	1.37	0.19	...	...
62	89	46.2	17.68	0.06	-0.28	0.08	...	...	175	171.9	172.4	19.13	0.05	0.02	0.10	-2.10	0.15
65	10.2	46.7	17.67	0.08	-0.26	0.10	-1.92	0.10	179	320.1	175.3	17.83	0.03	1.24	0.08	...	...
68	347.2	49.9	18.72	0.06	-0.07	0.08	-0.61	0.09	180	372.4	177.4	19.66	0.08	2.14	0.18	...	...
69	1212	51.4	20.05	0.12	-0.10	0.22	...	...	181	180.2	177.4	16.75	0.01	2.18	0.00	...	...
70	13.8	52.6	19.12	0.09	-0.08	0.16	...	...	186	376.4	182.3	19.80	0.17	0.00	0.24	-1.19	0.21
71	370.0	55.8	20.00	0.12	0.31	0.29	...	...	190	7.8	184.6	18.00	0.03	1.22	0.09	...	...
74	384.2	57.2	19.28	0.17	-0.06	0.22	-0.95	0.20	193	352.2	186.0	19.56	0.00	0.14	0.19	...	...
75	285.1	59.7	19.83	0.10	0.45	0.29	...	...	194	342.1	186.1	15.81	0.01	-0.51	0.02	-1.60	0.00
76	378.6	59.8	19.31	0.08	-0.15	0.12	...	...	199	59.8	191.8	1881	0.05	0.24	0.11	-0.44	0.19
78	318.8	63.6	19.77	0.09	0.27	0.20	-0.87	0.19	203	115.3	196.5	16.16	0.01	-0.02	0.00	-1.04	0.00
79	177.7	65.7	19.57	0.10	-0.21	0.17	-0.62	0.18	209	25.5	201.4	19.30	0.06	-0.32	0.14	-0.10	0.23
82	206.7	72.2	20.39	0.18	0.09	0.48	...	...	212	102.6	204.9	18.78	0.06	-0.28	0.09	-0.49	0.11
86	78.7	73.8	19.75	0.12	0.05	0.24	...	...	217	309.6	207.1	18.95	0.13	0.72	0.19	...	...
87	178.6	75.6	19.94	0.12	-0.23	0.18	...	...	218	149.6	207.3	19.70	0.12	-0.11	0.18	-1.04	0.18
89	244.5	85.1	1689	0.00	-0.14	0.03	-1.80	0.03	223	347.7	212.4	1906	0.05	-0.13	0.09	-0.56	0.14
98	173.6	85.6	1399	0.01	0.32	0.02	0.09	0.03	224	129.8	215.0	19.21	0.08	-0.55	0.13	-0.46	0.13
102	206.4	94.1	17.04	0.01	-0.05	0.03	-0.94	0.03	225	308.3	215.4	17.30	0.08	-0.41	0.12	-0.74	0.10
104	47.1	98.8	17.68	0.00	-0.05	0.05	-0.32	0.05	232	85.4	221.7	16.96	0.01	0.25	0.03	-0.05	0.05
107	299.6	102.2	15.96	0.01	-0.22	0.02	-0.98	0.02	233	20.8	222.1	19.36	0.06	0.82	0.20	...	...
111	112.6	106.0	18.90	0.05	0.84	0.17	...	...	238	302.4	224.6	15.20	0.03	-0.24	0.04	-0.67	0.04
115	162.4	108.9	1961	0.12	0.12	0.22	-0.10	0.28	239	89.6	224.7	19.41	0.10	0.00	0.19	0.10	0.33
119	246.2	109.9	19.89	0.12	-0.09	0.20	...	...	240	33.0	225.3	17.90	0.03	2.16	0.23	...	...
125	351.5	113.1	18.90	0.05	0.13	0.10	0.68	0.15	241	288.8	225.6	18.22	0.11	-0.24	0.16	-0.95	0.15
129	264.6	116.6	17.72	0.02	0.51	0.04	0.52	0.22	242	292.4	225.8	17.07	0.05	-0.02	0.07	-1.04	0.06
131	285.0	116.8	18.94	0.05	0.04	0.10	-0.81	0.14	243	297.7	226.5	1508	0.02	-0.22	0.03	-0.96	0.03
	367.2	117.1	19.47	0.09	0.08	0.18	...	...	246	179.9	227.2	18.09	0.03	-0.07	0.05	-0.75	0.06
	333.3	121.1	1961	0.10	0.17	0.25	-0.75	0.20	247	306.1	227.5	15.36	0.19	-0.15	0.16	-0.86	bono

Table 18: UBV Photometry for NGC 460

No.	z	y	V	σ_V	B - V	σ_{B-V}	U - B	σ_{U-B}	No.	z	y	V	σ_V	B − V	A - ED	U − B	σ_{U-B}
11	248.4	12.6	18.48	0.04	-0.18	800	-0.80	6(Y0	90	257.4	976	17.43	0.03	-0.24	0.04	088	0.04
12	1 768	13.2	19.54	LO"0	-0.29	11"0	. . . . .		16	229.1	98.9	19.46	0.11	0.15	91"0	-0.85	81"0
14	103.0	18.8	17.50	Z00	-0.14	0.03	LL"0	0.04	26	336.6	7.66	1861	11"0	-0.43	81"0	. . . . .	
16	121.2	19.5	18.98	0-0	00'1	61"0	. . . . .		93	245.8	100.1	19.91	0.10	-0.28	0.17	. . . . .	
21	283.3	24.9	19.42	0-0	sro-	01"0	LZ"0	0.13	94	207.4	100.5	17.06	10"0	-0.17	200	t'L"0	0.04
22	376.1	9"92	20"0	8081	-0.20	80-0	-0.73	LOO	96	252.2	6101	18.10	0.03	-0.09	0.04	-0.65	0.05
25	241.3	27.8	14.84	0.01	0.15	0.01	0.49	80-0	16	94.0	102.0	18.79	0.06	-0.11	008	-0.55	01"0
28	205.4	28.5	18.09	0.03	-0.22	70"0	f x o -	0.04	98	374.0	103.0	17.92	0.03	-0.06	so-o	- o 8 " b 8 q	0.06
29	164.1	30.4	18.94	0.06	-0.04	01"0	-0.67	0.11	101	164.8	106.2	19.56	0-60	200	91"0	. . . . .	
34	150.8	39.2	19.60	0.11	-0.01	61"0	-0.51	0.24	103	331.7	107.0	19.66	TWO	ot"o-	81"0	. . . . .	
35	146.2	39.3	19.38	0.11	-0.04	61"0	-0.78	02"0	104	344.4	111.5	17.99	0.04	-0.24	0-90	vso-	9(%)
40	329.2	45.0	14.45	10"0	-0.26	0.01	s60-	0.01	106	252.2	112.5	17.08	0.03	-0.23	0.04	-0.79	0.04
42	120.6	45.3	17.90	11"0	0.04	0.12	-0.60	LOO	107	49.7	112.7	19.73	0.12	-0.38	91"0	. . . . .	
44	33.9	47.8	17.28	Z00	-0.14	0.03	-0.76	70"0	108	340.2	114.0	16.34	ZOO	-0.07	Z00	LL"0	Z00
45	161.1	48.7	16.86	0.02	-0.15	Z00	W0-	0.03	109	9011	115.5	19.70	0.12	-0.06	02"0	. . . . .	
48	272.5	53.1	19.71	0.13	-0.15	0.22	. . . . .		112	274.0	116.0	17.70	0.04	-0.20	0.05	SL-0-	0.05
50	148.4	54.9	14.63	0.01	0.93	Z00	0.52	0.03	113	23.6	117.2	05"02	02"0	-0.13	82"0	. . . . .	
54	24.7	57.0	15.77	0.01	-0.13	0.02	-0.68	0.02	115	360.8	1"811	16.86	0.01	-0.15	0.03	LL"0	0.03
55	109.4	Z"LS	1861	0.13	-0.10	0.17	-0.45	0.21	117	307.8	121.2	16.06	20"0	-0.28	0.03	-0.98	20"0
56	153.8	S"LS	15.87	100	-0.19	0.02	-0.85	200	120	378.4	121.7	19.15	LOO	-0.12	21"0	ss"o-	91"0
58	225.1	6"8S	19.11	60"0	0.02	0.15	1so-	0.14	121	298.4	122.0	20.01	0.12	-0.49	0.17	. . . . .	
62	337.8	2"S9	20.08	0.14	-0.45	02"0	. . . . .		124	117.3	6"S21	19.18	0.14	0.04	91"0	vz"o-	61"0
63	308.3	66.4	18.80	0.05	-0.26	800	19"o-	0.09	125	377.6	6S21	18.62	0.04	-0.28	0.09	LVO	21"0
64	326.2	66.9	20.84	0.34	-1.22	0.39	. . . . .		129	191.7	129.0	19.48	800	0.43	0.18	. . . . .	
66	128.6	68.3	19.27	0.04	-0.06	0.11	t'vo-	0.14	130	130.7	129.2	9981	0.06	0.45	600	600	0.17
69	319.3	71.2	18.95	0.06	0.03	0.08	-0.71	0.08	132	986	131.1	19.14	0.05	0!%	0.12	-0.58	0.16
69	352.6	74.7	19.32	8C%	-0.08	0.11	-0.46	0.18	133	75.1	132.4	9961	11"0	0.18	02"0	-1.20	12"0
72	175.2	77.2	19.66	0.11	-0.19	0.16	-0.37	0.23	136	159.8	133.3	19.60	0.13	0.25	22"0	. . . . .	
74	52.3	L"LL	17.42	Z O O	1.14	0.06	060	0.15	137	115.4	134.6	19.23	01"0	100-	0.15	-L9"o-	0.13
75	317.4	2"08	17.22	0.03	-0.17	0.03	-0.70	0.03	139	322.8	136.4	19.35	0.12	1.58	0.49	. . . . .	
76	87.0	2"08	1861	0.10	,21"0	0.22	. . . . .		140	69.8	137.3	20.33	0.22	-0.76	0.26	. . . . .	
77	2"0S1	918	19.19	0.05	0.97	61"0	. . . . .		143	132.0	140.6	14.97	0.01	-0.25	Z00	C60-	Z00
80	332.3	6"L8	19.59	01"0	0.43	0.25	61"1	92"0	144	243.2	141.6	17.82	0.03	1.32	01"0	. . . . .	
86	252.4	95.0	19.87	0.13	-0.04	0.23	. . . . .		145	239.3	145.1	19.57	600	0.16	0.18	8S"0"	0.24
88	102.5	95.9	20.08	0.12	-0.06	0.20	. . . . .		147	306.1	146.9	19.77	0.14	-0.23	61"0	. . . . .	